Міністерство освіти і науки України
Харківський національний університет імені В. Н. Каразіна

ВІСНИК

Харківського національного університету імені В.Н. Каразіна

Серія
«Математичне моделювання.
Інформаційні технології.
Автоматизовані системи управління»

Випуск 56

Серія заснована 2003 р.

BULLETIN

of V.N. Karazin Kharkiv National University

Series
«Mathematical Modeling.
Information Technology.
Automated Control Systems»

Issue 56

First published in 2003

Харків
2022

Статті містять дослідження у галузі математичного моделювання та обчислювальних методів, інформаційних технологій, захисту інформації. Висвітлюються нові математичні методи дослідження та керування фізичними, технічними та інформаційними процесами, дослідження з програмування та комп'ютерного моделювання в наукоємних технологіях.

Для викладачів, наукових працівників, аспірантів, працюючих у відповідних або суміжних напрямках.

Наказом Міністерства освіти і науки України від 17.03.2020 № 409 наукове фахове періодичне видання Вісник Харківського національного університету імені В.Н. Каразіна серія «Математичне моделювання. Інформаційні технології. Автоматизовані системи управління» включено до Категорії «Б» Переліку наукових фахових видань України за наступними спеціальностями: 113 – Прикладна математика;122 – Комп'ютерні науки та інформаційні технології; 123 – Комп'ютерна інженерія; 125 – Кібербезпека.

Затверджено до друку рішенням Вченої ради Харківського національного університету імені В. Н. Каразіна (протокол № 19 від 26.12.2022 р.)

Адреса редакційної колегії: 61022, м. Харків, майдан Свободи, 6, ХНУ імені В. Н. Каразіна, к. 534.
Тел. +380 (57) 705-42-81, Email: journal-mia@karazin.ua.

Мова публікації: українська, англійська, російська.

Статті пройшли внутрішнє та зовнішнє рецензування.

Свідоцтво про державну реєстрацію КВ № 21578-11478 Р від 18.08.2015.

The articles are present research in the field of mathematical modeling and computing methods, information technologies, information security. New mathematical methods of research and management of physical, technical and information processes, research on programming and computer modeling in science-intensive technologies are covered.

For teachers, researchers, graduate students working in relevant or related fields.

By the order of the Ministry of Education and Science of Ukraine from 17.03.2020 № 409 scientific professional periodical Bulletin of V.N. Karazin Kharkiv National University series "Mathematical modeling. Information Technologies. Automated control systems" is included in Category "B" of the List of scientific professional publications of Ukraine in the following specialties: 113 – Applied Mathematics, 122 – Computer Science and Information Technology; 123 – Computer engineering; 125 – Cybersecurity.

Approved for publication by the decision of the Academic Council of V.N. Karazin Kharkiv National University (Minutes № 19 of 26.12.2022).

Editorial Address: 61022, Kharkiv, Svobodi sq., 6, V.N. Karazin Kharkiv National University, r. 534.
Phone. +380 (57) 705-42-81, Email: journal-mia@karazin.ua.

Language of publication: Ukrainian, English, Russian.

The articles pass internal and external review.

Certificate of state registration: KV № 21578-11478P dated 18.08.2015

ЗМІСТ

CONTENTS

DOI: https://doi.org/10.26565/2304-6201-2022-56-01

UDC 535.4

Bondarenko Kostiantyn *Ph.D student*
Department of Theoretical and Applied Systems Engineering, Faculty of Computer Science, V.N. Karazin Kharkiv National University, Svobody Sq., 4, 61022, Kharkiv, Ukraine
e-mail: konstantinb2016@gmail.com
https://orcid.org/0000-0002-2430-0716

Dolya Gregory *Doctor of Technical Sciences, professor*
Department of Theoretical and Applied Systems Engineering, Faculty of Computer Science, V.N. Karazin Kharkiv National University, Svobody Sq., 4, 61022, Kharkiv, Ukraine
e-mail: gdolya@karazin.ua
https://orcid.org/0000-0001-8888-5189

Mathematical models and approaches in simulation of RRS-based laser sensor system

The article is devoted to the research of mathematical models and approaches in simulation of laser sensor systems based on retroreflective sheeting (RRS) usage. The subject of the study is the mathematical model of the research object - the processes of propagation of a light in the medium and its transformation on retroreflectors with further analysis of the reflected radiation, which, being modulated by interaction with objects in the system, carries information about the state of the system. Overview of existing studies has been made. The analysis of existing approaches to simulation methods has been carried out, as well as the analysis of existing models. Common elements of models applicable in different fields and contexts of such systems have been determined. The scientific methods of research are outlined, such as comparative analysis while studying similar systems, conducting physical experiments in laboratory conditions with a prototype of a computerized detection system for observing phenomena in the system, their systematization and description, synthesis of a mathematical model based on the obtained data, creation of a computer model and, after its verification, and conducting computer experiments. The typical research schema is proposed, suggesting such main stages in simulation modeling of the laser sensing systems based on RRS as generation of the laser emission light field structure, interaction of the light field with environment, transformation of the APD inside the RRS, finding the APD in the reception zone, converting the resulting APD into a photocurrent, finding dependencies between parameters, evaluating detection efficiency, system optimization. The analysis of strong points of different approaches has been made. Some major aspects to be considered when choosing the appropriate method have been pointed out. The guiding principles for the general modeling of such systems illustrated with original concrete examples of such models verified in practice are presented.
Keywords: *laser, sensor, retroreflective sheeting, specklometry, simulation modeling.*

How to quote: K. Bondarenko, and G. Dolya, “Mathematical models and approaches in simulation of RRS-based laser sensor system.” *Bulletin of V.N. Karazin Kharkiv National University, series Mathematical modelling. Information technology. Automated control systems*, vol. 56, pp. 6-20, 2022. https://doi.org/10.26565/2304-6201-2022-56-01

Як цитувати: Бондаренко К. О., Доля Г. М., Математичні моделі та підходи до імітаційного моделювання лазерних датчиків на основі СПП. *Вісник Харківського національного університету імені В. Н. Каразіна, серія Математичне моделювання. Інформаційні технології. Автоматизовані системи управління*. 2022. вип. 56. С. 6-20.
https://doi.org/10.26565/2304-6201-2022-56-01

1. Introduction

Laser detectors have become widespread due to the properties of the emitters included in their composition. Coherent radiation generated by lasers makes it possible to use the features of the diffraction phenomenon, namely, observing the formed speckle pattern, which allows expanding the scope of application of relatively simple optical detectors significantly. As optical detectors, they have the advantage of low signal response delay, because the speed of light propagation is extremely high. Among other advantages, one cannot fail to mention the fact that laser detectors will allow observing

phenomena from a great distance, as this can be used in many fields of technology. In many cases, the condition is also fulfilled that the effect of detector radiation on the investigated system is so small that it can be neglected, which means that the system can be observed with their help without interfering with it, for example, mechanically, which is a great advantage. These devices allow solving a wide range of tasks - vibration control, laser ranging, velocimetry, turbulence control, as well as registration of acoustic oscillations and others [1-8].

One of the significant limitations when using the speckle measurement method is a wide angular spectrum of the laser light scattered on the rough object surface. This leads to a rapid decrease in power of the received radiation with an increase of measurement range. By covering the object surface with retro-reflecting sheeting (RRS) a significant increase of spatial concentration of the scattered radiation can be achieved. These coatings are currently widely used, for example, to enhance the visibility of the road signs, clothing, vehicles, etc. They consist of a large number of glass microspheres or microprisms [9] with characteristic dimensions ranging from tens to hundreds of micrometers and disposed on a substrate in random manner (microspheres) or relatively regular (microprisms). When the laser radiation falls on such surface, the light field is transformed in accordance with the laws of beam pass in each element of the RRS. The transformed radiation propagates in the direction of the laser source within a small angle of a few degrees. That process creates the speckle image within the receiving plane as a result of interference of waves re-emitted by each element. Use of RRS significantly increases the laser radiation capacity observed in a receiver plane. That allows us to increase observation distance and precision of measurements.

The study of the features of RRS-based laser sensor systems is of great interest. As part of the research, it is beneficial to develop simulation models of the system to assist in analyzing the influence of the variation of the system parameters on the quality of detection.

2. Overview of existing studies, analysis and goal definition

The design features of the retroreflectors provide for some useful properties. For example, as in case of the roughsurfaced objects, a speckle pattern is formed in the far zone when they are irradiated with laser radiation, which can be used for laser ranging. It is also possible to vary the microstructure, which opens up an opportunity to influence the transformation characteristics of the light field and intensity distribution of the reflected laser radiation in the far zone (receiving plane). The latter of these features is of particular interest and is the subject of the research [8-11], since it makes it possible to optimize the RRS used to improve the properties of a target, being a part of the specific optical subsystems.

The paper [12] describes the specklometric method of detecting acoustic vibrations, while reflective surfaces based on corner reflectors are used. The article [13] describes an approach to observing and measuring the acoustic dynamics of a gas after an ionizing pulse.

An extremely detailed study of using glass microbeads in road marking has been carried out at the University of Pretoria [14]. The work focuses on the creation of a thermoplastic road marking standard. It serves as a valuable source of both background information and information on different approaches to technology. The model that simulates the reflection of the car headlights from the marking back into the cabin is mentioned in the work. Statistical data on road marking wear over time are presented, an analysis of the dependence of light-reflective properties on the radius of the microspheres used in correlation with wear over time is carried out. The parameters of the structure of the reflective surface and the issues related to the choice of the substrate material are discussed.

Among other promising areas of use for RRS, the creation of reflective screens for image projection could be noted. For example, the article [11] describes a simulation model for studying the properties of such screens. Another similar direction of technology development is the creation of surfaces with a controlled degree of light reflection. The articles [15] and [16] describe such surfaces being developed in the University of Cincinnati. The authors propose a combined approach to the creation of reflective surfaces - prismatic microreflectors are suggested to be filled with an oily solution and light reflection could be controlled by changing the wettability (and thus the spatial shape of the structure) by changing the applied voltage. In [16], the mathematical model is described in detail and the results of physical modeling are presented. Such a serious study of prospective areas of retroreflector application shows us great relevance and broad prospects of using the RRS sensors.

Thus, the article [17] describes the use of RRS in scanning systems in conjunction with lidars. The article [18] describes the principle of creating a linear velocimeter based on the use of RRS and Doppler effect, the article [19] extends this idea to the case of rotating cylindrical objects. The article [20]

describes the use of a retroreflective surface for optical tracking of object vibration, providing a mathematical model of laser radiation diffraction on a vibrating surface covered with microprism-based RRS.

The analysis of the literature shows that laser sensor systems with retroreflectors are widely used in industry. Active research of RRS-based laser sensor systems, as well as prospective areas of their application, reflects the interest of the scientific community in their further improvement and development of new areas of their application.

Our goal is to carry out an analysis of existing approaches simulation methods, find common elements of models applicable in different fields and contexts of such systems, as well as analyze strong points of different approaches in order to help in selecting an appropriate method, taking into account coherent laser radiation properties, and provide original examples of such models verified in practice.

3. Typical research schema

From the overview and analysis of the existing models it can be concluded that there is a general underlying schema of research, which we are going to summarize.

The purpose of the research on the modeling of RRS-based laser sensor systems is developing mathematical models of such systems for their further practical optimization and efficiency improvement.

The subject of the study is the mathematical model of the research object - the processes of propagation of a light wave (in the case of lasers - partially coherent) in the medium and its transformation on retroreflectors (microbeads- or microprism-based) with further analysis of the reflected radiation, which, being modulated by interaction with objects in the system, carries information about the state of the system.

There are some widespread scientific research methods, such as comparative analysis, conducting physical experiments in laboratory conditions with a prototype of a computerized detection system for observing phenomena in the system, their systematization and description, synthesis of a mathematical model based on the obtained data, creation of a computer model and, after its verification, conducting computer experiments.

The result of such research is a developed mathematical and computer models describing the system consisting of laser emitters and RRS, which allow improving the efficiency of such systems by providing recommendations on the selection of system parameters. Depending on the type of sensor under consideration and the application field such parameters as the detection efficiency, which is expressed as the ratio of positive activations to all activations in notification systems, or the accuracy of detection of environmental fluctuations, and the speed of movement of the object of observation, etc., can be selected.

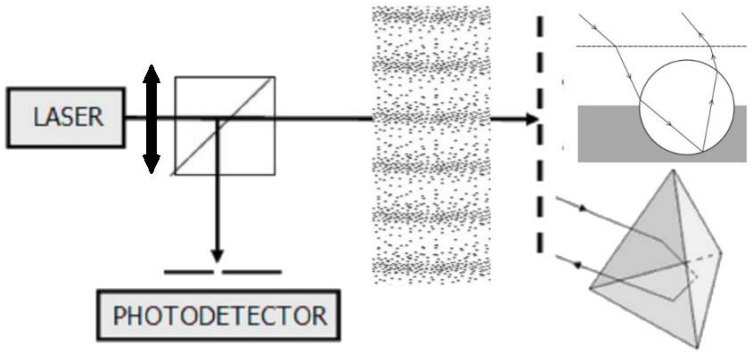

Fig.3.1 Typical setup for the research

A typical [11, 12, 15, 18, 19, 21, 22] setup of laser sensor with RRS, regardless of the application field shown in Fig. 3.1. It includes the main following elements: a source of laser radiation with an external focusing device, some kind of environment that laser beam transverses (might be turbulent atmosphere, regular acoustic oscillations, liquid, etc.) a reflecting surface with a reflective coating

applied to it (surface might be moving – simulating vibrations or spatial movements of the target), optical splitter, a radiation collector, a diaphragm, and a photodetector.

4. The main stages in simulation modeling of RRS-based laser sensor systems

4.1. Generation of the laser emission light field structure

In some studies, only the intensity of the emitter is taken into account and diffraction does not play a role in detection, the speckle pattern is not important, and only the change in the amplitude of the detected photocurrent is of interest [11, 14, 15, 17, 21]. This greatly simplifies modeling and is also justified in cases where not only laser but the emitter with a wide spectrum can be used.

In the case when it is necessary to take into account the coherence of laser radiation, one should use the representation of the emitter in the form of the Gaussian beam (in the general case, it is multi-mode, most often it is enough to study the single-mode case). Next, we will consider the multimode laser approach, because multimode lasers are required for the sensors to be applicable in practice. In this case to describe the light field at a point, one should use the multimode Gaussian beams [23]:

$$E_{l,m}(x,y,z) = E_0 \frac{w_0}{w(z)} H_l\left(\frac{\sqrt{2}x}{w(z)}\right) H_m\left(\frac{\sqrt{2}y}{w(z)}\right) \times \exp\left(-\frac{x^2+y^2}{w^2(z)}\right) \exp\left(-i\frac{k(x^2+y^2)}{2R(z)}\right) \exp(i\psi(z)) \exp(-ikz) \quad (4.1)$$

where l, m - a longitudinal mode and a transverse mode respectively, H - the Hermite polynomial.

The cross section of the intensity distribution across the beam propagation direction *l* is shown in the Fig. 4.1 (a), with TEM LM designating modes: L designating the longitudinal mode and M the transverse mode.

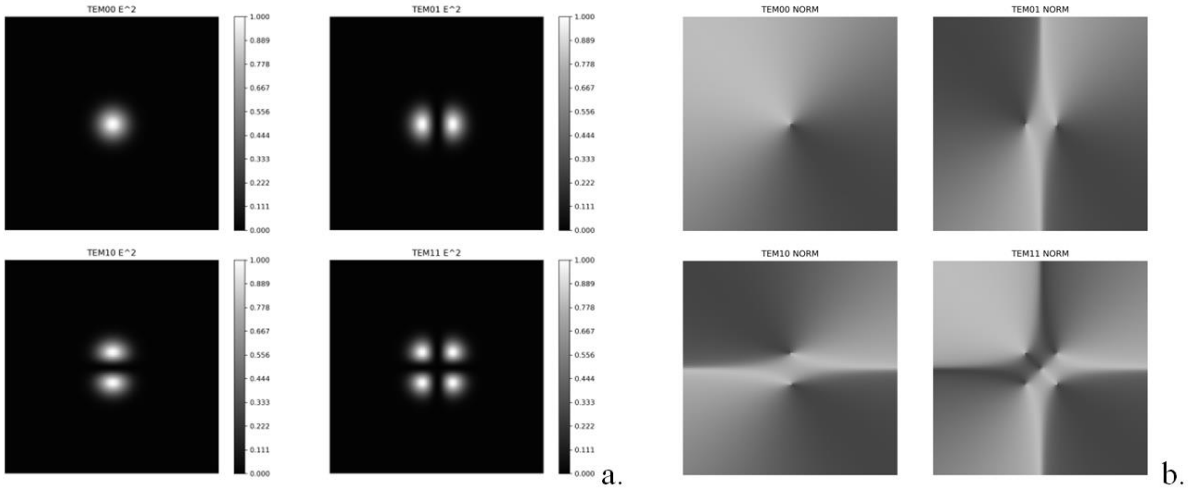

Fig.4.1 Intensity distribution (a) and normal map (b) of the multimode Gaussian beam cross section

For the further transition to the geometric optics, which is used in the model at the stage of calculating the field transformation inside of the RSS, it is necessary to restore the directional vector of the field at a point, as well as the polarization vector perpendicular to it and lying in a given polarization plane. To do this, it is enough to find the value of the gradient of the function at the desired point. One can use the numerical methods (e.g., finite differences methods) [24] for finding the derivative of the equation 4.1, considering the extreme cumbersomeness of the analytical calculation of the derivative function of the multimode Gaussian beam. The attractiveness of the numerical approach is largely explained by the presence of simple dependencies, with the help of which the derivatives at given points can be approximated by several values of the function at those points and points close to them. The construction of approximate differentiation equations based on a fact that the function on the given segment is replaced by the corresponding approximating function, and then it is assumed that the

derivatives of the functions coincide. At the same time, the approximating function is most often given in the form of a polynomial [25].

The Fig. 4.1 (b) shows an example of normal maps for the cross sections of the fields of the Gaussian beams of different combinations of the orders of longitudinal and transverse modes. It seems obvious that for a multimode emitter it is possible to carry out an experiment for each of the chosen order of the modes and then combine the obtained intensities in the far zone.

4.2. Interaction of the light field with environment

The environment that laser beam transverses might vary - turbulent atmosphere, regular acoustic oscillations, liquid, etc. Most often it is just regular atmosphere and distances are so small, that it could be ignored altogether. In some cases, atmosphere effects are to be taken into account, Rayleigh scattering and Beer–Lambert law, for example [26].

In case of turbulent atmosphere usage of models with phase screens [27] and ray tracing in context of the refraction are appropriate. The refraction approach can also be used to model liquid environment. When dealing with acoustic wavefront, if width of the laser beam is much smaller than acoustic wavelength, a simple refraction approach is appropriate and described below.

It is assumed that the laser beam width is smaller than the acoustic wavelength in air, therefore, the sound wave can be represented as an acousto-optic refractive deflector - the mechanical propagation of a sound wave is accompanied by a change in the air density, which creates a gradient of optical density and causes the beam to deviate from the axis of its initial propagation.

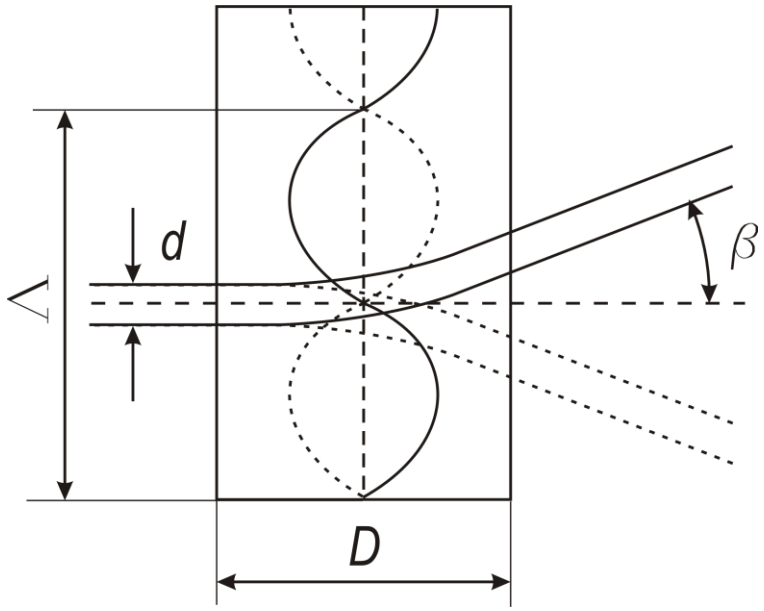

Fig.4.2 Acousto-optic refractive deflector

Then the following equation is applicable for the deflection angle [28]:

$$\beta = \frac{2\pi\Delta n D}{n\Lambda}\sin(2\pi(ft+\varphi)) \tag{4.2}$$

where Δn - a modulation amplitude of the refractive index of the medium, D - acoustic wave thickness, n - a refractive index, Λ - an acoustic wavelength, f - an acoustic frequency, t - time, φ - a phase shift.

For the model, the acoustic wave is assumed to be a plane with the wave propagation axis indicated on it. At a zero point of the axis, the phase is assumed to be zero. For the case of a multimodal laser, one should take into account that dielectric medium for propagation of radiation has a dispersion that can be described by the Sellmeier equation [26].

4.3. Transformation of the APD inside the RRS

Diffraction phenomena being neglected, and only the intensity is of interest, it is enough to calculate the initial aperture, limiting angles of reflection and the reflection coefficient, based on geometrical optics, both analytically as a whole, and by ray tracing, as in work [17], for example.

In the case of the scalar theory of diffraction and taking into account coherent radiation, two approaches are possible. If the RRS grid is strictly periodic (for example, obtained by stamping), analytical transformations according to the laws of diffraction grids are sufficient, as in the work [20], for example.

When the retroreflectors are disordered, as in the case of glass beads, it is necessary to find the transformation of amplitude-phase distribution (APD) on RRS by tracing rays (thus turning to geometric optics), as it is done in the works [11, 29]. We emphasize the fact that the transition to geometric optics is possible only if the retroreflective elements are at least an order of magnitude larger than the wavelength. At the same time, the decomposition of the polarization vector, transmission losses, and the calculation of the phase shift should be taken into account. An example of calculating the transformation of AFD on the retroreflector based on glass beads is given below.

Knowing the field amplitude, phase, directing vector and electric field vector in space at the given point, we can proceed to the second stage - the transformation of the field inside the RRS. To construct the ray trajectory, the directing vector $\overrightarrow{k_1}$ at a point P_1, selected on the RRS plane, transforms into vector $\overrightarrow{k_2}$ according to the Snell's law (Fig. 4.3 (a)). Next, the bead with which the intersection occurs and the point P_2 of the intersection of the ray $\left\{P_1, \overrightarrow{k_2}\right\}$ with the sphere representing the bead is determined. At the found point, a normal to the sphere is constructed, then similar actions are carried out.

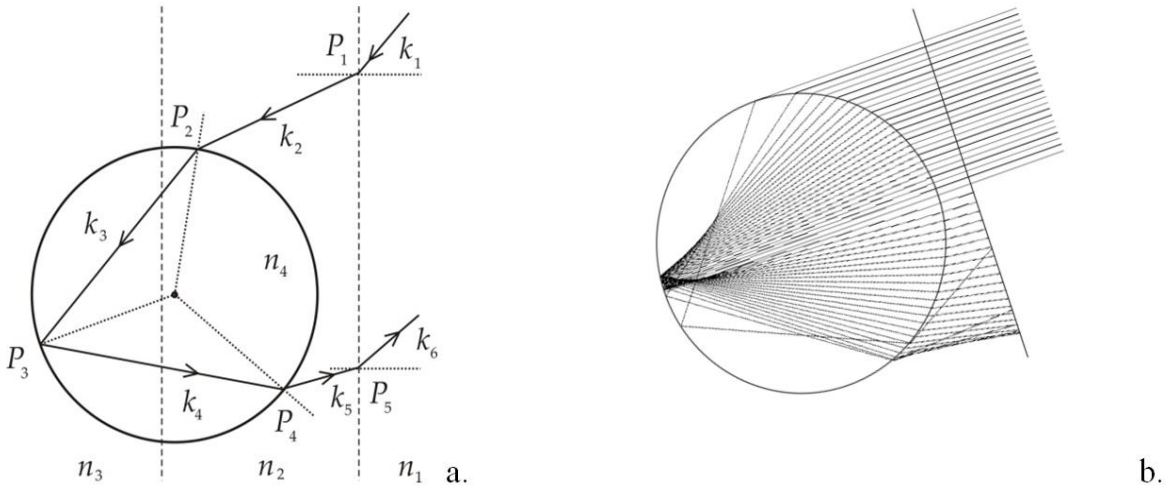

Fig.4.3 Ray trajectory inside glass beads RRS: calculations (a) and simulation example (b)

According to the model, the points P_2 and P_4 should lie on the border between the bead and the covering layer, and the point P_3 should lie on the border between the bead and the substrate; re-reflections inside the bead or between neighboring beads are not considered. The point P_5 is sampled and is the point of the output APD. In general case, the vectors $\overrightarrow{k_1}$ and $\overrightarrow{k_2}$ lie in one plane, and the vectors $\overrightarrow{k_2}$, $\overrightarrow{k_3}$, $\overrightarrow{k_4}$, $\overrightarrow{k_5}$, $\overrightarrow{k_6}$ lie in another. Given each of the segments $\overrightarrow{l_i = P_{i-1}P_i}$ that make up the trajectory of the light beam, the total phase shift φ is calculated:

$$\varphi = \frac{2\pi}{\lambda}\sum_{i=1}^{6} n_i l_i \tag{4.3}$$

where λ - a wavelength in vacuum, n_i - an absolute index of refraction of the medium for λ.

The phase shift when reflected at the point P_3 is considered separately, since the shift *i* for the parallel and perpendicular components *n* the general case is different. Also, for each transition from one medium to another, the amplitude transmission and reflection coefficients for both field components are calculated by using the Fresnel equations [26].

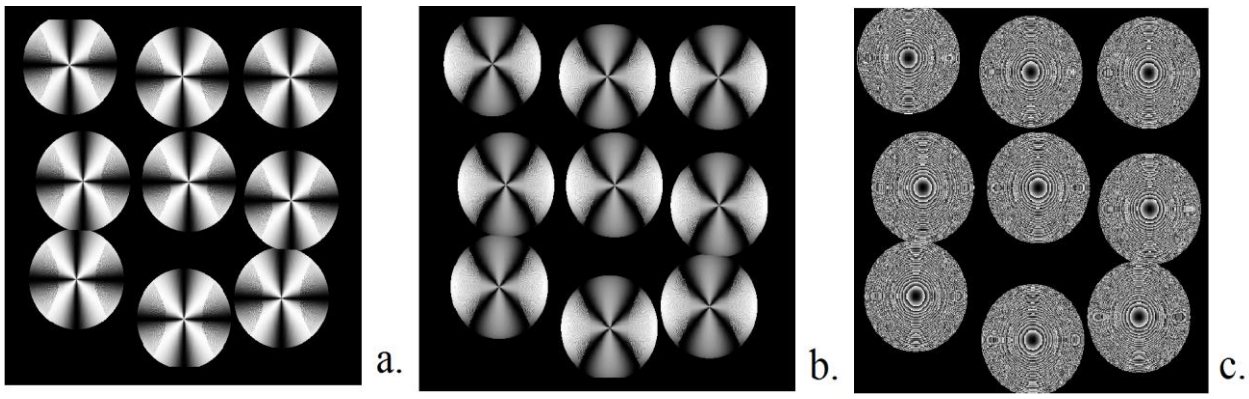

Fig.4.4 Example of the APD after the transformation on the glass beads RRS - parallel amplitude (a), perpendicular amplitude (b) and phase (c)

4.4. Finding the APD in the reception zone (far zone)

In the case of incoherent radiation, only intensity and aperture [11, 14, 15, 17, 21] are of interest. In this case, it is enough to account for the interaction with the environment, as in the modeling step above.

When the radiation is coherent and the RRS plays the role of a diffraction grating, it is necessary to take into account diffraction phenomena. In this case, it is possible to see the structure of the picture or individual speckles to use this information for detection. Then it is necessary to use the scalar theory of diffraction. We will present the general principle of finding speckle pattern in the far zone below.

After the APD is found on the surface of the reflector, one can start searching for the image formed in the far zone. APD on the plane can be considered as a collection of point sources of radiation, the coherence of which is given by the nature of the laser illuminating the surface. The expression for a monochromatic wave has the form [30]:

$$u(x, y, t) = A(x, y)\cos(2\pi\upsilon t + \varphi(x, y)) \tag{4.4}$$

or, alternatively

$$\begin{aligned} u(x, y, t) &= \mathrm{Re}\left[U(x, y)\exp(-j2\pi\upsilon t)\right] \\ U(x, y) &= A(x, y)\exp(-j\varphi(x, y)) \end{aligned} \tag{4.5}$$

The function $U(x, y)$ from (4.5) also called a phasor and describes the APD. Due to the linearity of the wave equation, as well as the coherence of radiation, the created diffraction pattern can be represented as the integral of a superposition:

$$U(x_0, y_0) = \int_{-\infty}^{\infty}\int_{-\infty}^{\infty} h(x_0, y_0; x_1, y_1)U(x_1, y_1)\,dx_1 dy_1 \tag{4.6}$$

In equation (4.6), the integrand function of transition has the form:

$$h(x_0, y_0; x_1, y_1) = \frac{1}{j\lambda} \frac{\exp(jkr_{01})}{r_{01}} \cos\left(\vec{n}, \overrightarrow{r_{01}}\right) \tag{4.7}$$

The limits of integration in (4.6) are written as infinite due to the fact that outside the source region the function $U(x_1, y_1)$ turns to zero, which satisfies the Kirchhoff boundary conditions.

If z is sufficiently large, it is possible to represent the integral of the superposition as the Fourier transform by using the Fraunhofer approximation:

$$U(x_0, y_0) = \int_{-\infty}^{\infty} \int_{-\infty}^{\infty} U(x_1, y_1) \exp\left(-j \frac{2\pi}{\lambda z}(x_0 x_1 + y_0 y_1)\right) dx_1 dy_1 \tag{4.8}$$

The resulting Fourier image is a diffraction pattern in the far zone [31]. It should be noted that in practice instead of the amplitude distribution of the received image, the squared one is being used allowing us to obtain a value proportional to the intensity. This is due to the fact that quadratic detectors are widely used, and therefore it is more convenient to evaluate the intensity. Regarding the model, it should be noted that two Fourier transforms are calculated - for parallel and perpendicular components relative to the common base, and then the listed intensities are added. This is due to the fact, that polarization plane shifts during refraction, because the parallel and perpendicular components being affected differently, so to stay within scalar diffraction theory one should consider components separately.

Of course, computer model is able to work only with a limited amount of data, therefore, in practice, only a discrete signal, that can be decomposed into finite Fourier series, can be calculated.

To calculate a two-dimensional DFT, it is enough to calculate one-dimensional complex DFTs of all rows of the image, and then calculate one-dimensional complex DFTs of all columns in the resulting image.

Direct computation of the discrete Fourier transform of the sequence $x(n)$ requires n^2 products (or additions) of complex numbers. Thus, for sufficiently large n, the direct calculation of the DFT requires an excessive number of computational operations. Thus, in practice the fast discrete Fourier transform (FDFT) algorithms are used for more efficient calculations [32].

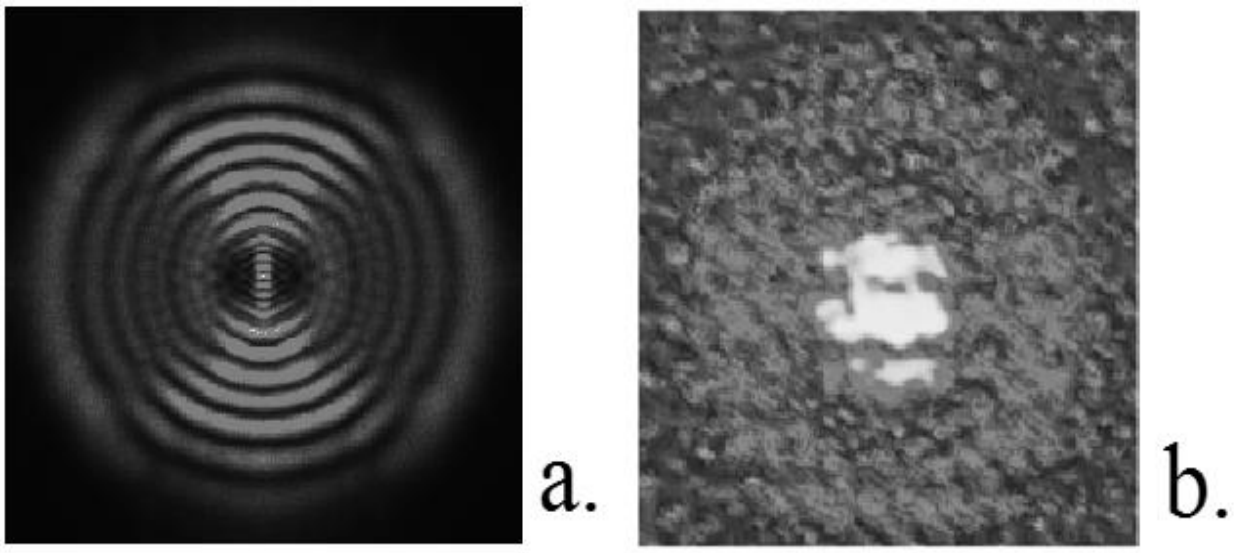

Fig.4.5 Intensity of the APD in far plane after the FDFT (a), speckle structure closeup (b)

4.5. Converting the resulting APD into a photocurrent

Regardless of the way APD is obtained in the far zone, most of the detectors end up converting observed intensity into the photocurrent for further analysis of the fluctuations. We will proceed with explanation on how this part of modeling is approached.

On the previous step we have obtained far-field APD for the perpendicular and parallel polarization components. To convert into a photocurrent, a few simple steps are enough. To begin with, let us translate the amplitude into intensity by squaring. The resulting intensities for the components can be

added. At this stage, one can simulate a different receiving aperture by imposing a bit mask on the resulting distribution - multiplying the distribution with an array of zeros and ones of the same size - this way we can cut out the central aperture, make it circular, etc. Further, it is enough to sum up all intensities for each of the polarizations - this is equivalent to the operation of integration over the area, which, in fact, is produced by the lens - the result will be the power. The obtained instantaneous energy characteristic can be represented as directly proportional to the photocurrent - the characteristic of the photodetector can be considered linear and the sensor is infinitely sensitive because this does not apply to detection and is solved in applied cases by typical methods.

Further, one can trace the dynamics of the photocurrent in time by simulating the behavior of the system at successive discrete moments in time. Thus, we receive a photocurrent. Now we need to get the spectral characteristics of this sampled signal. To do this, first we find and subtract the average - this is how we get rid of the constant component. Next, we apply the Fourier transform and obtain the spectrum of the photocurrent - it carries information about the detected acoustic vibrations, since the optical signal that formed it was modulated by a sound wave.

Below, shown on the Fig. 4.6, is an example of the use of FDFT for the analysis of the photocurrent spectrum when detected in the environment of an acoustic column with a frequency of 1100 Hz.

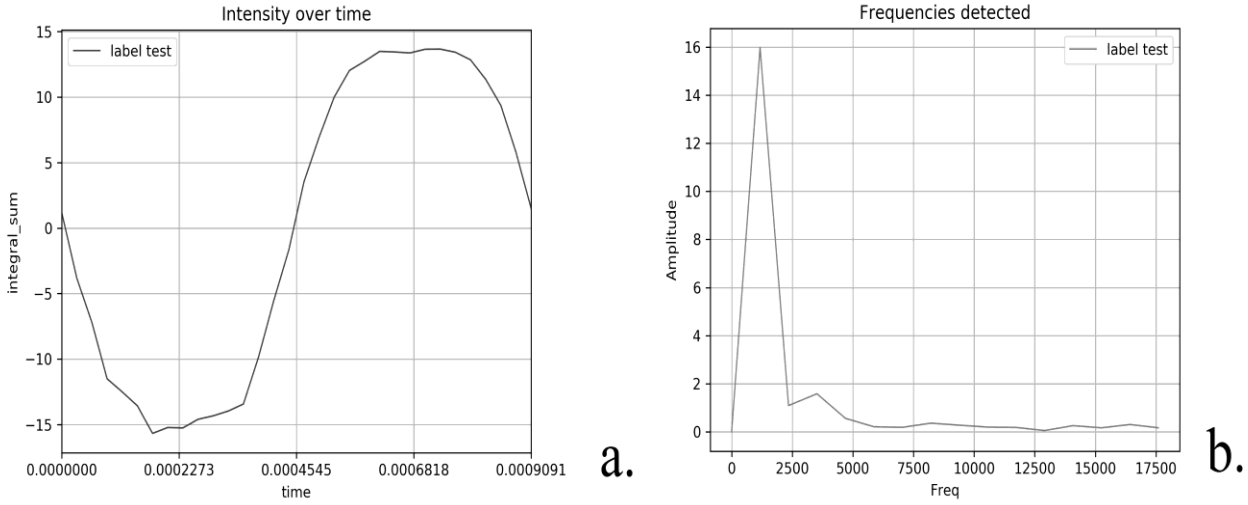

Fig.4.6 Example of the obtained via simulation photocurrent (a), and its spectral image (b)

It worth the mention, that in case you are aiming after modeling velocimetery application, then bumps on the higher frequencies will correspond to the speed of movement of the RRS-coated object, being result of the Doppler effect [18, 19].

4.6. An iterative pass with variation of parameter values of the system

Since for the components of real systems some deviations in the distributions of physical properties are present, it is necessary to conduct computer experiments for various implementations. It is simply impossible to assess whether the simulation model is correct or translate individual results into practice, because this is not a completely analytical mathematical modeling. In fact, the Monte Carlo approach [33] can be used to solve this problem. During iterative runs of experiments with different implementations of the system parts, slightly different results can be obtained. Averaging the results allows us to see which trajectory the system gravitates towards certain parameters, whether it is stable within given limits of deviations.

4.7. Finding dependencies between parameters, evaluating detection efficiency, system optimization

The imitation model ultimately allows, on the one hand, to better understand the processes in detection systems, and on the other hand, to investigate the relationships of parameters in the system without conducting a huge number of physical experiments - which are expensive to implement and

take a lot of time. Indeed, the approach to finding relationships between parameters can vary depending on the context of the system. Usually, they become clear quickly enough, since when observing the boundary conditions and constrains, they fall under the theories found in classical works on optics, being a simple combination of known laws. However, in cases where there are a lot of parameters in the system and they are interconnected in such a way that it is not possible to fix all other parameters and look at the influence of one of them on the result, it can be difficult to navigate. In this case, it is advisable to conduct a number of experiments, find correlation between parameters and use a regression model to identify the type of relations [34].

Moreover, based on the results of the experiments with the verified model, it is possible to make recommendations regarding the specific values of the system parameters for the optimal operating mode. In this case, the output parameter is selected, which must be maximized under the given input restrictions. To optimize the target function of efficiency it is necessary to use the method of mathematical programming [35]. The selection of the target metric depends entirely on the application of the model. An example of such a target metric can be, in the case of laser fire detectors, the notification efficiency, defined as the ratio of positive activations to all activations in the condition of external disturbances.

5. Conclusions

The subject of the study is the simulation models of the processes of light wave propagation (in the case of lasers - partially coherent) in the medium and its transformation on retroreflectors (microbeads- or microprism-based) with further analysis of the reflected radiation, which, being modulated by interaction with objects in the system, carries information about the state of the system. Overview of existing studies has been made. Analysis of existing approaches to simulation methods and overview of the existing models has been carried out.

As a result, common elements of models applicable in different fields and contexts of such systems have been found. Scientific methods of research have been outlined and typical research schema is proposed, suggesting the main stages in simulation modeling of RRS-based laser sensor systems. The following topics are covered: generation of the laser emission light field structure, interaction of the light field with environment, transformation of the APD inside the RRS, finding the APD in the reception zone, converting the resulting APD into a photocurrent, finding dependencies between parameters, evaluating detection efficiency, system optimization.

The analysis of strong points of different approaches has been made, the aspects important for choosing the appropriate method have been underlined. The guidance principles for the general modeling of such systems have been given, and original concrete examples of such models verified in practice is provided.

REFERENCES

1. Measures R. M. Laser Remote Sensing: Fundamentals and Applications. Malabar, FL: Krieger Publishing, 1992.
   URL: http://www.krieger-publishing.com/Titles/LthruO/STACKmno/stackmno_33.html
2. Tetsuo Fukuchi, Tatsuo Shiina. Industrial Applications of Laser Remote Sensing. Bentham Science Publishers, 2012.
   URL: https://doi.org/10.2174/97816080534071120101
3. Korpel, A. Acousto-Optics, Second Edition; Technology & Engineering, CRC Press, 1996.
   URL: https://www.academia.edu/8400584/Acousto-optics
4. Magdich, L.N. Acoustooptic Devices and Their Applications; Technology & Engineering, CRC Press, 1989.
   URL:https://books.google.com.ua/books/about/Acoustooptic_Devices_and_Their_Applicati.html?id=DPCNu9hQuA4C&redir_esc=y
5. Sirohi, R.S., Ed. Speckle Metrology; Technology & Engineering, CRC Press, 1993.
   URL: https://www.routledge.com/Speckle-Metrology/Sirohi/p/book/9780824789329
6. M. Kowalczyk, Pluta M. , Jabczynski J. K., and Szyjer M. Laser speckle velocimetry // Optical Velocimetry, Proc. SPIE 2729, 1996. Pp. 139–145. URL: https://spie.org/Publications/Proceedings/Paper/10.1117/12.233000

7. Raffel M., Willert C., Kompenhans J. Particle Image Velocimetry. A Practical Guide. Springer, 1998.
URL: https://link.springer.com/book/10.1007/978-3-662-03637-2
8. Dolya G. M., Lytvynova O. S. Modeling of fluctuations of laser radiation scattered on the reflector array in a turbulent atmosphere // Laser and Fiber-Optical Networks Modeling (LFNM), 2011. Pp. 108-111.
URL: https://doi.org/10.1109/LFNM.2011.6145015
9. Lloyd J. A brief history of retroreflective sign face sheet materials. The principles of retroreflection. REMA publications, 2008.
URL: http://www.rema.org.uk/pub/pdf/history-retroreflective-materials.pdf
10. Migletz J., Fish J. K., Grahm J. L. Roadway Delineation Practices Handbook. US Department of transportation, Federal highway administration, 1994.
URL: https://safety.fhwa.dot.gov/ped_bike/docs/rdwydelin.pdf
11. Héricz D., Sarkadi T., Erdei G., Lazuech T., Lenk S., Koppa P. Simulation of small- and wide-angle scattering properties of glass-bead retroreflectors // Applied Optics Vol. 56, Issue 14, 2017. Pp. 3969-3976.
URL: http://dx.doi.org/10.1364/AO.56.003969
12. Dolya G. M., Lytvynova O. S Modeling of speckle metrology technique of detecting the medium acoustic oscillations // Bulletin of V.N. Karazin Kharkiv National University, series "Mathematical modelling. Information technology. Automated control systems", 31(1), 2016. 38-46 p. [in Russian]
URL: https://periodicals.karazin.ua/mia/article/view/6807/6299
13. Wahlstrand J. K., Jhajj N., Rosenthal E. W., Zahedpour S., Milchberg H. M. Direct imaging of the acoustic waves generated by femtosecond filaments in air // Opt. Lett. 39, 2014. 1290-1293 c.
URL: https://doi.org/10.1364/OL.39.001290
14. Naidoo S. The development of thermoplastic road marking material stadart. University of Pretoria, 2016. 302 c.
URL: https://repository.up.ac.za/handle/2263/61319
15. Kilaru M., Yang J., Heikenfeld J. Advanced characterization of electrowetting retroreflectors // OSA, OPTICS EXPRESS, Vol. 17, No. 20, 2009. 17563-17569 c.
URL: https://doi.org/10.1364/OE.17.017563
16. Murali Krishna Kilaru. Electrowetting Switchable Retroreflectors: a dissertation for the degree of doctor of philosophy (Ph.D.), University of Cincinnati, 2009. 148 c.
URL:
https://etd.ohiolink.edu/apexprod/rws_etd/send_file/send?accession=ucin1282054545&disposition=inline
17. Anderson J., Massaro R., Lewis L., Moyers R., Wilkins J. Lidar-activated Phosphors and Infrared Retro-Reflectors: Emerging Target Materials for Calibration and Control // Photogrammetric Engineering & Remote Sensing, 2010. 875-879 c.
URL: https://www.researchgate.net/profile/Richard-Massaro/publication/228747484_Lidar-activated_Phosphors_and_Infrared_Retro-Reflectors_Emerging_Target_Materials_for_Calibration_and_Control/links/00b7d5208e69f0a972000000/Lidar-activated-Phosphors-and-Infrared-Retro-Reflectors-Emerging-Target-Materials-for-Calibration-and-Control.pdf
18. Dolya G. M., Lytvynova O. S. Modeling the Method of Laser Doppler Speckle-Velocimetry for Flat Objects with Retroreflective Surface // Asian Engineering Review Vol.4, No. 2, 2017. 7-13 c.
URL: https://doi.org/10.20448/journal.508.2017.42.7.13
19. Dolya G., Bondarenko K. Laser Doppler Velocimetry of Rotating Cylinder with Retroreflecting Surface // Asian Engineering Review, 5(1), 2018. 1-7 pp.
URL: https://doi.org/10.20448/journal.508.2018.51.1.7
20. Dolya G.N., Chudovskaya E.S., Kochin A.V. Mathematical modeling of diffraction of laser radiation on a vibrating surface with a reflective coating // Eastern European journal of advanced technologies 1/6 (37), 2009. 59-62 c. [in Russian]
URL: https://doi.org/10.15587/1729-4061.2009.3174
21. Ishikawa K., Asada K., Tamayama K., Ueda M., Optical Vibration Monitoring System by Means of CCD Camera and Retro-Reflector // The Review of Laser Engineering Vol.30, No.2, 2002 91-93.

URL: https://www.jstage.jst.go.jp/article/lsj/30/2/30_2_91/_pdf
22. Dolya G., Bondarenko K., Laser detector of acoustic oscillations utilizing a retroreflective surface with glass beads // EESA, Vol. 3, No. 11(63), 2020. 7-16 p.
URL: https://archive.eesa-journal.com/index.php/eesa/article/view/30
23. Siegman, Anthony E. Lasers. Revised ed. edition. University Science Books, 1986. 1283 p.
URL: https://uscibooks.aip.org/books/lasers/
24. Kryzhanivska T.V., Boytsova I.A. Synopsis of lectures on the discipline "Numerical methods". Odesa, 2013. – 152 c. [in Ukrainian]
URL:http://eprints.library.odeku.edu.ua/id/eprint/711/1/KryzhanivskaTV_BoitsovaIA_Chyselni_Metody_KL_2013.pdf
25. Feldman L.P. Numerical methods in computer science. - Textbook. K., 2006. – 480c.[in Ukrainian]
URL: http://library.kre.dp.ua/Books/2-4%20kurs/%D0%90%D0%BB%D0%B3%D0%BE%D1%80%D0%B8%D1%82%D0%BC%D0%B8%20%D1%96%20%D0%BC%D0%B5%D1%82%D0%BE%D0%B4%D0%B8%20%D0%BE%D0%B1%D1%87%D0%B8%D1%81%D0%BB%D0%B5%D0%BD%D1%8C/%D0%A4%D0%B5%D0%BB%D1%8C%D0%B4%D0%BC%D0%B0%D0%BD_%D0%A7%D0%B8%D1%81%D0%B5%D0%BB%D1%8C%D0%BD%D1%96_%D0%BC%D0%B5%D1%82%D0%BE%D0%B4%D0%B8_%D0%B2_%D1%96%D0%BD%D1%84%D0%BE%D1%80%D0%BC%D0%B0%D1%82%D0%B8%D1%86%D1%96_2007.pdf
26. Born M., Wolf E. Principles of optics: electromagnetic theory of propagation, interference and diffraction of light (7th expanded ed.). Cambridge: Cambridge University Press. 1999.
URL: https://www.worldcat.org/title/1151058062
27. M. Charnotskii. Comparison of four techniques for turbulent phase screens simulation. J. Opt. Soc. Am. A, 37(5):738–747, May 2020.
URL: https://doi.org/10.1364/JOSAA.385754
28. Giarola A.J., Billeter T.R., Electroacoustic deflection of a coherent light beam // Proc. IEEE 51, #8, 1150, 1963.
URL: https://doi.org/10.1109/PROC.1963.2463
29. Dolya G., Bondarenko K. Model of laser radiation transformation upon retroreflection from glass beads based surface // East European Scientific Journal, #5(45), 2019. 10-20 p.
URL: https://eesa-journal.com/wp-content/uploads/EESA_may1.pdf
30. Goodmam J.W. Introduction to Fourier Optics., New York: W. H. Freeman, 2017. 546 p.
URL: https://www.worldcat.org/title/introduction-to-fourier-optics/oclc/958780856
31. H.L. Kononchuk, V.M. Prokopets, V.V. Stukalenko Introduction to Fourier Optics: A Study Guide. - Kyiv: Publishing and printing center "Kyiv University", 2009. – 320 p.[in Ukrainian]
URL:http://exp.phys.univ.kiev.ua/ua/Study/Lib/Navch_posibnyky/NP%20-%20Fure%20optyka%20-%20Kononchuk.pdf
32. Fedorov E.E., Nechyporenko O.V., Utkina T.Yu., Korpan Ya.V. Models and methods of computer systems for visual image recognition: monograph. – Cherkasy: ChDTU, 2021. – 482 p. [in Ukrainian]
URL: https://er.chdtu.edu.ua/bitstream/ChSTU/3502/1/mono_FEE.pdf
33. Kroese, D. P.; Taimre, T.; Botev, Z.I. Handbook of Monte Carlo Methods. New York: John Wiley & Sons. 2011 p. 772.
URL: https://www.wiley.com/en-au/Handbook+of+Monte+Carlo+Methods-p-9780470177938
34. Rouaud M. Probability, Statistics and Estimation. 2013, p 191.
URL: http://www.incertitudes.fr/book.pdf
35. Bilogurova G.V., Samoilenko M.I. Mathematical programming: Synopsis of lectures. – Kharkiv: KhNAMG, 2009. – 72 p. [in Ukrainian]
URL: https://core.ac.uk/download/pdf/11322845.pdf

СПИСОК ЛІТЕРАТУРИ

1. Measures R. M. Laser Remote Sensing: Fundamentals and Applications. Malabar, FL : Krieger Publishing, 1992.
URL: http://www.krieger-publishing.com/Titles/LthruO/STACKmno/stackmno_33.html

2. Tetsuo Fukuchi, Tatsuo Shiina. Industrial Applications of Laser Remote Sensing. Bentham Science Publishers, 2012.
URL: https://doi.org/10.2174/9781608053407112010 1
3. Korpel, A. Acousto-Optics, Second Edition; Technology & Engineering, CRC Press, 1996.
URL: https://www.academia.edu/8400584/Acousto-optics
4. Magdich, L.N. Acoustooptic Devices and Their Applications; Technology & Engineering, CRC Press, 1989.
URL:https://books.google.com.ua/books/about/Acoustooptic_Devices_and_Their_Applicati.html?id=DPCNu9hQuA4C&redir_esc=y
5. Sirohi, R.S., Ed. Speckle Metrology; Technology & Engineering, CRC Press, 1993.
URL: https://www.routledge.com/Speckle-Metrology/Sirohi/p/book/9780824789329
6. M. Kowalczyk, Pluta M. , Jabczynski J. K., and Szyjer M. Laser speckle velocimetry // Optical Velocimetry, Proc. SPIE 2729, 1996. Pp. 139–145.
URL: https://spie.org/Publications/Proceedings/Paper/10.1117/12.233000
7. Raffel M., Willert C., Kompenhans J. Particle Image Velocimetry. A Practical Guide. Springer, 1998.
URL: https://link.springer.com/book/10.1007/978-3-662-03637-2
8. Dolya G. M., Lytvynova O. S. Modeling of fluctuations of laser radiation scattered on the reflector array in a turbulent atmosphere // Laser and Fiber-Optical Networks Modeling (LFNM), 2011. Pp. 108-111.
URL: https://doi.org/10.1109/LFNM.2011.6145015
9. Lloyd J. A brief history of retroreflective sign face sheet materials. The principles of retroreflection. REMA publications, 2008.
URL: http://www.rema.org.uk/pub/pdf/history-retroreflective-materials.pdf
10. Migletz J., Fish J. K., Grahm J. L. Roadway Delineation Practices Handbook. US Department of transportation, Federal highway administration, 1994.
URL: https://safety.fhwa.dot.gov/ped_bike/docs/rdwydelin.pdf
11. Héricz D., Sarkadi T., Erdei G., Lazuech T., Lenk S., Koppa P. Simulation of small- and wide-angle scattering properties of glass-bead retroreflectors // Applied Optics Vol. 56, Issue 14, 2017. Pp. 3969-3976.
URL: http://dx.doi.org/10.1364/AO.56.003969
12. Dolya G. M., Lytvynova O. S Modeling of speckle metrology technique of detecting the medium acoustic oscillations // Вісник Харківського національного університету імені В.Н. Каразіна, серія «Математичне моделювання. Інформаційні технології. Автоматизовані системи управління», 31(1), 2016. 38-46 с.
URL: https://periodicals.karazin.ua/mia/article/view/6807/6299
13. Wahlstrand J. K., Jhajj N., Rosenthal E. W., Zahedpour S., Milchberg H. M. Direct imaging of the acoustic waves generated by femtosecond filaments in air // Opt. Lett. 39, 2014. 1290-1293 с.
URL: https://doi.org/10.1364/OL.39.001290
14. Naidoo S. The development of thermoplastic road marking material stadart. University of Pretoria, 2016. 302 с.
URL: https://repository.up.ac.za/handle/2263/61319
15. Kilaru M., Yang J., Heikenfeld J. Advanced characterization of electrowetting retroreflectors // OSA, OPTICS EXPRESS, Vol. 17, No. 20, 2009. 17563-17569 с.
URL: https://doi.org/10.1364/OE.17.017563
16. Murali Krishna Kilaru. Electrowetting Switchable Retroreflectors: a dissertation for the degree of doctor of philosophy (Ph.D.), University of Cincinnati, 2009. 148 с.
URL:
https://etd.ohiolink.edu/apexprod/rws_etd/send_file/send?accession=ucin1282054545&disposition=inline
17. Anderson J., Massaro R., Lewis L., Moyers R., Wilkins J. Lidar-activated Phosphors and Infrared Retro-Reflectors: Emerging Target Materials for Calibration and Control // Photogrammetric Engineering & Remote Sensing, 2010. 875-879 с.
URL: https://www.researchgate.net/profile/Richard-Massaro/publication/228747484_Lidar-activated_Phosphors_and_Infrared_Retro-Reflectors_Emerging_Target_Materials_for_Calibration_and_Control/links/00b7d5208e69f0a9720

00000/Lidar-activated-Phosphors-and-Infrared-Retro-Reflectors-Emerging-Target-Materials-for-Calibration-and-Control.pdf
18. Dolya G. M., Lytvynova O. S. Modeling the Method of Laser Doppler Speckle-Velocimetry for Flat Objects with Retroreflective Surface // Asian Engineering Review Vol.4, No. 2, 2017. 7-13 c. URL: https://doi.org/10.20448/journal.508.2017.42.7.13
19. Dolya G., Bondarenko K. Laser Doppler Velocimetry of Rotating Cylinder with Retroreflecting Surface // Asian Engineering Review, 5(1), 2018. 1-7 pp. URL: https://doi.org/10.20448/journal.508.2018.51.1.7
20. Доля Г. Н., Чудовская Е. С., Кочин А. В. Математическое моделирование дифракции лазерного излучения на вибрирующей поверхности со световозвращающим покрытием // Восточно-Европейский журнал передовых технологий 1/6 (37), 2009. 59-62 с. URL: https://doi.org/10.15587/1729-4061.2009.3174
21. Ishikawa K., Asada K., Tamayama K., Ueda M., Optical Vibration Monitoring System by Means of CCD Camera and Retro-Reflector // The Review of Laser Engineering Vol.30, No.2, 2002 91-93. URL: https://www.jstage.jst.go.jp/article/lsj/30/2/30_2_91/_pdf
22. Dolya G., Bondarenko K., Laser detector of acoustic oscillations utilizing a retroreflective surface with glass beads // EESA, Vol. 3, No. 11(63), 2020. 7-16 p. URL: https://archive.eesa-journal.com/index.php/eesa/article/view/30
23. Siegman, Anthony E. Lasers. Revised ed. edition. University Science Books, 1986. 1283 p. URL: https://uscibooks.aip.org/books/lasers/
24. Крижанівська Т.В., Бойцова І.А. Конспект лекцій з дисципліни „Чисельні методи". Одеса, 2013. – 152 с. URL:http://eprints.library.odeku.edu.ua/id/eprint/711/1/KryzhanivskaTV_BoitsovaIA_Chyselni_Metody_KL_2013.pdf
25. Фельдман Л.П. Чисельні методи в інформатиці. – Підручник. К., 2006. – 480с. URL: http://library.kre.dp.ua/Books/2-4%20kurs/%D0%90%D0%BB%D0%B3%D0%BE%D1%80%D0%B8%D1%82%D0%BC%D0%B8%20%D1%96%20%D0%BC%D0%B5%D1%82%D0%BE%D0%B4%D0%B8%20%D0%BE%D0%B1%D1%87%D0%B8%D1%81%D0%BB%D0%B5%D0%BD%D1%8C/%D0%A4%D0%B5%D0%BB%D1%8C%D0%B4%D0%BC%D0%B0%D0%BD_%D0%A7%D0%B8%D1%81%D0%B5%D0%BB%D1%8C%D0%BD%D1%96_%D0%BC%D0%B5%D1%82%D0%BE%D0%B4%D0%B8_%D0%B2_%D1%96%D0%BD%D1%84%D0%BE%D1%80%D0%BC%D0%B0%D1%82%D0%B8%D1%86%D1%96_2007.pdf
26. Born M., Wolf E. Principles of optics: electromagnetic theory of propagation, interference and diffraction of light (7th expanded ed.). Cambridge: Cambridge University Press. 1999. URL: https://www.worldcat.org/title/1151058062
27. M. Charnotskii. Comparison of four techniques for turbulent phase screens simulation. J. Opt. Soc. Am. A, 37(5):738–747, May 2020. URL: https://doi.org/10.1364/JOSAA.385754
28. Giarola A.J., Billeter T.R., Electroacoustic deflection of a coherent light beam // Proc. IEEE 51, #8, 1150, 1963. URL: https://doi.org/10.1109/PROC.1963.2463
29. Dolya G., Bondarenko K. Model of laser radiation transformation upon retroreflection from glass beads based surface // East European Scientific Journal, #5(45), 2019. 10-20 c URL: https://eesa-journal.com/wp-content/uploads/EESA_may1.pdf
30. Goodmam J.W. Introduction to Fourier Optics., New York: W. H. Freeman, 2017. 546 p. URL: https://www.worldcat.org/title/introduction-to-fourier-optics/oclc/958780856
31. Г.Л. Конончук, В. М. Прокопець, В.В. Стукаленко. Вступ до фур'є-оптики: навчальний посібник. –К.: Видавничополіграфічний центр «Київський університет», 2009. – 320 с. URL:http://exp.phys.univ.kiev.ua/ua/Study/Lib/Navch_posibnyky/NP%20-%20Fure%20optyka%20-%20Kononchuk.pdf
32. Федоров Є. Є., Нечипоренко О. В., Уткіна Т. Ю., Корпань Я. В. Моделі та методи комп'ютерних систем розпізнавания зорових образів : монографія. – Черкаси : ЧДТУ, 2021. – 482 с. URL: https://er.chdtu.edu.ua/bitstream/ChSTU/3502/1/mono_FEE.pdf

33. Kroese, D. P.; Taimre, T.; Botev, Z.I. Handbook of Monte Carlo Methods. New York: John Wiley & Sons. 2011 p. 772.
URL: https://www.wiley.com/en-au/Handbook+of+Monte+Carlo+Methods-p-9780470177938
34. Rouaud M. Probability, Statistics and Estimation. 2013, p 191.
URL: http://www.incertitudes.fr/book.pdf
35. Білогурова Г.В., Самойленко М.І. Математичне програмування: Конспект лекцій. – Харків: ХНАМГ, 2009. – 72 с.
URL: https://core.ac.uk/download/pdf/11322845.pdf

Бондаренко Костянтин Олексійович *аспірант*
Кафедра теоретичної і прикладної систематехніки, факультет комп'ютерних наук, Харківський національний університет ім. В. Н. Каразіна, майдан Свободи 4, 61022, Харків, Україна
e-mail: konstantinb2016@gmail.com
https://orcid.org/0000-0002-2430-0716

Доля Григорій Миколайович *д.т.н., професор*
Кафедра теоретичної і прикладної систематехніки, факультет комп'ютерних наук, Харківський національний університет ім. В. Н. Каразіна, майдан Свободи 4, 61022, Харків, Україна
e-mail: gdolya@karazin.ua
https://orcid.org/0000-0001-8888-5189

Математичні моделі та підходи до імітаційного моделювання лазерних датчиків на основі СПП

Стаття присвячена дослідженню математичних моделей і підходів до моделювання лазерних датчиків, які базуються на використанні світлоповертаючих поверхонь. Предметом дослідження є математична модель об'єкта дослідження – процесів поширення світла в середовищі та його трансформації на ретрорефлекторах з подальшим аналізом відбитого випромінювання, яке, модулюючись взаємодією з об'єктами системи, несе інформацію про стан системи. Зроблено огляд існуючих досліджень. Проведено аналіз існуючих підходів до методів моделювання, та аналіз існуючих моделей. Знайдено спільні елементи моделей що можуть бути застосовані в різних прикладних областях та контекстах таких систем. Наведено такі наукові методи дослідження, як порівняльний аналіз при дослідженні подібних систем, проведення фізичних експериментів у лабораторних умовах з прототипом комп'ютеризованої системи детектування для спостереження явищ у системі, їх систематизація та опис, синтез математичної моделі на основі отриманих даних, створення імітаційної комп'ютерної моделі та проведення комп'ютерних експериментів після її верфікації. Запропоновано типову схему дослідження, яка передбачає основні етапи імітаційного моделювання систем лазерного детектування на основі СПП. Розглядаються такі теми, як: генерація структури світлового поля лазерного випромінювання, взаємодія світлового поля з навколишнім середовищем, трансформація АФР всередині СПП, знаходження АФР в зоні прийому, перетворення отриманого АФР у фотострум, знаходження залежностей між параметрами, оцінка ефективності виявлення, оптимізація системи. Проведено аналіз сильних сторін різних підходів, вказано деталі, які необхідно враховувати при виборі відповідного методу з урахуванням властивостей когерентного лазерного випромінювання. Наведено керівні принципи загального моделювання таких систем, що проілюстровані оригінальними конкретними прикладами таких моделей, перевірених на практиці.

Ключові слова: *лазер, датчик, світлоповертаюче покриття, спеклометрія, імітаційне моделювання*.

Надійшла у першій редакції 12.09.2022, в останній - 18.11.2022.
The first version has been received on 12.09.2022, the final version - on 18.11.2022.

DOI: https://doi.org/10.26565/2304-6201-2022-56-02

UDC 517.95 : 517.988

Konchakovska Oksana *postgraduate student of the Department of Applied Mathematics; Kharkiv National University of Radio Electronics, Nauky Avenue 14, Kharkiv, Ukraine, 61166*
e-mail: oksana.konchakovska@nure.ua
https://orcid.org/0000-0002-0836-6045

Sidorov Maxim *Doctor of Physical and Mathematical Sciences, Full Professor, Head of the Department of Applied Mathematics; Kharkiv National University of Radio Electronics, Nauky Avenue 14, Kharkiv, Ukraine, 61166*
e-mail: maxim.sidorov@nure.ua;
https://orcid.org/0000-0001-8022-866X

Using the two-sided approximations method for the numerical research of nanoelectromechanical systems under the action of the Casimir force

O. Konchakovska, M. Sidorov

Relevance. Developing the method of two-sided approximations for finding a positive solution to a nonlinear boundary value problem that models an electrostatic nanoelectromechanical system under external pressure has been considered. The presented mathematical model takes into account the influence of Casimir forces as an additional force of attraction between the components of nanosystems. Such systems feature the nonlinear phenomenon of pull-in instability, which occurs due to the interaction of conductive plates under a critical electric voltage. This phenomenon significantly limits the range of system's stable states and is typical of many nanodevices, in particular, accelerometers, switches, micromirrors, microresonators, etc. It is suggested to study the model parameters and estimate their values in order to analyze the stable states of nanoelectromechanical systems.

Goal. To develop a method of two-sided approximations for solving the given problem by using the methods of the nonlinear operator theory in semi-ordered Banach spaces.

Research methods. The nonlinear elliptic equation that models the operation of the electrostatic nanoelectromechanical system using the Green's function method is replaced by its Hammerstein integral equation equivalent. The specified integral equation is considered to be a nonlinear operator equation with a monotone operator in the space of continuous functions, semi-ordered by using a cone of non-negative functions. The conditions for the existence of a unique positive solution to the specified problem and the two-sided convergence of successive approximations to such a solution have been obtained.

The results. The developed method has been implemented and investigated by solving test problems. The results of computational experiment are shown in graphical and tabular form.

Conclusions. The performed computational experiments have confirmed the effectiveness of the developed method and can be used to solve the problems of mathematical modeling of nonlinear processes in micro- and nanoelectromechanical systems. The prospects for further research may lie in applying the method of two-sided approximations for models of nanoelectromechanical systems with repulsive Casimir forces.

Keywords: *method of two-sided approximations, Green's function, invariant conical segment, monotone operator, nanoelectromechanical system, external pressure, Casimir force.*

How to quote: O. Konchakovska, M. Sidorov, "Using the two-sided approximations method for the numerical research of nanoelectromechanical systems under the action of the Casimir force." *Bulletin of V.N. Karazin Kharkiv National University, series Mathematical modelling. Information technology. Automated control systems*, vol. 56, pp. 21-34, 2022. https://doi.org/10.26565/2304-6201-2022-56-02

Як цитувати: Кончаковська О.С., Сидоров М.В. Використання методу двобічних наближень для чисельного дослідження наноелектромеханічних систем під дією сили Казимира". *Вісник Харківського національного університету імені В. Н. Каразіна, серія. Математичне моделювання. Інформаційні технології. Автоматизовані системи управління*. 2022. вип. 56. С. 21-34. https://doi.org/10.26565/2304-6201-2022-56-02

1. Introduction

The development of microelectromechanical systems (MEMS) has been driven by combining the principles of mechanics and electrostatics [1, 2]. Mathematical and numerical modeling of MEMS has been a key principle, initially focusing on stationary states [3-5] and later expanding to models including external pressure and non-stationary states governed by parabolic laws [4, 6].

Such systems in mathematical modeling are usually presented in partial differential equations with appropriate initial and boundary conditions. The most common method of solving such non-stationary problems is to reduce them (according to Rothe's method) to a system of ordinary differential equations in the time variable and then to solve the resulting equations numerically or analytically. Some discretization approaches are also used: the finite element method, the boundary element method, and the finite difference method [7]. For the numerical analysis of the corresponding stationary problems, it is convenient to use numerical methods with a two-sided nature of convergence. This approach allows a posteriori estimation of the error of the approximate solution at each step of the iterative process [8].

Therefore, developing and improving existing approaches to mathematical modeling and numerical analysis of the problems arising while studying electromechanical systems is a relevant field of research.

2. NEMS and the impact of Casimir's forces

When the scale of these systems decreases to the nanoscale, it is necessary to consider nanoelectromechanical systems (NEMS). Most typical models of electrostatic NEMS consist of two conductive plates: an elastic plate fixed along the boundary at the top and a fixed, rigid plate at the bottom. The applied electric voltage between the two plates leads to the deflection of the elastic plate and the following change in the system's capacitance [9]. The operation scheme of the simplest NEMS is shown in Figure 2.1.

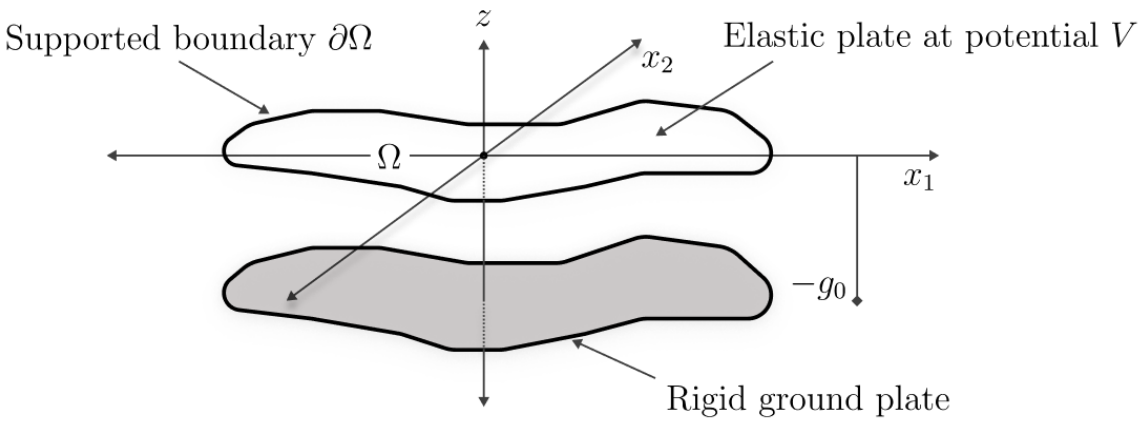

Fig. 2.1 Scheme of the electrostatic NEMS operation

The so-called pull-in instability is a distinguishing feature that limits the effectiveness of electrostatic NEMS. This effect occurs when the applied voltage exceeds a specific critical value. As a result, the plates snap together, limiting the range of stable operation of the devices. Many researchers have investigated pull-in instability [9-12]. Moreover, the miniaturization of devices requires considering the Casimir force along with the Coulomb force in a mathematical model.

An essential effect of quantum electrodynamics, namely, the effect of quantum fluctuations on non-quantum objects, was theoretically demonstrated by Hendrik Casimir in 1948 [13]. He considered the interaction of two conducting parallel plates in a vacuum and determined the force of gravity between them

$$F = -\frac{\pi^2 \eta c}{240 g_0^4},$$

where g_0 is the distance between the plates, η is a Planck constant, c is the speed of light in a vacuum.

The presence of Planck's constant indicates the purely quantum nature of the phenomenon.

The Casimir force for NEMS models is related to the interaction of plates. It is well-known that each wave presses the plate, and the closer the plates are, the fewer waves can exist between them, and the weaker their pressure is. At the same time, there is no limitation for the external space, so there can be much more waves outside. This creates a relatively sizeable converging force from the outside, which is illustrated in Figure 2.2. It turns out that the smaller the distance between the plates, the more they are attracted. This effect restricts the stability of micro- and nanoscale systems, as the parts of the mechanisms tend to snap together.

Consequently, to develop reliable, high-performance devices, it is necessary to determine stable modes of operation to prevent the occurrence of pull-in instability.

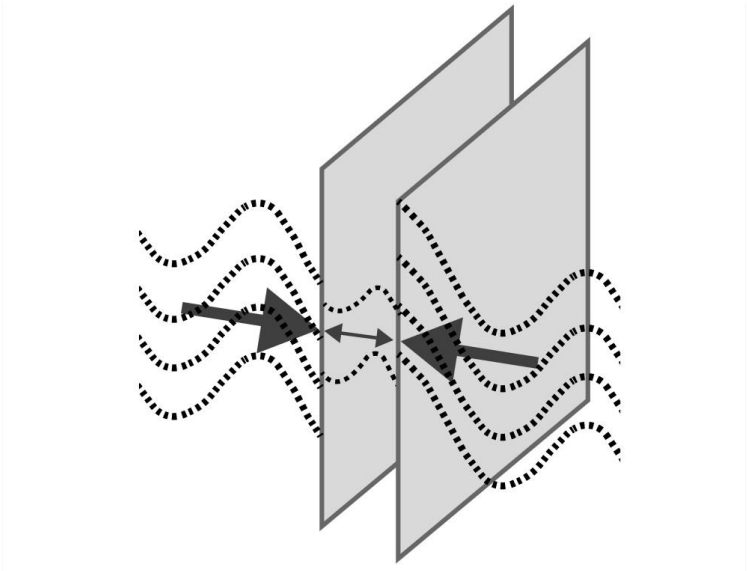

Fig. 2.2 Casimir forces acting on conductive plates

3. The research method

Let us consider a nonlinear boundary value problem modeling an electrostatic NEMS under the influence of external pressure [14, 15]:

$$-\Delta u = \frac{\lambda f(\mathbf{x})}{(1-u)^2} + \frac{\mu g(\mathbf{x})}{(1-u)^4} + P(\mathbf{x}),\ \mathbf{x} \in \Omega, \tag{3.1}$$

$$u(\mathbf{x}) > 0,\ \mathbf{x} \in \Omega, \tag{3.2}$$

$$u(\mathbf{x}) = 0,\ \mathbf{x} \in \partial\Omega, \tag{3.3}$$

where Ω is a plane domain with a piecewise smooth border $\partial\Omega$, $\mathbf{x} = (x_1, x_2)$, $P(\mathbf{x})$ is the external pressure, $P(\mathbf{x}) \geq 0$, the functions $f(\mathbf{x})$ and $g(\mathbf{x})$ describe the dielectric properties of the plate, the parameters λ and μ are the Coulomb and Casimir forces, respectively

$$\lambda = \frac{\varepsilon_0 V^2 L^2}{2\sigma_0 h g_0^3}, \quad \mu = \frac{\eta c \pi^2 L^2}{240\sigma_0 h g_0^5},$$

σ_0 is the tension in the plate, g_0 is the distance between the plates, h is the thickness of the deformed plate, ε_0 is the vacuum dielectric constant, L is the length of the plate, V is the applied voltage, η is a Planck constant, c is the speed of light in a vacuum.

From the physical content of the problem, it follows that the functions $f(\mathbf{x})$, $g(\mathbf{x})$ and $P(\mathbf{x})$ are continuous and non-negative at $\mathbf{x} \in \bar{\Omega}$.

The problem (3.1) – (3.3) is equivalent to the Hammerstein integral equation

$$u(\mathbf{x}) = \int_\Omega G(\mathbf{x},\mathbf{s}) \left[\frac{\lambda f(\mathbf{s})}{(1-u(\mathbf{s}))^2} + \frac{\mu g(\mathbf{s})}{(1-u(\mathbf{s}))^4} + P(\mathbf{s}) \right] d\mathbf{s}, \tag{3.4}$$

where $G(\mathbf{x},\mathbf{s})$ is the Green's function of this problem, $\mathbf{s} = (s_1, s_2)$.

Let $C(\bar{\Omega})$ be the Banach space of functions continuous in the domain $\bar{\Omega} = \Omega \cup \partial\Omega$, with the norm $\|u\| = \max\limits_{\mathbf{x}\in\bar{\Omega}} |u(\mathbf{x})|$. Let us consider a normal (and even an acute) cone of non-negative functions $K_+ = \{u \in C(\bar{\Omega}) : u(\mathbf{x}) \geq 0,\ \mathbf{x} \in \bar{\Omega}\}$ in space $C(\bar{\Omega})$. And let us define semi-ordering in the $C(\bar{\Omega})$ with a cone K_+ by the rule: for $u, v \in C(\bar{\Omega})$ $u \,,\!, v$, if $v - u \in K_+$. It means that [16]

$$u \,,\!, v, \text{ if } u(\mathbf{x}) \leq v(\mathbf{x}) \text{ for all } \mathbf{x} \in \bar{\Omega}.$$

The nonlinear integral equation (3.4) semi-ordered by a cone K_+ will be considered in $C(\bar{\Omega})$ as an operator equation $u = T(u)$, where operator T acts in the $C(\bar{\Omega})$ according to the rule

$$T(u)(\mathbf{x}) = \int\limits_{\Omega} G(\mathbf{x},\mathbf{s}) \left[\frac{\lambda f(\mathbf{s})}{(1-u(\mathbf{s}))^2} + \frac{\mu g(\mathbf{s})}{(1-u(\mathbf{s}))^4} + P(\mathbf{s}) \right] d\mathbf{s}. \tag{3.5}$$

It should be noted that if a classical solution of the problem (3.1) – (3.3) exists as a function $u^* \in C^2(\Omega) \cap C(\bar{\Omega})$ that satisfies equation (3.1) and conditions (3.2), (3.3), this function will also satisfy the integral equation (3.4). If the problem (3.1) – (3.3) does not have a classical solution, then the equation (3.4) will be taken as the definition of the generalized solution of the problem (3.1) – (3.3).

Definition. The generalized solution of the boundary value problem (3.1) – (3.3) will be the function $u^* \in K_+$, which is the solution of the integral equation (3.4).

The properties of the operator T (3.5) has been stated in the following lemma.

Lemma. The operator T (3.5) is:

a) a positive operator;

b) is a u_0 -positive operator, where the function $u_0(\mathbf{x})$ is defined by the equality

$$u_0(\mathbf{x}) = \int\limits_{\Omega} G(\mathbf{x},\mathbf{s}) d\mathbf{s}; \tag{3.6}$$

c) is an isotonic operator;

d) has an invariant conical segment $< 0, \beta >$, and the constant β, $0 < \beta < 1$, is a solution of the inequality

$$\lambda M_f (1-\beta)^2 + \mu M_g \leq (\beta - M_P)(1-\beta)^4, \tag{3.7}$$

where

$$M_f = \max_{\mathbf{x}\in\bar{\Omega}} \int\limits_{\Omega} G(\mathbf{x},\mathbf{s}) f(\mathbf{s}) d\mathbf{s}, \quad M_g = \max_{\mathbf{x}\in\bar{\Omega}} \int\limits_{\Omega} G(\mathbf{x},\mathbf{s}) g(\mathbf{s}) d\mathbf{s}, \quad M_P = \max_{\mathbf{x}\in\bar{\Omega}} \int\limits_{\Omega} G(\mathbf{x},\mathbf{s}) P(\mathbf{s}) d\mathbf{s};$$

e) is a Lipschitz-continuous operator on $< 0, \beta >$, i.e., for all $v, w \in < 0, \beta >$ the following inequality

$$\|T(v) - T(w)\| \leq \gamma \|v - w\|, \tag{3.8}$$

where $\gamma = \dfrac{2\lambda M_f}{(1-\beta)^3} + \dfrac{4\mu M_g}{(1-\beta)^5}$ is true.

Proof. a) The Green's function $G(\mathbf{x},\mathbf{s})$ of the first boundary value problem for the operator $-\Delta$ in the domain is continuous for $\mathbf{x}, \mathbf{s} \in \bar{\Omega}$, $\mathbf{x} \neq \mathbf{s}$ and

$$0 \leq G(\mathbf{x},\mathbf{s}) \leq k_0 \left| \ln \frac{1}{r_{\mathbf{xs}}} \right|,$$

where $r_{\mathbf{xs}} = |\mathbf{x} - \mathbf{s}| = \sqrt{(x_1 - s_1)^2 + (x_2 - s_2)^2}$ is the distance between the points $\mathbf{x}$ and $\mathbf{s}$ [17].

Taking into account the non-negativity and continuity of the functions $u(\mathbf{x})$, $f(\mathbf{x})$, $g(\mathbf{x})$ and $P(\mathbf{x})$ at $\mathbf{x} \in \bar{\Omega}$, the integral expression in (3.5) will also be non-negative and continuous at $\mathbf{x}, \mathbf{s} \in \bar{\Omega}$, $\mathbf{x} \neq \mathbf{s}$, and, therefore, the function $T(u)(\mathbf{x})$ is non-negative and continuous at $\mathbf{x} \in \bar{\Omega}$. This means that the operator T (3.5) acts in the space $C(\bar{\Omega})$ and leaves the cone K_+ invariant, i.e., converts the function from K_+ to the function from K_+. Therefore, T is a positive operator.

b) It is obvious that the function $u_0(\mathbf{x})$ of the form (3.6) belongs to $K_+ \setminus \{\theta\}$. If Ω_0 is a subdomain of the domain Ω, and $\mu(\Omega_0) > 0$, then there will be a such number $\gamma = \gamma(\Omega_0) > 0$ that the inequality

holds [17]

$$\gamma \int_{\Omega} G(\mathbf{x},\mathbf{s})d\mathbf{s} \le \int_{\Omega_0} G(\mathbf{x},\mathbf{s})d\mathbf{s}\,.$$

On the other hand, if $u \in \mathrm{K}_+ \setminus \{\theta\}$, then for some $\alpha_0 > 0$ there is a set $\Omega_0 \subset \Omega$ that $\mu(\Omega_0) > 0$ and $\frac{\lambda f(\mathbf{x})}{(1-u(\mathbf{x}))^2} + \frac{\mu g(\mathbf{x})}{(1-u(\mathbf{x}))^4} + P(\mathbf{x}) \ge \alpha_0$ for all $\mathbf{x} \in \Omega_0$. Then for all $\mathbf{x} \in \bar{\Omega}$

$$T(u)(\mathbf{x}) = \int_{\Omega} G(\mathbf{x},\mathbf{s})\left[\frac{\lambda f(\mathbf{s})}{(1-u(\mathbf{s}))^2} + \frac{\mu g(\mathbf{s})}{(1-u(\mathbf{s}))^4} + P(\mathbf{s})\right]d\mathbf{s} \ge$$

$$\ge \int_{\Omega_0} G(\mathbf{x},\mathbf{s})\left[\frac{\lambda f(\mathbf{s})}{(1-u(\mathbf{s}))^2} + \frac{\mu g(\mathbf{s})}{(1-u(\mathbf{s}))^4} + P(\mathbf{s})\right]d\mathbf{s} \ge \alpha_0 \int_{\Omega_0} G(\mathbf{x},\mathbf{s})d\mathbf{s} \ge \alpha_0\gamma \int_{\Omega} G(\mathbf{x},\mathbf{s})d\mathbf{s} = \alpha_0\gamma u_0(\mathbf{x})\,.$$

is true.

Next, for all $\mathbf{x} \in \bar{\Omega}$

$$T(u)(\mathbf{x}) = \int_{\Omega} G(\mathbf{x},\mathbf{s})\left[\frac{\lambda f(\mathbf{s})}{(1-u(\mathbf{s}))^2} + \frac{\mu g(\mathbf{s})}{(1-u(\mathbf{s}))^4} + P(\mathbf{s})\right]d\mathbf{s} \le$$

$$\le \max_{\mathbf{x}\in\bar{\Omega}}\left[\frac{\lambda f(\mathbf{x})}{(1-u(\mathbf{x}))^2} + \frac{\mu g(\mathbf{x})}{(1-u(\mathbf{x}))^4} + P(\mathbf{x})\right] \cdot \int_{\Omega} G(\mathbf{x},\mathbf{s})d\mathbf{s} = \max_{\mathbf{x}\in\bar{\Omega}}\left[\frac{\lambda f(\mathbf{x})}{(1-u(\mathbf{x}))^2} + \frac{\mu g(\mathbf{x})}{(1-u(\mathbf{x}))^4} + P(\mathbf{x})\right] \cdot u_0(\mathbf{x})\,.$$

Therefore, for all $\mathbf{x} \in \bar{\Omega}$ there will be a double inequality

$$\alpha u_0(\mathbf{x}) \le \int_{\Omega} G(\mathbf{x},\mathbf{s})\left[\frac{\lambda f(\mathbf{s})}{(1-u(\mathbf{s}))^2} + \frac{\mu g(\mathbf{s})}{(1-u(\mathbf{s}))^4} + P(\mathbf{s})\right]d\mathbf{s} \le \beta u_0(\mathbf{x})\,,$$

where $\alpha = \alpha_0\gamma > 0$, $\beta = \max_{\mathbf{x}\in\bar{\Omega}}\left[\frac{\lambda f(\mathbf{x})}{(1-u(\mathbf{x}))^2} + \frac{\mu g(\mathbf{x})}{(1-u(\mathbf{x}))^4} + P(\mathbf{x})\right] > 0$, which means that the operator T is the u_0 -positive.

c) Let $v, w \in \mathrm{K}_+$ and $v \,,\!,\, w$, that is $v(\mathbf{x}) \le w(\mathbf{x})$ for all $\mathbf{x} \in \bar{\Omega}$. Then for all $\mathbf{x} \in \bar{\Omega}$

$$\frac{\lambda f(\mathbf{x})}{(1-v(\mathbf{x}))^2} + \frac{\mu g(\mathbf{x})}{(1-v(\mathbf{x}))^4} + P(\mathbf{x}) \le \frac{\lambda f(\mathbf{x})}{(1-w(\mathbf{x}))^2} + \frac{\mu g(\mathbf{x})}{(1-w(\mathbf{x}))^4} + P(\mathbf{x})\,,$$

and hence, in view of the non-negativity of the Green's function $G(\mathbf{x},\mathbf{s})$,

$$T(v)(\mathbf{x}) = \int_{\Omega} G(\mathbf{x},\mathbf{s})\left[\frac{\lambda f(\mathbf{s})}{(1-v(\mathbf{s}))^2} + \frac{\mu g(\mathbf{s})}{(1-v(\mathbf{s}))^4} + P(\mathbf{s})\right]d\mathbf{s} \le$$

$$\le \int_{\Omega} G(\mathbf{x},\mathbf{s})\left[\frac{\lambda f(\mathbf{s})}{(1-w(\mathbf{s}))^2} + \frac{\mu g(\mathbf{s})}{(1-w(\mathbf{s}))^4} + P(\mathbf{s})\right]d\mathbf{s} = T(w)(\mathbf{x})\,.$$

Therefore, it follows from $v, w \in \mathrm{K}_+$ and $v \,,\!,\, w$ that $T(v) \le T(w)$. Therefore, the operator T (3.5) is isotonic.

d) The invariant conical segment $< v_0, w_0 >$ is defined by the inequalities $T(v_0) \ldots v_0$ and $T(w_0) \,,\!,\, w_0$. Let us take $v_0 = 0$ and $w_0 = \beta$. Then the specified inequalities will take form

$$\int_{\Omega} G(\mathbf{x},\mathbf{s})[\lambda f(\mathbf{s}) + \mu g(\mathbf{s}) + P(\mathbf{s})]d\mathbf{s} \ge 0 \text{ for all } \mathbf{x} \in \Omega\,, \tag{3.9}$$

$$\int_{\Omega} G(\mathbf{x},\mathbf{s})\left[\frac{\lambda f(\mathbf{s})}{(1-\beta)^2} + \frac{\mu g(\mathbf{s})}{(1-\beta)^4} + P(\mathbf{s})\right]d\mathbf{s} \le \beta \text{ for all } \mathbf{x} \in \Omega\,. \tag{3.10}$$

The inequality (3.9) will always hold, since the Green's function $G(\mathbf{x},\mathbf{s})$ at $\mathbf{x}, \mathbf{s} \in \bar{\Omega}$, $\mathbf{x} \ne \mathbf{s}$, and functions $f(\mathbf{x})$, $g(\mathbf{x})$ and $P(\mathbf{x})$ at $\mathbf{x} \in \bar{\Omega}$ are non-negative, and parameters λ and μ are positive. The inequality (3.10) can be written as

$$\frac{\lambda}{(1-\beta)^2}\int_\Omega G(\mathbf{x},\mathbf{s})f(\mathbf{s})d\mathbf{s}+\frac{\mu}{(1-\beta)^4}\int_\Omega G(\mathbf{x},\mathbf{s})g(\mathbf{s})d\mathbf{s}+\int_\Omega G(\mathbf{x},\mathbf{s})P(\mathbf{s})d\mathbf{s}\le\beta \text{ for all } \mathbf{x}\in\Omega.$$

Taking the maximum in the last inequality leads to

$$\frac{\lambda M_f}{(1-\beta)^2}+\frac{\mu M_g}{(1-\beta)^4}+M_P\le\beta, \tag{3.11}$$

where $M_f=\max\limits_{\mathbf{x}\in\bar\Omega}\int_\Omega G(\mathbf{x},\mathbf{s})f(\mathbf{s})d\mathbf{s}$, $M_g=\max\limits_{\mathbf{x}\in\bar\Omega}\int_\Omega G(\mathbf{x},\mathbf{s})g(\mathbf{s})d\mathbf{s}$, $M_P=\max\limits_{\mathbf{x}\in\bar\Omega}\int_\Omega G(\mathbf{x},\mathbf{s})P(\mathbf{s})d\mathbf{s}$.

It follows from physical considerations that $0<\beta<1$. Then after multiplying by $(1-\beta)^4$ the inequality (3.11) takes the form (3.7).

e) Let us denote

$$F(\mathbf{x},u(\mathbf{x}))=\frac{\lambda f(\mathbf{x})}{(1-u(\mathbf{x}))^2}+\frac{\mu g(\mathbf{x})}{(1-u(\mathbf{x}))^4}+P(\mathbf{x}).$$

Let us choose $v,w\in<0,\beta>$ and consider the expression

$$\left|F(\mathbf{x},v(\mathbf{x}))-F(\mathbf{x},w(\mathbf{x}))\right|=$$

$$=\left|\left(\frac{\lambda f(\mathbf{x})}{(1-v(\mathbf{x}))^2}+\frac{\mu g(\mathbf{x})}{(1-v(\mathbf{x}))^4}+P(\mathbf{x})\right)-\left(\frac{\lambda f(\mathbf{x})}{(1-w(\mathbf{x}))^2}+\frac{\mu g(\mathbf{x})}{(1-w(\mathbf{x}))^4}+P(\mathbf{x})\right)\right|=$$

$$=\left|\lambda f(\mathbf{x})\left(\frac{1}{(1-v(\mathbf{x}))^2}-\frac{1}{(1-w(\mathbf{x}))^2}\right)+\mu g(\mathbf{x})\left(\frac{1}{(1-v(\mathbf{x}))^4}-\frac{1}{(1-w(\mathbf{x}))^4}\right)\right|.$$

The triangle inequality leads to

$$\left|F(\mathbf{x},v(\mathbf{x}))-F(\mathbf{x},w(\mathbf{x}))\right|\le\lambda f(\mathbf{x})\left|\frac{1}{(1-v(\mathbf{x}))^2}-\frac{1}{(1-w(\mathbf{x}))^2}\right|+\mu g(\mathbf{x})\left|\frac{1}{(1-v(\mathbf{x}))^4}-\frac{1}{(1-w(\mathbf{x}))^4}\right|.$$

Since at $0<v,\ w<\beta$

$$\left|\frac{1}{(1-v)^2}-\frac{1}{(1-w)^2}\right|\le\frac{2}{(1-\beta)^3}|v-w|,\quad \left|\frac{1}{(1-v)^4}-\frac{1}{(1-w)^4}\right|\le\frac{4}{(1-\beta)^5}|v-w|,$$

then the inequality holds

$$\left|F(\mathbf{x},v(\mathbf{x}))-F(\mathbf{x},w(\mathbf{x}))\right|\le\left[\frac{2\lambda f(\mathbf{x})}{(1-\beta)^3}+\frac{4\mu g(\mathbf{x})}{(1-\beta)^5}\right]\left|v(\mathbf{x})-w(\mathbf{x})\right|.$$

Therefore

$$\left\|T(v)-T(w)\right\|=\max_{\mathbf{x}\in\bar\Omega}\left|T(v)(\mathbf{x})-T(w)(\mathbf{x})\right|=\max_{\mathbf{x}\in\bar\Omega}\left|\int_\Omega G(\mathbf{x},\mathbf{s})[F(\mathbf{s},v(\mathbf{s}))-F(\mathbf{s},w(\mathbf{s}))]d\mathbf{s}\right|\le$$

$$\le\left[\frac{2\lambda}{(1-\beta)^3}\max_{\mathbf{x}\in\bar\Omega}\int_\Omega G(\mathbf{x},\mathbf{s})f(\mathbf{s})d\mathbf{s}+\frac{4\mu}{(1-\beta)^5}\max_{\mathbf{x}\in\bar\Omega}\int_\Omega G(\mathbf{x},\mathbf{s})g(\mathbf{s})d\mathbf{s}\right]\cdot\max_{\mathbf{x}\in\bar\Omega}\left|v(\mathbf{x})-w(\mathbf{x})\right|=$$

$$=\left[\frac{2\lambda M_f}{(1-\beta)^3}+\frac{4\mu M_g}{(1-\beta)^5}\right]\cdot\left\|v-w\right\|=\gamma\left\|v-w\right\|.$$

The lemma has been proven.

Obviously, the operator T (3.5) is continuous and completely continuous.

Let us proceed to constructing the method of two-sided approximations for finding the positive solution of the integral equation (3.4) (and, therefore, the boundary value problem (3.1) – (3.3)).

Since the ends of the invariant conical segment $<0,\beta>$ will be chosen as the initial approximation, let us investigate the inequality (3.7) under the condition $0<\beta<1$ and denote $\varphi(\beta)=\lambda M_f(1-\beta)^2+\mu M_g$, $\psi(\beta)=(\beta-M_P)(1-\beta)^4$. Then the inequality (3.7) takes the form

$\varphi(\beta) \le \psi(\beta)$. It is obvious that $\varphi(\beta) > \mu M_g > 0$ if $0 < \beta < 1$. On the other hand $\psi(0) = -M_P \le 0$, $\psi(1) = \psi(M_P) = 0$ and if $M_P \ge 1$, then $\psi(\beta) < 0$ for $0 < \beta < 1$ and the inequality (3.7) will not hold. Therefore, the condition $0 \le M_P < 1$ must be fulfilled and $\psi(\beta) > 0$, if $M_P < \beta < 1$. In addition, the inequality (3.7) cannot be satisfied if $\sup\limits_{0<\beta<1} \psi(\beta) \le \inf\limits_{0<\beta<1} \varphi(\beta)$.

Accordingly, $\sup\limits_{0<\beta<1} \psi(\beta) = \psi\left(\dfrac{4M_P+1}{5}\right) = \dfrac{2^8(1-M_P)^5}{5^5}$, $\inf\limits_{0<\beta<1} \varphi(\beta) = \mu M_g$. If the inequality (3.7) has a solution, then the following inequality should be satisfied

$$\mu M_g < \frac{2^8(1-M_P)^5}{5^5}. \tag{3.12}$$

It is obvious that the inequality (3.7) has the solution $\underline{\beta} \le \beta \le \overline{\beta}$ when

$$\sup_{0<\beta<1} \psi(\beta) = \psi\left(\frac{4M_P+1}{5}\right) = \frac{2^8(1-M_P)^5}{5^5} > \varphi\left(\frac{4M_P+1}{5}\right) = \frac{2^4}{5^2}\lambda M_f (1-M_P)^2 + \mu M_g,$$

namely

$$2^4 5^3 \lambda M_f (1-M_P)^2 + 5^5 \mu M_g < 2^8 (1-M_P)^5. \tag{3.13}$$

It is clear that the inequality (3.12) is a consequence of the inequality (3.13).

It should be noted that the inequality (3.7) will hold only at one point $\beta = \beta_0$ if

$$2^4 5^3 \lambda M_f (1-M_P)^2 + 5^5 \mu M_g = 2^8 (1-M_P)^5.$$

Therefore, the set of solutions of the inequality (3.7) for β forms the segment $[\underline{\beta}, \overline{\beta}]$, only under the conditions:

$$0 \le M_P < 1,\ 2^4 5^3 \lambda M_f (1-M_P)^2 + 5^5 \mu M_g < 2^8 (1-M_P)^5.$$

Consequently,

$$\lambda < \frac{2^8(1-M_P)^5 - 5^5 \mu M_g}{2^4 5^3 M_f (1-M_P)^2},$$

and the positivity of the parameter λ leads to

$$\mu < \frac{2^8(1-M_P)^5}{5^5 M_g},$$

or

$$\mu < \frac{2^8(1-M_P)^5 - 2^4 5^3 \lambda M_f (1-M_P)^2}{5^5 M_g} \text{ and } \lambda < \frac{2^8(1-M_P)^5}{2^4 5^3 M_f (1-M_P)^2}. \tag{3.14}$$

At the same time $M_P < \underline{\beta} < \overline{\beta} < 1$.

Let us form an iterative process according to the scheme

$$v^{(k+1)}(\mathbf{x}) = \int_\Omega G(\mathbf{x},\mathbf{s}) \left[\frac{\lambda f(\mathbf{s})}{(1-v^{(k)}(\mathbf{s}))^2} + \frac{\mu g(\mathbf{s})}{(1-v^{(k)}(\mathbf{s}))^4} + P(\mathbf{s}) \right] d\mathbf{s},\ k = 0, 1, 2, \ldots; \tag{3.15}$$

$$w^{(k+1)}(\mathbf{x}) = \int_\Omega G(\mathbf{x},\mathbf{s}) \left[\frac{\lambda f(\mathbf{s})}{(1-w^{(k)}(\mathbf{s}))^2} + \frac{\mu g(\mathbf{s})}{(1-w^{(k)}(\mathbf{s}))^4} + P(\mathbf{s}) \right] d\mathbf{s},\ k = 0, 1, 2, \ldots; \tag{3.16}$$

$$v^{(0)}(\mathbf{x}) = 0,\ w^{(0)}(\mathbf{x}) = \beta. \tag{3.17}$$

The sequence $\{v^{(k)}(\mathbf{x})\}$ is non-decreasing under the cone K_+ and the sequence $\{w^{(k)}(\mathbf{x})\}$ is non-increasing under the cone K_+, since the conical segment $< 0, \beta >$ is invariant for the isotonic operator T (3.5). The existence of boundaries $v^*(\mathbf{x})$ and $w^*(\mathbf{x})$ of these sequences follows from the normality

of the cone K_+ and the complete continuity of the operator T. Therefore, the chain of inequalities holds

$$0 = v^{(0)} \,,\, v^{(1)} \,,\, ...,\, v^{(k)} \,,\, ...,\, v^* \,,\, w^* \,,\, ...,\, w^{(k)} \,,\, ...,\, w^{(1)} \,,\, w^{(0)} = \beta .$$

There are two possible cases: $v^* < w^*$ and $v^* = w^*$. In the second case $u^* := v^* = w^*$ is unique fixed point of the operator T on the conical segment $< 0, \beta >$, and therefore u^* is unique positive solution of the considered boundary value problem (3.1) – (3.3).

To obtain the conditions for the case $v^* = w^*$, let us estimate the norm $\left\| w^{(k+1)} - v^{(k+1)} \right\|$. Taking the inequality (3.8) into account leads to

$$\left\| w^{(k+1)} - v^{(k+1)} \right\| = \left\| T(w^{(k)}) - T(v^{(k)}) \right\| \le \gamma \left\| w^{(k)} - v^{(k)} \right\| = \gamma \left\| T(w^{(k-1)}) - T(v^{(k-1)}) \right\| \le$$

$$\le \gamma^2 \left\| w^{(k-1)} - v^{(k-1)} \right\| \le ... \le \gamma^{k+1} \left\| w^{(0)} - v^{(0)} \right\| = \gamma^{k+1} \beta .$$

It follows that $\lim\limits_{k \to \infty} \left\| w^{(k+1)} - v^{(k+1)} \right\| = 0$, i.e. $v^* = w^*$, if $\gamma < 1$.

So, the following theorem is true.

Theorem 3.1. Let $< 0, \beta >$ be an invariant conical segment for the operator T (3.5) and $\gamma < 1$. Then the iterative process (3.15) – (3.17) converges from two sides in the space $C(\bar{\Omega})$ norm to the continuous positive solution u^* of the boundary value problem (3.1) – (3.3), which is unique for the segment.

For the approximate solution of the boundary value problem (3.1) – (3.3) at the k -th iteration let us choose the function

$$u^{(k)}(\mathbf{x}) = \frac{v^{(k)}(\mathbf{x}) + w^{(k)}(\mathbf{x})}{2},$$

considering the mentioned above, the error of this approximation will be estimated by the inequality

$$\left\| u^* - u^{(k)} \right\| \le \frac{1}{2} \left\| w^{(k)} - v^{(k)} \right\| \le \frac{1}{2} \gamma^k \beta . \qquad (3.18)$$

Therefore, if the accuracy $\varepsilon > 0$ is specified, the iterative process (3.15) – (3.17) should be carried out until the inequality

$$\left\| w^{(k)} - v^{(k)} \right\| = \max_{\mathbf{x} \in \bar{\Omega}} (w^{(k)}(\mathbf{x}) - v^{(k)}(\mathbf{x})) < 2\varepsilon$$

or inequalities $\gamma^k \beta < 2\varepsilon$ are satisfied, so with the accuracy ε it can be stated that $u^*(x) \approx u^{(k)}(x)$.

The number of iterations required to achieve the specified accuracy ε can be estimated from a priori estimation (3.18) and the inequality $\frac{1}{2} \gamma^k \beta < \varepsilon$, i.e.

$$k_0(\varepsilon) = \left[\frac{\ln \frac{\beta}{2\varepsilon}}{\ln \frac{1}{\gamma}} \right] + 1,$$

where the square brackets denote the whole part of the number.

Thus, it is necessary to choose $\beta = \underline{\beta}$ for the fastest convergence of the iterative process.

4. Numerical experiments

Let us consider the problem (3.1) – (3.3) in the domain $\Omega = \{\mathbf{x} = (x_1, x_2) \mid x_1^2 + x_2^2 < 1\} \subset \mathbf{R}^2$. Green's function in this case has the form

$$G(\mathbf{x}, \mathbf{s}) = \frac{1}{2\pi} \ln \frac{1}{r_{\mathbf{xs}}} - \frac{1}{2\pi} \ln \frac{1}{\rho r_{\mathbf{xs}^1}},$$

where $\mathbf{x} = (x_1, x_2)$, $\mathbf{s} = (s_1, s_2)$, $\rho = \sqrt{s_1^2 + s_2^2}$, points $\mathbf{s}$, $\mathbf{s}^1$ are symmetrical about the unit circle, $r_{\mathbf{xs}}$,

$r_{\mathbf{xs}^1}$ is the distance between the points $\mathbf{x}$, $\mathbf{s}$ and $\mathbf{x}$, $\mathbf{s}^1$ respectively.

The researchers [4] suggest using functions of the plate's dielectric properties for the circle domain in the form

$$f(\mathbf{x}) = e^{\zeta(|\mathbf{x}|^2-1)} = e^{\zeta(x_1^2+x_2^2-1)}, \quad g(\mathbf{x}) = e^{\zeta(|\mathbf{x}|^2-1)} = e^{\zeta(x_1^2+x_2^2-1)},$$

where ζ is a non-negative constant.

To simulate the influence of external pressure, let us select a function

$$P(\mathbf{x}) = \kappa(1-|\mathbf{x}|^2)(e^{-\chi|\mathbf{x}-\mathbf{a}|^2} + e^{-\varpi|\mathbf{x}-\mathbf{b}|^2}),\ \kappa, \chi, \varpi > 0,\ \mathbf{a} = (0.75; 0.75),\ \mathbf{b} = (-0.15; -0.15)$$

($\kappa = 0$ is the case of no external pressure).

Let $\zeta = 3$, $\kappa = 0.5$, $\chi = 3$, $\varpi = 5$. Then $M_f = 0.0343$, $M_g = 0.0343$, $M_P = 0.0510$. The graph of the surface of the functions $f(\mathbf{x})$ and $g(\mathbf{x})$ is presented in Figure 4.1, and the graph of the function $P(\mathbf{x})$ surface is presented in Figure 4.2.

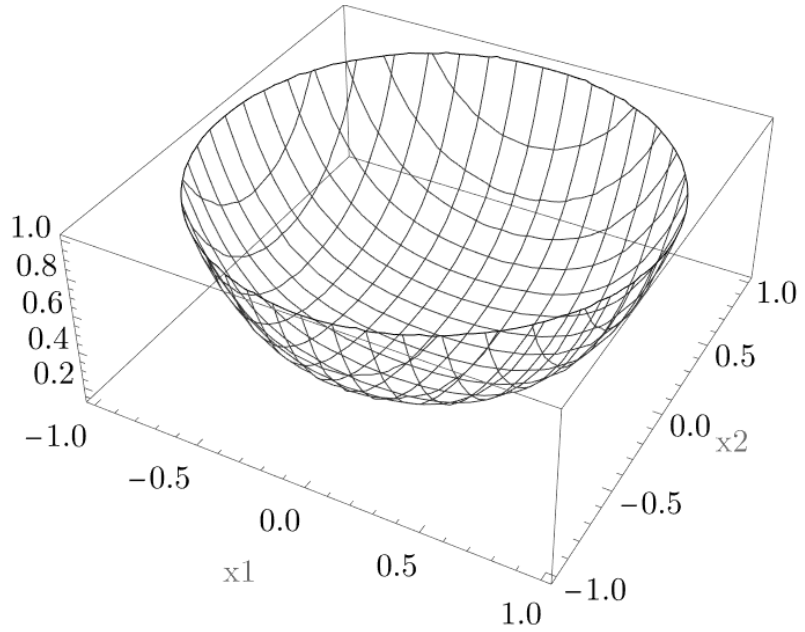

Fig. 4.1 The surface of the functions $f(\mathbf{x})$ and $g(\mathbf{x})$

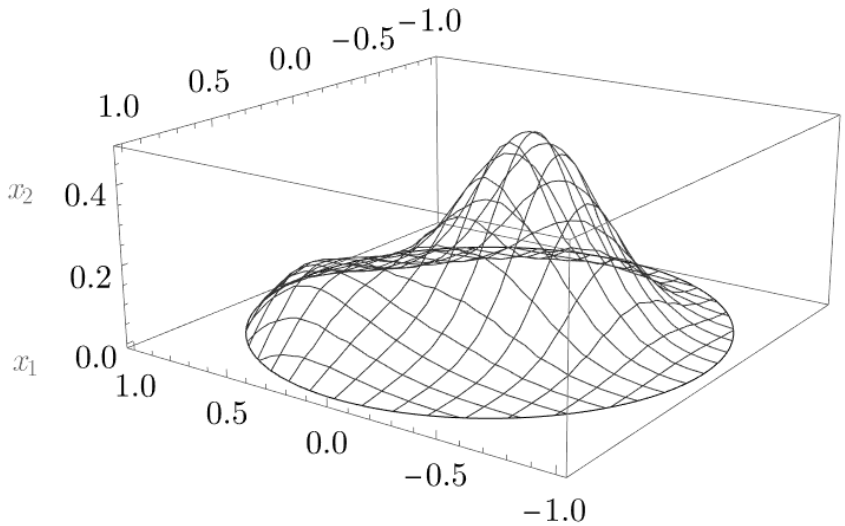

Fig. 4.2 The surface of the function $P(\mathbf{x})$

The condition (3.14) leads to a set of solutions for the parameters λ and μ, which is shown in Figure 4.3. According to (3.14): $\lambda < 3.1929$. Let $\lambda = 2$, so $\mu < 0.6875$. Let us choose $\mu = 0.5$. Then according to (3.7): $0.1998 \le \beta \le 0.4363$. Thus, the conical segment has the form $<0, \beta> =< 0, \underline{\beta} > =< 0, 0.1998 >$. In this case $\gamma = 0.4764$. Since $\gamma < 1$, according to Theorem 3.1, the successive approximations formed by the scheme (3.15) – (3.17) converge from two sides to the positive solution of the problem, which is unique on the cone $<0, \beta>$.

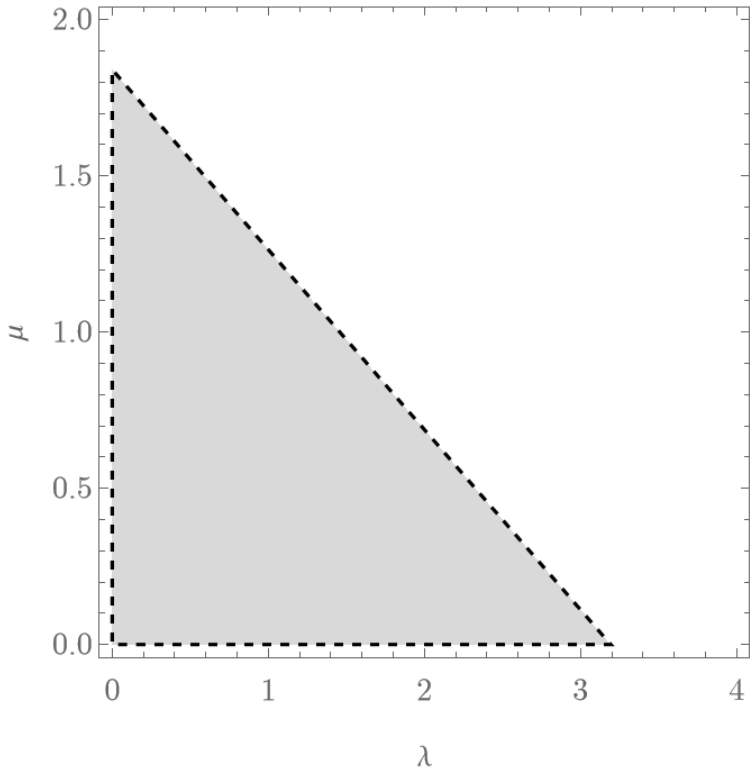

Fig. 4.3 The set of solutions for the parameters λ and μ

Let the accuracy be $\varepsilon = 10^{-4}$. Since the condition is fulfilled on the fifth iteration

$$\max_{\mathbf{x}\in\bar{\Omega}} (w^{(5)}(\mathbf{x}) - v^{(5)}(\mathbf{x})) = 0.285 \cdot 10^{-3},$$

and with the accuracy $0.57 \cdot 10^{-4}$, $u^*(\mathbf{x}) \approx u^{(5)}(\mathbf{x}) = \dfrac{w^{(5)}(\mathbf{x}) + v^{(5)}(\mathbf{x})}{2}$ can be chosen.

In this case $\left\| u^{(5)} \right\| = 0.1621$. The two-sided nature of the convergence of successive approximations is illustrated in Figure 4.4, where the graphs of the upper (solid line) and lower (dashed line) approximations to the solution at $x_2 = 0$ are shown. The contour lines and the surface of the approximate solution $u^{(5)}(\mathbf{x})$ are shown in Figures 4.5 and 4.6, respectively.

A computational experiment has been performed for different values of λ. Table 1 presents the value of the approximate solution norm of the problem (3.1) – (3.3) depending on the parameters λ and μ.

Table 1. The value of the approximate solution norm depending on the problem parameters

ζ	$\lambda_{\max}(\zeta)$	λ	$\mu_{\max}(\lambda)$	μ	$\|u\|$
3	3.1929	0	1.8403	1.80	0.1389
		1	1.2639	1.20	0.1545
		2	0.6875	0.50	0.1621
		3	0.1112	0.10	0.1896

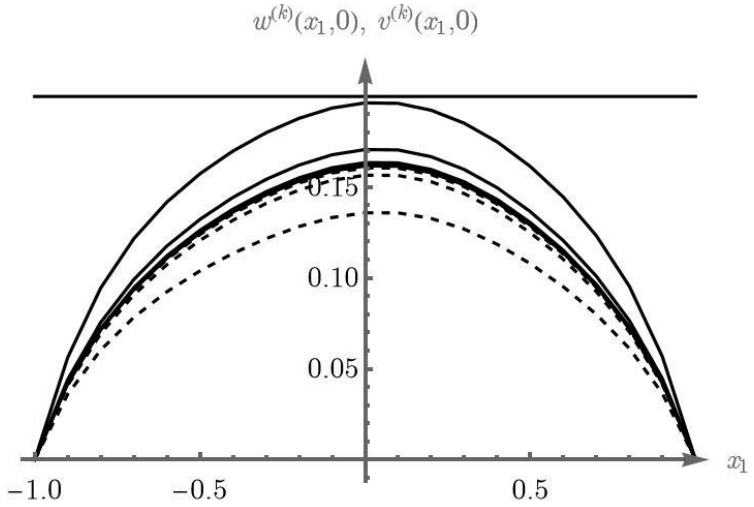

Fig. 4.4 Cross-sections of upper and lower approximations to the solution at $x_2 = 0$

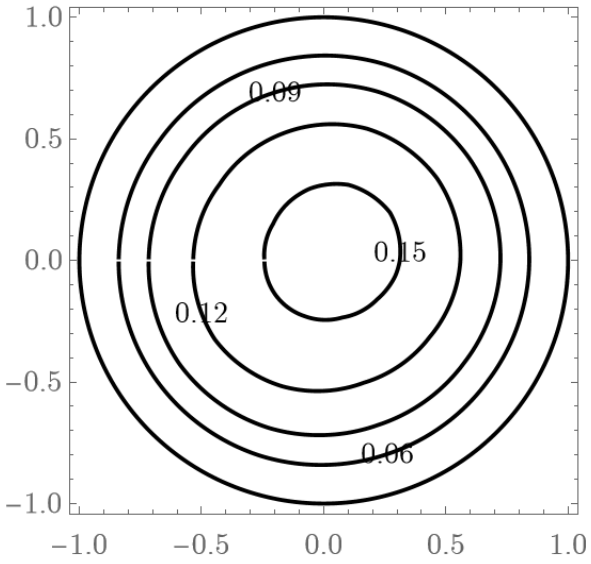

Fig. 4.5 The contour lines of the approximate solution

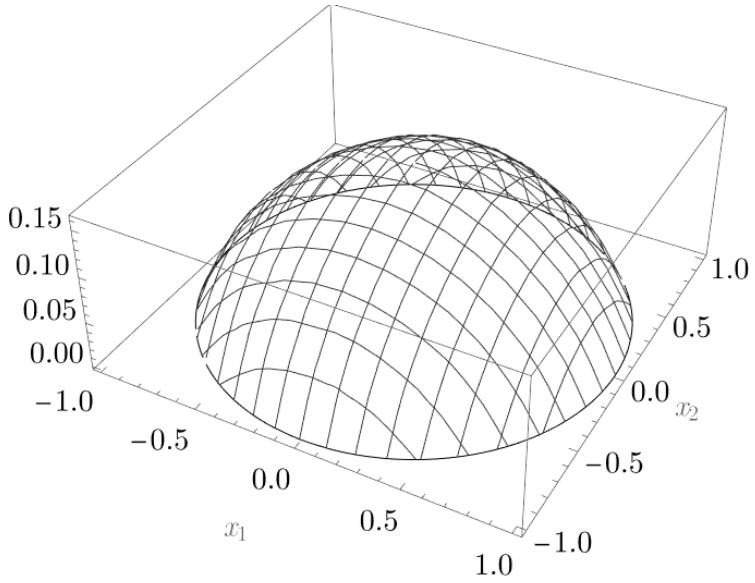

Fig. 4.6 The surface of the approximate solution

The analysis of the results of computational experiment shows that for a fixed value ζ, the parameter value $\mu_{\max}(\lambda)$ decreases with the increase of λ, and the norm $\|u\|$ increases. Those results define stable modes of operation for electrostatic NEMS. It should be noted that the choice of an unevenly and asymmetrically distributed external pressure leads to a violation of the radial symmetry of the solution.

5. Conclusions

The paper considers a generalized mathematical model of electrostatic nanoelectromechanical systems, which takes into account the Coulomb and Casimir forces and the external pressure. The method of two-sided approximations based on the usage of Green's function has been applied for the first time to the analysis of the proposed mathematical model, therefore, making it possible to obtain both the conditions for the existence of a unique positive solution of the problem and the two-sided convergence of successive approximations to it. The computational experiment conducted for the test values of the parameters has shown that this novel method is effective and can be used to study the parameters and modes of operation of real NEMS.

The research into Casimir's repulsive forces is a promising area of study due to the potential application in developing ultra-low friction and eliminating pull-in instability. The experiments have shown that repulsion occurs in one specific configuration; a plate and a sphere, instead of two flat plates, have been used in the model, as it is difficult to arrange the plates in parallel at such a small distance.

REFERENCES

1. B. McLellan, L. Medina, C. Xu, Y. Yang "Critical pull-in curves of MEMS actuators in presence of Casimir force" *ZAMM Journal of Applied Mathematics and Mechanics/Zeitschrift für Angewandte Mathematik und Mechanik*, vol. 96, no. 12, pp. 1406-1422, 2016.
2. J. A. Pelesko, D. H. Bernstein *Modeling MEMS and NEMS*, Cleveland: CRC Press, 2002. 351 p.
3. J. Davila, I. Flores, I. Guerra "Multiplicity of solutions for a fourth order equation with power-type nonlinearity" *Mathematische Annalen*, vol. 348, no. 1, pp. 143-193, 2010.
4. P. Esposito, N. Ghoussoub and Y. Guo *Mathematical analysis of partial differential equations modeling electrostatic MEMS*, Providence: American Mathematical Society, 2010. 262 p.
5. Z. Guo, J. Wei "On a fourth order nonlinear elliptic equation with negative exponent" *SIAM journal on mathematical analysis*, vol. 40, no. 5, pp. 2034-2054, 2008.
6. D. Ye, F. Zhou "On a general family of nonautonomous elliptic and parabolic equations" *Calculus of Variations and Partial Differential Equations*, vol. 37, pp. 259-274, 2010.
7. A. H. Nayfeh, M. I. Younis, E. M. Abdel-Rahman "Reduced-order models for MEMS applications" *Nonlinear dynamics*, vol. 41, no. 1, pp. 211-236, 2005.
8. M. V. Sidorov "Green-Rvachev's quasi-function method for constructing two-sided approximations to positive solution of nonlinear boundary value problems", *Carpathian Mathematical Publications*, vol. 10, no. 2, pp. 360-375, 2018.
9. R. C. Batra, M. Porfiri, D. Spinello "Effects of Casimir force on pull-in instability in micro-membranes" *Europhysics Letters*, vol. 77, no. 2, pp. 20010, 2007.
10. J. A. Pelesko "Mathematical modeling of electrostatic MEMS with tailored dielectric properties", *SIAM Journal on Applied Mathematics*, vol. 62, no. 3, pp. 888-908, 2002.
11. Y. Guo, Z. Pan and M. J. Ward "Touchdown and pull-in voltage behavior of a MEMS device with varying dielectric properties", *SIAM Journal on Applied Mathematics*, vol. 66, no. 1, pp. 309-338, 2005.
12. F. Lin and Y. Yang "Nonlinear non-local elliptic equation modeling electrostatic actuation", *Proceedings of the Royal Society of London A: Mathematical, Physical and Engineering Sciences*, vol. 463, no. 2081, pp. 1323-1337, 2007.
13. Gusejnov K. *Foton: uchebnoe posobie / pod redakciej professora B.S. Ishhanova*. M.: "KDU", "Universitetskaja kniga", 2020. 276 p. [in Russian].
14. J. R. Beckham, J. A. Pelesko "An electrostatic-elastic membrane system with an external pressure", *Mathematical and computer modelling*, vol. 54, no. 11-12, pp. 2686-2708, 2011.
15. Y. Guo, Y. Zhang and F. Zhou "Singular behavior of an electrostatic–elastic membrane system with

an external pressure", *Nonlinear Analysis*, vol. 190, pp. 111611, 2020.
16. V. I. Opojtsev, T. A. Khurodze *Nonlinear Operators in Spaces with a Cone*, Tbilisi, USSR: Izdatel'stvo Tbilisskogo Universiteta, 1984. 246 p. [in Russian].
17. M. A. Krasnosel'skij *Positive Solutions of Operator Equations*. M: Fizmatgiz, 1962. 394 p. [in Russian].

СПИСОК ЛІТЕРАТУРИ

1. McLellan B., Medina L., Xu C., Yang Y. Critical pull-in curves of MEMS actuators in presence of Casimir force. *ZAMM Journal of Applied Mathematics and Mechanics/Zeitschrift für Angewandte Mathematik und Mechanik*. 2016. Vol. 96, № 12. P. 1406-1422.
2. Pelesko J. A., Bernstein D. H. Modeling MEMS and NEMS. Cleveland: CRC Press, 2002. 351 p.
3. Davila J., Flores I., Guerra I. Multiplicity of solutions for a fourth order equation with power-type nonlinearity. *Mathematische Annalen*. 2010. Vol. 348, № 1. P. 143–193.
4. Esposito P., Ghoussoub N., Guo Y. Mathematical analysis of partial differential equations modeling electrostatic MEMS. Providence: American Mathematical Society, 2010. 262 p.
5. Guo Z., Wei J. On a fourth order nonlinear elliptic equation with negative exponent. *SIAM journal on mathematical analysis*. 2008. Vol. 40, № 5. P. 2034–2054.
6. Ye D., Zhou F. On a general family of nonautonomous elliptic and parabolic equations. *Calculus of Variations and Partial Differential Equations*. 2010. Vol. 37. P. 259–274.
7. Nayfeh A. H., Younis M. I., Abdel-Rahman E. M. Reduced-order models for MEMS applications. *Nonlinear dynamics*. 2005. Vol. 41, № 1. P. 211–236.
8. Sidorov M. V. Green-Rvachev's quasi-function method for constructing two-sided approximations to positive solution of nonlinear boundary value problems. *Carpathian Mathematical Publications*. 2018. Vol. 10, № 2. P. 360–375.
9. Batra R. C., Porfiri M., Spinello D. Effects of Casimir force on pull-in instability in micro-membranes. *Europhysics Letters*. 2007. Vol. 77, № 2. P. 20010.
10. Pelesko J. A. Mathematical modeling of electrostatic MEMS with tailored dielectric properties. *SIAM Journal on Applied Mathematics*. 2002. Vol. 62, № 3. P. 888–908.
11. Guo Y., Pan Z., Ward M. J. Touchdown and pull-in voltage behavior of a MEMS device with varying dielectric properties. *SIAM Journal on Applied Mathematics*. 2005. Vol. 66, № 1. P. 309–338.
12. Lin F., Yang Y. Nonlinear non-local elliptic equation modeling electrostatic actuation. *Proceedings of the Royal Society of London A: Mathematical, Physical and Engineering Sciences*. 2007. Vol. 463, № 2081. P. 1323–1337.
13. Гусейнов К. Фотон: учебное пособие / под редакцией профессора Б.С. Ишханова. Москва: "КДУ", "Университетская книга", 2020. 276 с.
14. Beckham J. R., Pelesko J. A. An electrostatic-elastic membrane system with an external pressure. *Mathematical and computer modelling*. 2011. Vol. 54, №11–12. P. 2686–2708.
15. Guo Y., Zhang Y., Zhou F. Singular behavior of an electrostatic–elastic membrane system with an external pressure. *Nonlinear Analysis*. 2020. Vol. 190. P. 111611.
16. Опойцев В. И., Хуродзе Т. А. Нелинейные операторы в пространствах с конусом. Тбилиси: Изд-во Тбилис. ун-та, 1984. 246 с.
17. Красносельский М. А. Положительные решения операторных уравнений. Москва: Физматгиз, 1962. 394 с.

Кончаковська Оксана Сергіївна *аспірант кафедри прикладної математики Харківський національний університет радіоелектроніки, пр. Науки 14, Харків-166, Україна, 61166*
e-mail: oksana.konchakovska@nure.ua
https://orcid.org/0000-0002-0836-6045

Сидоров Максим Вікторович *доктор фіз.-мат. наук, професор; завідувач кафедри прикладної математики Харківського національного університету радіоелектроніки, пр. Науки 14, Харків-166, Україна, 61166*
e-mail: maxim.sidorov@nure.ua;
https://orcid.org/0000-0001-8022-866X

Використання методу двобічних наближень для чисельного дослідження наноелектромеханічних систем під дією сили Казимира

Актуальність. Розглянуто питання побудови методу двобічних наближень знаходження додатного розв'язку нелінійної крайової задачі, що моделює електростатичну наноелектромеханічну систему під дією зовнішнього тиску. Наведена математична модель враховує вплив сил Казимира як додаткову силу тяжіння між компонентами наносистем. Особливістю таких систем є нелінійне явище нестабільності відхиляння, яке виникає внаслідок взаємодії струмопровідних пластин під дією критичної електричної напруги. Це явище значно обмежує діапазон стійких станів системи та характерне для багатьох нанопристроїв, зокрема, акселерометрів, перемикачів, мікродзеркал та мікрорезонаторів тощо. Для дослідження стійких станів наноелектромеханічних систем запропоновано дослідити параметри моделі та отримати їх оцінки.

Мета. Користуючись методами теорії нелінійних операторів у напівупорядкованих банахових просторах розробити метод двобічних наближень розв'язання поставленої задачі.

Методи дослідження. Нелінійне еліптичне рівняння, що моделює роботу електростатичної наноелектромеханічної системи за допомогою методу функцій Гріна замінюється еквівалентним інтегральним рівнянням Гаммерштейна. Зазначене інтегральне рівняння розглядається як нелінійне операторне рівняння з монотонним оператором у просторі неперервних функцій, напівупорядкованому за допомогою конуса невід'ємних функцій. Отримано умови існування єдиного додатного розв'язку розглядуваної задачі та двобічної збіжності до нього послідовних наближень.

Результати. Розроблений метод програмно реалізовано та досліджено при розв'язанні тестових задач. Результати обчислювального експерименту наведено у вигляді графічної та табличної інформації.

Висновки. Проведені обчислювальні експерименти підтвердили ефективність розробленого метода і можуть бути використанні на практиці при розв'язання задач математичного моделювання нелінійних процесів у мікро- та наноелектромеханічних системах. Перспективи подальших досліджень можуть полягати у застосуванні методу двобічних наближень для моделей наноелектромеханічних системах з відштовхуючими силами Казимира.

Ключові слова: *метод двобічних наближень, функція Гріна, інваріантний конусний відрізок, монотонний оператор, наноелектромеханічна система, зовнішній тиск, сили Казимира.*

Надійшла у першій редакції 18.01.2022, в останній - 11.09.2022.
The first version has been received on 18.01.2022, the final version - on 11.09.2022.

DOI: https://doi.org/10.26565/2304-6201-2022-56-03

UDC 004.93

Malyha Ihor Yevheniyovych *postgraduate*
Kharkiv National University of V.N. Karazin,4 Svobody Square, Kharkiv, Ukraine, 61077
e-mail: igormalyga@gmail.com;
https://orcid.org/0000-0002-5708-7739

Shmatkov Serhiy Ihorovych *doctor of science, professor; Head of the Department of Theoretical Theoretical and Applied System Engineering*
Kharkiv National University of V.N. Karazin,4 Svobody Square, Kharkiv, Ukraine, 61077
e-mail: s.shmatkov@karazin.ua
https://orcid.org/0000-0002-6328-988X
Scopus Author ID: 57203141869

Machine learning methods for solving semantics and context problems in processing textual data

Topicality. As machine learning capabilities expand and impact many aspects of modern life, such as natural language processing, understanding semantics and context in textual data is becoming increasingly important. Semantics and context play a significant role in the ability of machines to understand human language. They are central elements in various applications such as machine translation, sentiment analysis, spam detection, voice recognition, and others. However, these aspects are often neglected or underestimated when processing textual data. Despite significant progress in this area, the problem of semantics and context remains unresolved, which reduces the efficiency and accuracy of many machine learning systems.

Goal: The main goal of this article is to investigate the problem of understanding semantics and context in machine learning in the textual data processing. The article aims to identify the main challenges associated with understanding semantics and context, and how they affect various aspects of text processing. Additionally, current techniques and approaches used in the field of machine learning for solving those problems have been analyzed and their limitations identified.

Research methods. Analysis, explanation, classification.

The results. It has been found that despite significant advances in machine learning technologies, problems of semantics and context in processing textual data are still existing. They affect the quality and accuracy of decisions made by machine learning based systems, which can lead to incorrect analysis and distortion of data. It has been found that even modern transformer-based models can face challenges in understanding semantics and context, especially in complex and multi-valued scenarios.

Conclusions. On the basis of the conducted research, it has been concluded that the problem of semantics and context in the processing of textual data is significant and requires further study. The existing methods and technologies show high results in some cases, but may be insufficient in others, especially complex ones. It is proposed to continue research in this area, to develop new methods and approaches that will be able to effectively solve these problems. It is also important to study how different contextual factors affect the semantics of textual data and how these effects can be taken into account when designing and using machine learning systems.

Keywords: *Machine learning, natural language processing, semantics, context, textual data, neural networks, transformers, BERT, GPT-3, data analysis, sentiment analysis, semantic analysis.*

How to quote: I. Malyha, and I. Shmatkov, "Machine learning methods for solving semantics and context problems in processing textual data." *Bulletin of V.N. Karazin Kharkiv National University, series "Mathematical modelling. Information technology. Automated control systems*, vol. 56, pp. 35-42, 2022. https://doi.org/10.26565/2304-6201-2022-56-03

Як цитувати: І. Є. Малига, С. І. Шматков. «Методи машинного навчання для вирішенні проблем семантики та контексту при обробці текстових даних». *Вісник В.Н. Каразіна Харків Національний університет, серія "Математичне моделювання. Інформаційні технології. Автоматизоване управління системи*, вип. 56. с.35-42, 2022.
https://doi.org/10.26565/2304-6201-2022-56-03

1. Introduction

Machine learning is one of the fastest growing sectors of the technology industry, where textual data processing plays an important role. Applying machine learning to textual data, including sentiment

analysis, emotion recognition, automatic translation, information retrieval, and more, opens up endless possibilities for advancing science, technology, and enterprise.

However, understanding and processing a text in machine learning faces several challenges, particularly in understanding semantics and context. Semantics, that is, understanding the meaning of a word or phrase, is one of the biggest problems in processing textual data. Intelligent systems often have difficulty in understanding that words can have different meanings in different contexts.

In addition, the problem of the context is also a big challenge for machine learning. Understanding how the meaning of a word can change depending on its context in the text is a complex task that machines are not yet able to perform effectively.

Given this, the relevance of those problems is topical. Solving them will improve the ability of machine learning to process textual data, paving the way for further progress.

2. Statement of the problem in a general form and its connection with important scientific or technical tasks. Review of topical publications.

Machine learning and artificial intelligence create many opportunities to transform large amounts of unstructured textual data into valuable information. However, applying these technologies to real world situations often leads to complex problems, especially in the context of natural language processing (NLP).

One of the main problems lies in semantic understanding. Artificial intelligence cannot yet fully comprehend the meaning of words, especially when used in different contexts. This is a natural for humans, but machines cannot yet sufficiently reproduce this ability.

The issue of context is also critical. Context can greatly affect the meaning of words or phrases, and it is difficult for machines to take this into account. For example, they may not understand cultural or historical context, which can lead to misinterpretation of textual data.

These issues limit the potential effectiveness and accuracy of machine learning algorithms that process textual data. Solving those problems will open new opportunities for the application of machine learning in various fields, including text analysis, automatic translation, text generation, and many others.

In the field of machine learning and natural language processing, the importance of semantics and context has been emphasized in a number of important studies.

First of all, a significant contribution to the study of semantics in machine learning is the work of Tomas Mikulov and his colleagues. They developed the word2vec model, which became one of the main methods of representing words in a vector space. The word2vec model uses large volumes of text for training aimed at learning high-dimensional vector representations of words that can represent semantic relations between them. However, this method still has limitations because it does not take into account the different meaning of a word in different contexts. This model uses neural network architectures to learn high-dimensional vector word representations from a large dataset. An important point is that Word2Vec can learn the semantic relations between words by displaying them in a vector space [1].

In addition, Bahdanau, Cho, and Bengio have made significant contributions to our understanding of how machines can better learn to recognize context. They proposed an attention model that allows focusing attention on specific parts of the input while generating the output. This provides more flexibility in context understanding and can help in various tasks including machine translation and automatic generalization [2].

In recent years, the BERT (Bidirectional Encoder Representations from Transformers) model, developed by Devlin and colleagues, has attracted special attention. BERT uses bidirectional transformers, which allows the model to better understand the context of a word because it analyzes the text in both directions. This made it possible to significantly improve the results in some NLP tasks, but at the same time new challenges arose, such as the large quantity of resources required for training the model and the weak ability to interpret [3].

We should also note the work of Vaswani et al., who developed the Transformer architecture for machine translation. This architecture, based on self-attention mechanisms, favored several previous approaches to semantics and context, including recurrent neural networks (RNNs) and convolutional neural networks (CNNs). However, Transformer also has its limitations, especially regarding the processing of long texts and taking into account the global context [4].

3. Highlighting previously unresolved parts of the general problem, to which the article is devoted, with justification of the relevance of the solution. Research of other authors on the topic.

The main theoretical approaches to understanding semantics and context in textual data processing are based on word embedding models and neural networks.

However, despite the success of the Word2Vec model, it struggled to cope with polysemy - cases where one word has several meanings depending on the context. This has led to the development of context-aware models, such as the GloVe (Global Vectors for Word Representation) model, which additionally uses statistical information from the word correlation matrix [5].

A more recent advance has been the development of models that can better understand the contextual information of a word. One such model is BERT (Bidirectional Encoder Representations from Transformers), proposed by Devlin. BERT uses bidirectional transformers, which allows the model to better understand the context of a word by analyzing the text in both directions.

These and other studies have made valuable contributions to understanding the challenges of semantics and context in machine learning. However, those problems are still open and require further research.

3. Statement of the task.

The purpose of the article is to analyze the problem of semantics and context when processing textual data in machine learning. The article highlights how relevant this problem is, how it affects the quality of machine learning systems, and what possible consequences may arise from underestimating this issue.

It is necessary to identify the main problem situations where semantics and context are crucial, and to analyze how effectively modern machine learning techniques and algorithms can cope with these cases.

The latest theories and practices in this area need to be reviewed to determine whether they can offer meaningful progress to the solution of this problem.

The final purpose of this paper is to formulate recommendations for further research in this area and ways that can improve the use of machine learning for semantic and context-aware processing of textual data.

To achieve this goal, it is necessary to solve the following tasks.

- To reveal the relevance and importance of the problem of semantics and context. To show how deep this problem is, it is necessary to identify the key problematic points that researchers and practitioners face when processing textual data in machine learning.
- Identify and analyze the main problem situations. It is intended to consider typical situations where the consideration of semantics and context is particularly important, and to analyze how effectively modern machine learning techniques and algorithms can cope with these cases.
- Overview of modern methods and techniques of textual data processing. This requires analyzing how existing techniques and technologies handle semantics and context to identify their potential weaknesses and opportunities for improvement.
- Identify possible directions for further research. Based on the analysis, it is planned to identify the key areas, in which the further research needs to be conducted, and formulate the practical recommendations.

4. Presentation of the main material with a full justification of the obtained scientific results.

Increasingly, machine learning-based systems depend on the efficient understanding and processing of textual data. However, there are significant challenges related to semantics and context that still require further research and development.

Polysemy, the problem of distinguishing different meanings of the same word in different contexts, is one of the most obvious challenges in this area. Standard natural language processing (NLP) models such as Word2Vec or GloVe, which are based on vector representations of words, do not take this problem into account. They create one vector for each word, regardless of the context in which it is used. Therefore, words with multiple meanings can be problematic [6].

Another problem that arises when processing textual data is the identification and processing of sarcasm and irony. This is difficult because sarcasm often requires a deep understanding of the context and situation in which it is used. A study conducted on the Twitter sources revealed that most machine learning models cannot effectively cope with this task [7].

Please note that the meaning of words may change depending on the context in which they are used. In particular, context can be related to culture, social conditions, era or even individual characteristics of

the person using the language. This creates problems for machine learning models trying to learn the general rules of language, because these models may not take such variations in context into account.

That becomes particularly important when dealing with such phenomena as slang or dialects, where the use and meaning of words may differ significantly from those adopted in the standard language. For example, the study of Curtis and colleagues has shown that machine learning displays difficulties when trying to understand and generate texts written in African American Variants of English (AAVE) [8].

In addition, there are problems with processing implicit content such as metaphors, allegories, and other figurative expressions. These expressions usually require a deep understanding of the context and cultural background to be correctly interpreted, which is beyond the capabilities of most modern machine learning systems.

The issue of processing texts that contain descriptive, emotional or subjective information is especially difficult. These types of information often require a deep understanding of context and personal experience, which is difficult to model in machine learning systems.

To solve these problems, a number of problems and technologies have been developed recently, namely.

- Using contextual vector representations of words. To solve the problem of polysemy, so-called contextual vector word representations are used in machine learning and NLP research. One such model is BERT (Bidirectional Encoder Representations from Transformers), which was introduced in 2018 by Google. It uses an attention mechanism that allows the model to look at the context from both sides of a word to determine its meaning.
- Using fine-tuning of models. Researchers have also begun to use a technique known as "fine-tuning" to adapt general machine learning models to specific tasks or domains. This may involve pre-training a model on a large dataset and then fine-tuning it on a smaller, more specialized dataset. This approach shows promising results in solving the problem of language variability in different contexts [9-10].
- Use of ensembles and multimodal models. Researchers also use ensemble techniques and multimodal models to combine different types of information and solve complex language processing problems. For example, a combination of text, audio and visual information can be used to better understand the context in a dialogue [11-13].
- Using deep learning to understand implicit content. Recent research shows that deep learning can help in understanding implicit content in texts, such as identifying sarcasm or irony. This can be achieved using complex neural network architectures, which include recurrent neural networks (RNNs), long-term memory networks (LSTMs), and the attention mechanism [14-16].
- Using transformative models for speech generation: Transformers such as OpenAI's GPT (Generative Pretrained Transformer) use the attention mechanism and other state-of-the-art techniques for high-quality text generation. These models can generate much more naturalistic text sequences compared to older models, but they also have their own challenges in terms of context processing and semantics [17-18].
- Semantic multi-task learning: Some researchers are working on using multi-task learning to solve multiple language processing problems simultaneously. This means that the model tries to perform several tasks at the same time, using a common semantic space. For example, the model can simultaneously try to classify emotions in the text, determine sentiment and recognize named entities [19].
- Generalized machine learning models: Some researchers are also working on generalized models that can adapt to a wide range of language processing tasks without the need for fine-tuning. These models use universal architectures and algorithms that can effectively handle a variety of language tasks and domains [20].

However, it should be noted that all these methods have their own limitations and challenges. For example, contextual models of dictionary representations often require enormous computing resources and data to train. Nevertheless, these approaches open up new possibilities for improving the processing of textual data in machine learning.

Research findings show that to improve understanding semantics and context, practical research can be conducted in the following direction.

- Selection of dataset. Selecting a corpus of text that includes a wide range of contexts and semantic interactions that machine learning models often encounter in the real world. This data set should

include a variety of language styles, from academic texts to everyday spoken language, allowing us to evaluate how the models perform on a variety of tasks.

- Data pre-processing. Before training the models, several important data preprocessing steps must be performed. This includes removing noise (such as non-standard characters or URLs), using tokenization to break text into individual words, and using stemming or lemmatization to reduce words to their base form.
- Model training. To train the models, it is proposed to use several types of machine learning models to understand the semantics and context in our textual data. This includes lexical representation models such as Word2Vec and GloVe, contextual lexical representation models such as BERT and GPT-3, and transformative models for language generation.
- Assessment of models. Evaluation of the models will include the use of a set of metrics commonly used to evaluate the quality of machine learning in processing textual data. These can be, for example, accuracy, completeness (recall), precision, F1-score, or metrics considered in the context of tasks, such as BLEU for translation tasks or ROUGE for text generation tasks. Additionally, semantic-specific metrics such as the distance between word vectors in the representation space can be considered.
- Statistical analysis. After evaluating the models, it is necessary to conduct a statistical analysis of the results, using tests to compare the results of the models and determine the statistical significance of the difference between them. Tests such as Student's t-test, ANOVA, or non-parametric tests can be used for this, depending on the nature of our data.
- Processing of results. Finally, one can start processing and analyzing the results, interpreting them in the context of the study. It is necessary to compare the results with existing research and theories, and to determine what implications these results have for the field of machine learning and textual data processing.

5. Conclusions

In this article, the problems of semantics and context in textual data when using machine learning have been considered and analyzed. The article identified the main challenges associated with understanding semantics and context, and how they affect various aspects of text processing. In addition, the current techniques and approaches used in the field of machine learning to solve these problems and their limitations have been considered.

The analytical nature of this article allows us to better understand the current problems that arise when processing textual data in machine learning. The issues of semantics and context in processing textual data in machine learning are becoming increasingly relevant at the intersection of disciplines such as computer science and linguistics. This article analyzed those problems, examining them from different angles and trying to find possible ways to solve them.

From a practical point of view, the research is important for developers of machine learning systems. Challenges they may face have been identified, and directions for the further research that may help address these challenges are suggested. One such direction is the development of new machine learning methods and techniques that relies more on the semantics and context. Another direction may focus on finding effective ways to incorporate those aspects into the existing models.

REFERENCES

1. Mikolov, T., Chen, K., Corrado, G., & Dean, J. (2013). Efficient Estimation of Word Representations in Vector Space.
   Available at: https://arxiv.org/abs/1301.3781.
2. Bahdanau, D., Cho, K., & Bengio, Y. (2014). Neural Machine Translation by Jointly Learning to Align and Translate.
   Available at: https://arxiv.org/abs/1409.0473.
3. Devlin, J., Chang, M. W., Lee, K., & Toutanova, K. (2018). BERT: Pre-training of Deep Bidirectional Transformers for Language Understanding. Available at: https://www.aclweb.org/anthology/N19-1423/.

4. Vaswani, A., Shazeer, N., Parmar, N., Uszkoreit, J., Jones, L., Gomez, A. N., Kaiser, Ł., & Polosukhin, I. (2017). Attention is All you Need. Available at: https://papers.nips.cc/paper/2017/hash/3f5ee243547dee91fbd053c1c4a845aa-Abstract.html.
5. Pennington, J., Socher, R., & Manning, C. (2014). Glove: Global Vectors for Word Representation. Available at: https://www.aclweb.org/anthology/D14-1162/.
6. Mikolov, T., Sutskever, I., Chen, K., Corrado, G. S., & Dean, J. (2013). Distributed Representations of Words and Phrases and their Compositionality. Available at: https://papers.nips.cc/paper/2013/hash/9aa42b31882ec039965f3c4923ce901b-Abstract.html.
7. Davidov, D., Tsur, O., & Rappoport, A. (2010). Semi-supervised recognition of sarcastic sentences in Twitter and Amazon. Available at: https://aclanthology.org/W10-2914/.
8. Blodgett, S. L., Green, L., & O'Connor, B. (2018). Demographic Dialectal Variation in Social Media: A Case Study of African-American English. Available at: https://aclanthology.org/D16-1120/.
9. Howard, J., & Ruder, S. (2018). Universal Language Model Fine-tuning for Text Classification. Available at: https://www.aclweb.org/anthology/P18-1031/.
10. Peters, M. E., Neumann, M., Iyyer, M., Gardner, M., Clark, C., Lee, K., & Zettlemoyer, L. (2018). Deep contextualized word representations. Available at: https://www.aclweb.org/anthology/N18-1202/.
11. Huang, P. S., He, X., Gao, J., Deng, L., Acero, A., & Heck, L. (2013). Learning Deep Structured Semantic Models for Web Search using Clickthrough Data. Available at: https://posenhuang.github.io/papers/cikm2013_DSSM_fullversion.pdf.
12. Xu C., McAuley J., (2018). The Importance of Generation Order in Language Modeling. Available at: https://www.aclweb.org/anthology/D18-1324/.
13. Suzuki M., Matsuo Y., (2020). A survey of multimodal deep generative models. Available at: https://arxiv.org/abs/2207.02127.
14. Felbo, B., Mislove, A., Søgaard, A., Rahwan, I., & Lehmann, S. (2017). Using Millions of Emoji Occurrences to Learn Any-domain Representations for Detecting Sentiment, Emotion and Sarcasm. Available at: https://www.aclweb.org/anthology/D17-1169/.
15. Reyes A., Rosso P., (2016). Mining Subjective Knowledge from Customer Reviews: A Specific Case of Irony Detection. Available at: https://aclanthology.org/W11-1715.pdf.
16. Yang, Z., Yang, D., Dyer, C., He, X., Smola, A., & Hovy, E. (2016). Hierarchical Attention Networks for Document Classification. Available at: https://www.aclweb.org/anthology/N16-1174/.
17. Radford, A., Wu, J., Child, R., Luan, D., Amodei, D., Sutskever, I. (2019). Better language models and their implications. Available at: https://openai.com/blog/better-language-models/.
18. Brown, T. B., Mann, B., Ryder, N., Subbiah, M., Kaplan, J., Dhariwal, P., Neelakantan, A., Shyam, P., Sastry, G., Askell, A., Agarwal, S., Herbert-Voss, A., Krueger, G., Henighan, T., Child, R., Ramesh, A., Ziegler, D. M., Wu, J., Winter, C., ... Amodei, D. (2020). Language Models are Few-Shot Learners Available at: https://proceedings.neurips.cc/paper/2020/file/1457c0d6bf5478631ec67e564d04505b-Paper.pdf.
19. Wang, A., Singh, A., Michael, J., Hill, F., Levy, O., & Bowman, S. R. (2019). GLUE: A Multi-Task Benchmark and Analysis Platform for Natural Language Understanding. Available at: https://openreview.net/pdf?id=rJ4km2R5t7.
20. Lu, X., Xiong, C., Parikh, A. P., & Socher, R. (2019). ViLBERT: Pretraining Task-Agnostic Visiolinguistic Representations for Vision-and-Language Tasks. Available at: https://arxiv.org/abs/1908.02265.

СПИСОК ЛІТЕРАТУРИ

1. Mikolov, T., Chen, K., Corrado, G., & Dean, J. (2013). Efficient Estimation of Word Representations in Vector Space. Available at: https://arxiv.org/abs/1301.3781.

2. Bahdanau, D., Cho, K., & Bengio, Y. (2014). Neural Machine Translation by Jointly Learning to Align and Translate.
Available at: https://arxiv.org/abs/1409.0473.
3. Devlin, J., Chang, M. W., Lee, K., & Toutanova, K. (2018). BERT: Pre-training of Deep Bidirectional Transformers for Language Understanding. Available at: https://www.aclweb.org/anthology/N19-1423/.
4. Vaswani, A., Shazeer, N., Parmar, N., Uszkoreit, J., Jones, L., Gomez, A. N., Kaiser, Ł., & Polosukhin, I. (2017). Attention is All you Need. Available at: https://papers.nips.cc/paper/2017/hash/3f5ee243547dee91fbd053c1c4a845aa-Abstract.html.
5. Pennington, J., Socher, R., & Manning, C. (2014). Glove: Global Vectors for Word Representation. Available at: https://www.aclweb.org/anthology/D14-1162/.
6. Mikolov, T., Sutskever, I., Chen, K., Corrado, G. S., & Dean, J. (2013). Distributed Representations of Words and Phrases and their Compositionality. Available at: https://papers.nips.cc/paper/2013/hash/9aa42b31882ec039965f3c4923ce901b-Abstract.html.
7. Davidov, D., Tsur, O., & Rappoport, A. (2010). Semi-supervised recognition of sarcastic sentences in Twitter and Amazon.
Available at: https://aclanthology.org/W10-2914/.
8. Blodgett, S. L., Green, L., & O'Connor, B. (2018). Demographic Dialectal Variation in Social Media: A Case Study of African-American English.
Available at: https://aclanthology.org/D16-1120/.
9. Howard, J., & Ruder, S. (2018). Universal Language Model Fine-tuning for Text Classification. Available at: https://www.aclweb.org/anthology/P18-1031/.
10. Peters, M. E., Neumann, M., Iyyer, M., Gardner, M., Clark, C., Lee, K., & Zettlemoyer, L. (2018). Deep contextualized word representations. Available at: https://www.aclweb.org/anthology/N18-1202/.
11. Huang, P. S., He, X., Gao, J., Deng, L., Acero, A., & Heck, L. (2013). Learning Deep Structured Semantic Models for Web Search using Clickthrough Data. Available at: https://posenhuang.github.io/papers/cikm2013_DSSM_fullversion.pdf.
12. Xu C., McAuley J., (2018). The Importance of Generation Order in Language Modeling. Available at: https://www.aclweb.org/anthology/D18-1324/.
13. Suzuki M., Matsuo Y., (2020). A survey of multimodal deep generative models.
Available at: https://arxiv.org/abs/2207.02127.
14. Felbo, B., Mislove, A., Søgaard, A., Rahwan, I., & Lehmann, S. (2017). Using Millions of Emoji Occurrences to Learn Any-domain Representations for Detecting Sentiment, Emotion and Sarcasm. Available at: https://www.aclweb.org/anthology/D17-1169/.
15. Reyes A., Rosso P., (2016). Mining Subjective Knowledge from Customer Reviews: A Specific Case of Irony Detection.
Available at: https://aclanthology.org/W11-1715.pdf.
16. Yang, Z., Yang, D., Dyer, C., He, X., Smola, A., & Hovy, E. (2016). Hierarchical Attention Networks for Document Classification.
Available at: https://www.aclweb.org/anthology/N16-1174/.
17. Radford, A., Wu, J., Child, R., Luan, D., Amodei, D., Sutskever, I. (2019). Better language models and their implications.
Available at: https://openai.com/blog/better-language-models/.
18. Brown, T. B., Mann, B., Ryder, N., Subbiah, M., Kaplan, J., Dhariwal, P., Neelakantan, A., Shyam, P., Sastry, G., Askell, A., Agarwal, S., Herbert-Voss, A., Krueger, G., Henighan, T., Child, R., Ramesh, A., Ziegler, D. M., Wu, J., Winter, C., ... Amodei, D. (2020). Language Models are Few-Shot Learners Available at: https://proceedings.neurips.cc/paper/2020/file/1457c0d6bf5478631ec67e564d04505b-Paper.pdf.
19. Wang, A., Singh, A., Michael, J., Hill, F., Levy, O., & Bowman, S. R. (2019). GLUE: A Multi-Task Benchmark and Analysis Platform for Natural Language Understanding. Available at: https://openreview.net/pdf?id=rJ4km2R5t7.
20. Lu, X., Xiong, C., Parikh, A. P., & Socher, R. (2019). ViLBERT: Pretraining Task-Agnostic Visiolinguistic Representations for Vision-and-
Language Tasks. Available at: https://arxiv.org/abs/1908.02265.

Малига Ігор Євгенійович
аспірант
Харківський Національний Університет ім. В.Н. Каразіна, майдан Свободи 4, Харків, Україна, 61022
e-mail: igormalyga@gmail.com;
https://orcid.org/0000-0002-5708-7739

Шматков Сергій Ігорович
д.т.н., професор; завідуючий кафедри теоретичної теоретичної та прикладної системотехніки
Харківський Національний Університет ім. В.Н. Каразіна, майдан Свободи 4, Харків, Україна, 61022
e-mail: s.shmatkov@karazin.ua
https://orcid.org/0000-0002-6328-988X
Scopus Author ID: 57203141869

Методи машинного навчання для вирішенні проблем семантики та контексту при обробці текстових даних

Актуальність. З розширенням можливостей машинного навчання та його впливом на багато аспектів сучасного життя, включаючи обробку природної мови, розуміння семантики та контексту в текстових даних стає все більш актуальним. Семантика та контекст відіграють значну роль у здатності машин розуміти людську мову. Вони є центральними елементами в різних програмах, таких як машинний переклад, аналіз настроїв, виявлення спаму, розпізнавання голосу тощо. Однак цими аспектами часто нехтують або недооцінюють під час обробки текстових даних. Незважаючи на значний прогрес у цій галузі, проблема семантики та контексту залишається невирішеною, що знижує ефективність і точність багатьох систем машинного навчання.

Мета: Основна мета цієї статті — дослідити проблему семантики та контексту в машинному навчанні, а саме в обробці текстових даних. Стаття має на меті визначити основні проблеми, пов'язані з розумінням семантики та контексту, а також те, як вони впливають на різні аспекти обробки тексту. Крім того, буде проаналізовано поточні методи та підходи, які використовуються в галузі машинного навчання для вирішення цих проблем, і визначено їх обмеження.

Методи дослідження. Аналіз, пояснення, класифікація.

Результати. Було встановлено, що незважаючи на значні досягнення в технологіях машинного навчання, проблеми семантики та контексту в обробці текстових даних все ще існують. Вони впливають на якість і точність рішень, що приймаються системами на основі машинного навчання, що може призвести до некоректного аналізу та спотворення даних. Було виявлено, що навіть сучасні моделі на основі трансформаторів можуть зіткнутися з проблемами розуміння семантики та контексту, особливо в складних і багатозначних сценаріях.

Висновки. На основі проведеного дослідження зроблено висновок, що проблема семантики та контексту при обробці текстових даних є суттєвою та потребує подальшого вивчення. Існуючі методи і технології, хоч і показують високі результати в одних завданнях, можуть виявитися недостатніми в інших, особливо складних, ситуаціях. Пропонується продовжити дослідження в даному напрямку, розробити нові методи та підходи, які б змогли ефективно вирішити ці проблеми. Також важливо вивчити, як різні контекстуальні фактори впливають на семантику текстових даних і як ці ефекти можна врахувати при проектуванні та використанні систем машинного навчання.

Ключові слова: *Машинне навчання, обробка природної мови, семантика, контекст, текстові дані, нейронні мережі, трансформатори, BERT, GPT-3, аналіз даних, аналіз настроїв, семантичний аналіз.*

Надійшла у першій редакції 12.08.2022, в останній - 11.11.2022.
The first version has been received on 12.08.2022, the final version - on 11.11.2022.

DOI: https://doi.org/10.26565/2304-6201-2022-56-04

УДК (UDC) 004.052.42

Мороз Ольга Юріївна *старший викладач кафедри теоретичної та прикладної системотехніки факультету комп'ютерних наук; Харківський національний університет імені В. Н. Каразіна, майдан Свободи, 4, м. Харків, Україна, 61022, e-mail:* o.moroz@karazin.ua
https://orcid.org/0000-0002-4920-4093.

Компіляційно-семантична верифікація часопараметризованих мультипаралельних програм для інформаційних управляючих систем

У статті наводиться визначення часопараметризованих мультипаралельних програм, які (на відміну від загальноприйнятого трактування паралельних програм) містять специфікації моментів початку виконання операцій / функцій, а також підмножини таких операцій / функцій. Обгрунтовується необхідність розробки нових методів верифікації часопараметризованих паралельних програм. Розкриваються етапи виконання завдання компіляційного-семантичної верифікації часопараметризованих мультипаралельних програм в інтересах створення систем автоматичного синтезу високоефективних паралельних програм для обчислювальних систем різних класів.
Актуальність. Необхідність рішення наукової задачі розробки нових методів верифікації часопараметризованих мультипаралельних програм, орієнтованих на застосування формату структур семантико-числової специфікації робить. **Метою** є опис методу компіляційно-семантичної верифікації часопараметризованих мультипаралельних програм в інтересах створення систем автоматичного синтезу високоефективних паралельних програм для обчислювальних систем різних класів. **Метод дослідження.** Компіляційно-семантична верифікація часопараметризованих мультипаралельних програм. **Результати:** використання реального часу як один з основних параметрів формального синтезу паралельних програм і часових паралельних процесів, що їм відповідають; явне відображення в конструкціях паралельних програм складу фактично використовуваних методів паралельної обробки даних; явне відображення в конструкціях паралельних програм одиниць виміру (семантики) даних, що обробляються. Наводиться приклад, що ілюструє основні етапи методу. **Висновки.** Розроблений метод компіляційно-семантичної верифікації часопараметризованих мультипаралельних програм забезпечує облік наступних груп чинників, що роблять істотний вплив на ефективність програмних засобів паралельних обчислювальних систем.
***Ключові слова**: часопараметризовані мільтипаралельні програми, верифікація паралельних програм, компіляційно-семантична верифікація, семантично-числові специфікації.*

Як цитувати: Мороз О. Ю. Компіляційно-семантична верифікація часопараметризованих мультипаралельних програм для інформаційних управляючих систем. *Вісник Харківського національного університету імені В.Н.Каразіна, серія. Математичне моделювання. Інформаційні технології. Автоматизовані системи управління*. 2022. випуск 56. С.43-50. https://doi.org/10.26565/2304-6201-2022-56-04

How to quote: Moroz O. Yu. "Technology of semantic-numerical verification of time-parameterized parallel programs for information and control systems." *Bulletin of V.N. Karazin Kharkiv National University, series Mathematical modelling. Information technology. Automated control systems*, vol. 56. P.43-50. 2022. https://doi.org/10.26565/2304-6201-2022-53-04 [In Ukrainian].

1. Аналіз останніх досягнень і публікацій. Постановка проблеми.

Аналіз літератури показує, що одним з перспективних напрямів розвитку технологій паралельного програмування є дослідження в області автоматичного програмування часопараметризованих мультипаралельних програм [1–4].

Часопараметризована мультипаралельна програма визначається (на відміну від прийнятого нині трактування статичних паралельних програм) як конструкція, яка містить в явному виді специфікації наступних категорій інформації:

– множину об'єктів - даних, над якими повинні виконуватися дії (що задаються складом операцій/функцій алгоритмічної мови високого рівня);

– множину дій (операцій/функцій), які мають бути виконані над даними для вирішення завдання;

– множину статичних зв'язків, що задають стосунки впорядкованості операцій/функцій за даними і по управлінню;

– впорядкованість операцій/функцій в динаміці паралельного обчислювального процесу, що задається множиною моментів часу початку виконання операцій/функцій;

– розділення множини операцій/функцій на часові фрагменти (множинні часові оператори, МВО), що включають сукупність операцій/функцій, виконання яких починається одночасно в конкретний момент дискретного часу;

– розділення множини даних фрагменти даних, поставлені в однозначну відповідність множинним часовим операторам і використовувані у відповідні моменти дискретного часу;

– наявність інформації про розбиття множини команд різних фрагментів на підмножини (нитки), що виконуються відповідними модулями/процесорами;

– наявність інформації про одиниці виміру фізичних величин даних.

Новизна класу часопараметризованих мультипаралельних програм робить необхідним рішення наукової задачі розробки нових методів верифікації, орієнтованих на застосування формату структур семантико-числової специфікації [4]. В якості одного з етапів верифікації часопараметризованих мультипаралельних програм пропонується використовувати компіляційно-семантичну верифікацію. Основою компіляційно-семантичної верифікації є використання одиниць виміру (семантики) початкових даних і вихідних результатів задач, що задаються користувачем, автоматичне визначення в процесі рішення задач одиниць виміру проміжних і вихідних результатів і їх порівняння з одиницями виміру вихідних результатів, заданими користувачем.

Метою статті є опис методу компіляційно-семантичної верифікації часопараметризованих мультипаралельних програм в інтересах створення систем автоматичного синтезу високоефективних паралельних програм для обчислювальних систем різних класів.

2. Дослідження та результати

Початкові дані компіляційно-семантичної верифікації:

– початкова статична Сі-програма задачі;

– Сі-текст часової мультипаралельної програми, що відповідає початковій Сі-програмі і задовольняє вимогам/обмеженням користувача;

– семантична база даних БД «SEM» одиниць виміру фізичних величин;

– семантика (одиниці виміру) початкових даних і вихідних Сі-програми, що задаються користувачем, – структура US _ SEM.

– Вимагається:

– перевірити семантичну коректність початкової Сі-програми задачі;

– перевірити семантичну коректністьчасопараметризованої мультипаралельної програми.

– перевірити логічну еквівалентність часової мультипаралельної програми і початкової Сі-програми задачі.

Вихідними даними є:

1. Семантико-числова специфікація початкового коду програми (список одиниць виміру початкових даних завданняадачі, значень розмірності результатів проміжних обчислень і значень розмірності результатів виконання Сі-програми).

2. Результати перевірки ідентичності значень розмірності результатів виконання Сі-програми і призначеної для користувача семантичної специфікації задачі.

3. Результати перевірки семантичної коректності часової моделі і текстучасопараметризованої мультипаралельної програми.

Основні етапи методу компіляційно-семантичної верифікації часопараметризованих мультипаралельних програм показані на рис. 1.

Розглянемо зміст основних етапів методу компіляційно-семантичної верифікації.

Етап 1 (символ 2 рис. 1) забезпечує синтез для Сі-програми (рис.2) структур BF і CF семантико-числовой специфікації (таблиця. 3 представляє BF).

На етапі 2 (символ 3 рис. 1) забезпечується графічна візуалізація початкової Сі-програми у вигляді Сі-графа (рис. 3), виходячи із структур СЧС BF, сформованих при виконанні першого етапу. Побудова Сі-графа здійснюється за допомогою засобів візуалізації паралельних апаратно-програмних об'єктів, описаних в [1].

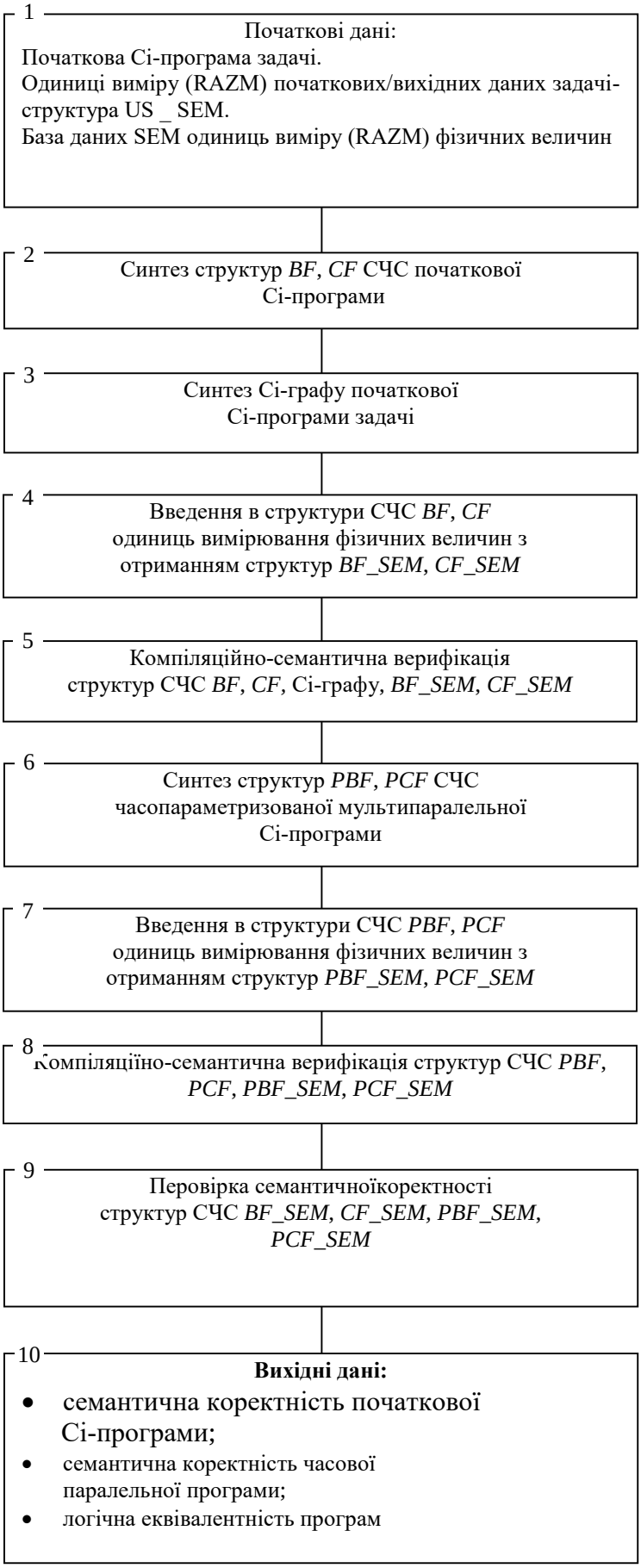

Рис. 1. Основні етапи методу компіляційно-семантичної верифікації часопараметризованих мультипаралельних програм

Третій етап (символ 4 рис. 1) забезпечує синтез одиниць виміру даних, що формуються "внутрішніми" і "вихідними" операторами P_j структур СЧС і Сі-графа, виходячи із заданих користувачем одиниць виміру початкових і вихідних даних Сі-програми задачі, типів операцій, що виконуються операторами P_j, сі-програми, і загальноприйнятої бази даних одиниць виміру фізичних величин.

Етап четвертий (символ 5 рис. 1) виконує шляхом компіляційної верифікації перевірку синтезу структур СЧС Сі-програми і відповідного Сі-графа. Методика компіляційної верифікації розглянута в [1, 4]. А також забезпечує перевірку семантичної коректності структур СЧС BF _ SEM, CF _ SEM початкової Сі-програми шляхом порівняння розрахованих одиниць вимірювання даних, що відповідають вихідним операторам синтезованої структури BF _ SEM початкової Сі-програми, з одиницями вимірювання вихідних даних, що задаються використачем.

Синтез структур PBF, PCF СЧС часопараметризованої мультипаралельної програми виконується на етапі 6 (символ 6 рис. 1) аналогічно етапу 1 (символ 2 рис. 1).

На етапі 7 (символ 7 рис. 1) здійснюється введення в структури СЧС PBF, PCF одиниць виміру фізичних величин з отриманням структур PBF _ SEM, PCF _ SEM.

Етап 8 (символ 8 рис. 1). Верифікація компіляції структур СЧС PBF, PCF з одночасною перевіркою семантичної коректності розширених структур СЧС PBF _ SEM, PCF _ SEM часопараметризованої мультипаралельної програми шляхом порівняння розрахованих одиниць виміру даних, що відповідають вихідним операторам синтезованої структури PBF _ SEM, з одиницями виміру вихідних даних, заданими користувачем.

Проілюструємо зміст основних етапів методу семантичної для компіляції верифікації за допомогою Сі-програми, представленої на рис. 2. До складу початкових даних входять також фрагмент бази цих одиниць виміру фізичних величин (табл. 1) і перелік даних, що задаються користувачем (табл. 2).

```
#include <stdio.h>
void main(void)
{
int a,b,c,r, k,l,m,p, s,t;
     scanf("%d %d
%d\n",&a,&b,&c);
     k = a * b;
     l = b % a;
     if(k < a-c)
     { m = (k % 2) * 2;
      r = l * 2;
     p = k + l;
     }
     else
     { p = 2 * l;
      r = l - k;
      m = p + l;
     }
     s = p - r;
     t = (m * 2) / a;
     printf ("%4d
%4d\n",s,t);
}
```

Рис. 2. Початкова Сі-програма

Базова структура BF (табл. 3) описує номери і склад операторів P_j задачі (масив N), їх типи (масив TYP), число вхідних (масив SJD) і вихідних (массивWJD) зв'язків кожного оператора P_j, ідентифікатори операторів (масив RES), покажчики на початок ланцюжків спряжених і зовнішніх операторів (масиви NSJ, NWJ) для кожного оператора Сі-програми. Синтез структур BF і CF СЧС здійснюється відповідно до методики, викладеної в [1].

Таблиця 1. Фрагмент семантичної бази даних «SEM»

KOD_RAZM	*RAZM*	*KOD_RAZM*	*SEM*
2	м	14	рад/с
3	кг	15	м/(с*с)
4	с	16	рад/(с*с)
5	А	17	1/м
6	К	18	кг/(м*м*м)
7	моль	19	м*м*м/кг
8	кд	20	А/(м*м)
9	рад	21	А/м
10	ср	22	моль/(м*м*м)
11	м*м	23	1/с
12	м*м*м	24	м*м/с
13	м/с	25	кд/(м*м)

Таблиця 2. Структура US_SEM одиниць вимірювання, що задаються користувачем

N_OP	*REZ*	*VHOD_VIH*	*KOD_SEM*
3	a	0	2
4	b	0	2
5	c	0	2
11	s	1	2
12	t	1	11

Таблиця 3. Базова структура BF операторів початкової Сі-програми

N	*MET*	*TYP*	*NSJ*	*SJD*	*BJ*	*NWJ*	*WJD*	*MP1*	*MP2*	*VH*	*VIH*	*RES*	*N*	*MET*	*TYP*	*NSJ*	*SJD*	*BJ*	*NWJ*	*WJD*	*MP1*	*MP2*	*VH*	*VIH*	*RES*
0	0	58	–1	0	0	0	1	0	0	0	1	a_in	26	0	12	24	2	1	48	2	0	0	2	2	=
1	0	58	–1	0	0	1	1	0	0	0	1	b_in	27	0	3	26	3	1	50	1	0	0	3	1	*
2	0	58	–1	0	0	2	1	0	0	0	1	c_in	28	0	12	29	2	1	51	2	0	0	2	2	=
3	0	47	–1	0	0	3	1	0	0	0	2	a	29	0	1	31	3	1	53	1	0	0	3	1	+
4	0	47	–1	0	0	4	1	0	0	0	2	b	30	0	12	34	2	1	54	2	0	0	2	2	=
5	0	47	–1	0	0	5	1	0	0	0	2	c	31	0	50	36	3	1	56	1	3	0	3	1	bp
6	0	47	–1	0	0	6	2	0	0	0	2	r	32	2	3	39	3	2	57	1	0	0	3	1	*
7	0	47	–1	0	0	8	1	0	0	0	2	k	33	0	12	42	2	2	58	2	0	0	2	1	=
8	0	47	–1	0	0	9	1	0	0	0	2	l	34	0	2	44	3	2	60	1	0	0	3	1	–
9	0	47	–1	0	0	10	2	0	0	0	2	m	35	0	12	47	2	2	61	2	0	0	2	2	=
10	0	47	–1	0	0	12	2	0	0	0	2	P	36	0	1	49	2	2	63	1	0	0	2	1	+
11	0	47	–1	0	0	14	1	0	0	0	2	s	37	0	12	51	2	2	64	2	0	0	2	2	=
12	0	47	–1	0	0	15	1	0	0	0	2	t	38	0	50	53	2	2	66	1	3	0	2	1	bp
13	0	12	0	2	0	16	4	0	0	2	1	=	39	3	54	55	2	3	67	1	0	0	2	1	l.o
14	0	12	2	2	0	20	2	0	0	2	1	=	40	0	53	57	2	3	68	1	0	0	2	1	a.o
15	0	12	4	2	0	22	1	0	0	2	1	=	41	0	53	59	2	3	69	1	0	0	2	1	a.o
16	0	3	6	2	0	23	1	0	0	2	1	*	42	0	53	61	2	3	70	1	0	0	2	1	a.o
17	0	12	8	2	0	24	4	0	0	2	1	=	43	0	2	63	3	3	71	1	0	0	3	1	–
18	0	5	10	2	0	28	1	0	0	2	1	%	44	0	12	66	2	3	72	2	0	0	2	2	=
19	0	12	12	2	0	29	5	0	0	2	1	=	45	0	3	68	2	3	74	1	0	0	2	1	*
20	0	2	14	2	0	34	1	0	0	2	1	–	46	0	4	70	2	3	75	1	0	0	2	1	/
21	0	25	16	2	0	35	1	0	0	2	1	<	47	0	12	72	2	3	76	2	0	0	2	2	=
22	0	51	18	1	0	36	5	1	2	1	2	upl	48	0	50	74	2	3	78	1	980	0	2	1	bp
23	0	57	–1	0	1	41	5	0	0	0	1	C2_	49	980	49	76	1	4	–1	0	0	0	1	0	stop
24	1	5	19	3	1	46	1	0	0	3	1	%	50	0	48	77	1	4	–1	0	0	0	1	0	s out
25	0	3	22	2	1	47	1	0	0	2	1	*	51	0	48	78	1	4	–1	0	0	0	1	0	t_out

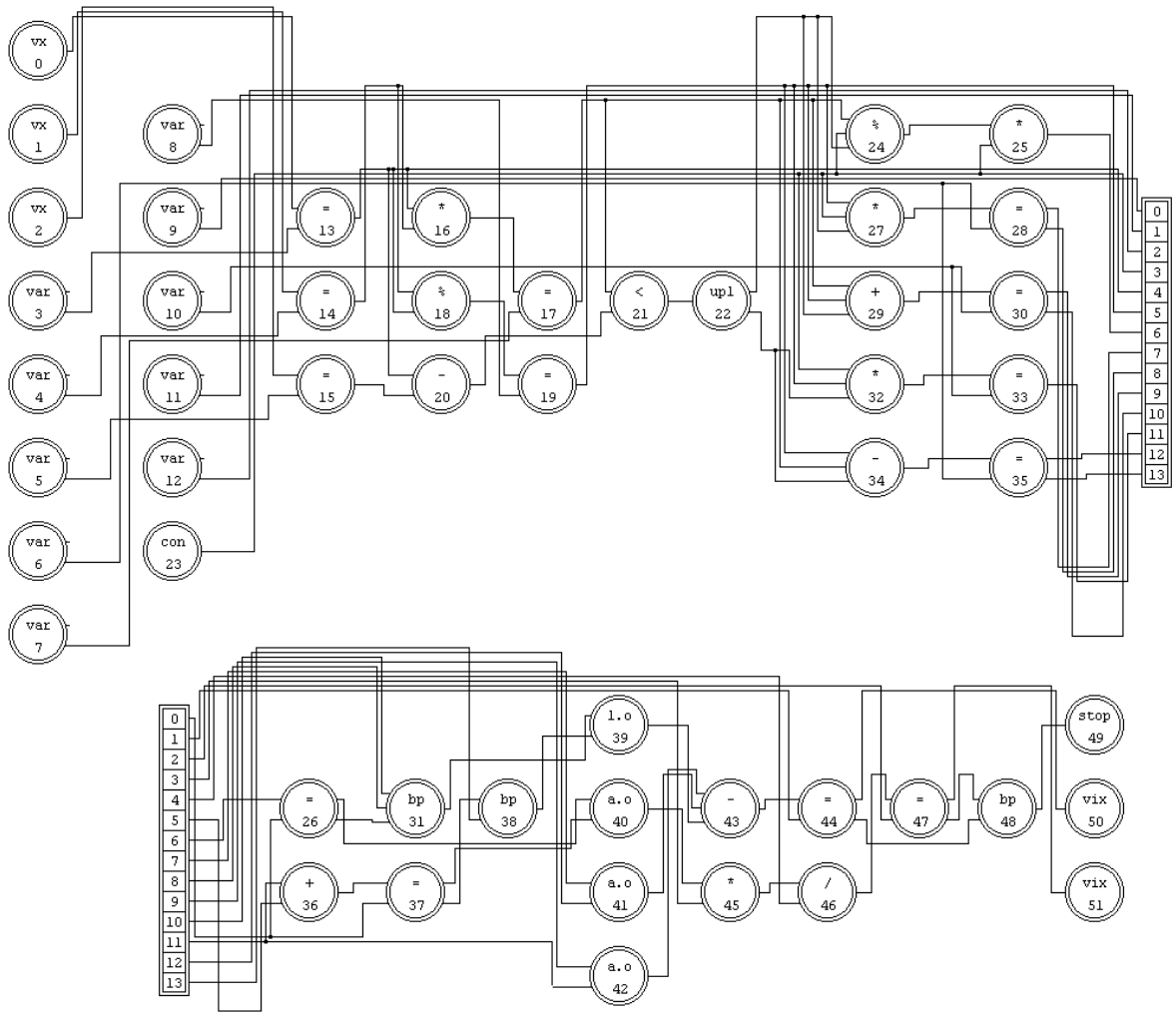

Рис. 3. Сі-граф початкової Сі-програми, що розгалужується

```
Файл елементів:                C:\My_prog\C\Result\CNSVWVIXVIX1.TXT
Файл зв'язків елементів:       C:\My_prog\C\Result\CNSVWVIXVIX2.TXT

 ТЕСТ КОРЕКТНОСТІ ФАЙЛІВ:
 максимальна кількість елементів:  0-35
 максимальна кількість зв'язків    0-38

 ТЕСТ ВІДПОВІДНОСТІ ЧИСЛА, СПОРУЖЕНИХ І ЗОВНІШНІХ ЗВ'ЯЗКІВ: ОК

 ТЕСТ ЧИСЛА ЗВ'ЯЗКІВ ПО СПОРУЖЕНИХ ЕЛЕМЕНТАХ: ОК

 ТЕСТ ЧИСЛА ЗВ'ЯЗКІВ ПО ЗОВНІШНІМ ЕЛЕМЕНТАМ: ОК

 ТЕСТ ВІДПОВІДНОСТІ ВИСНОВКІВ ПО СПОРУЖЕНИХ ЕЛЕМЕНТАХ: ОК

 ТЕСТ ВІДПОВІДНОСТІ ВИСНОВКІВ ПО ЗОВНІШНІМ ЕЛЕМЕНТАМ: ОК

 ТЕСТ ВІДПОВІДНОСТІ ЧИСЛА ВХОДІВ ЕЛЕМЕНТУ І КІЛЬКОСТІ ЙОГО СПОЛУЖЕНИХ: ОК
```

Рис. 4. Результати компіляційної верифікації структур семантико-числової специфікації Сі-програми та Сі-графу (View of test results)

Результати синтезу семантико-числовой специфікації *BF_SEM* Сі-програми показані в табл. 4. Результати синтезу семантико-числовой специфікації *BF_SEM* Сі-програми показані в таблиці. 4. У таблиці прийняті наступні позначення: масив *RAZM* – одиниці виміру початкових даних і даних – результатів виконання операцій : «м» - метр, «ні» - відсутність вичисленого значення вихідної змінної, «б/роз» - безрозмірна величина, «м*м», «м*м*м» - синтезовані одиниці виміру довільних величин.

Таблица 4. Структура BF_SEM – результат синтезу одиниць виміру операторів початкової Сі-програми

N	*TYP*	*NSJ*	*SJD*	*BJ*	*NWJ*	*WJD*	*RES*	*SEM*	*N*	*TYP*	*NSJ*	*SJD*	*BJ*	*NWJ*	*WJD*	*RES*	*SEM*
0	58	–1	0	0	0	1	a_in	*м*	26	12	24	2	1	48	2	=	*м*м*
1	58	–1	0	0	1	1	b_in	*м*	27	3	26	3	1	50	1	*	б/роз.
2	58	–1	0	0	2	1	c_in	*м*	28	12	29	2	1	51	2	=	б/роз.
3	47	–1	0	0	3	1	a	*м*	29	1	31	3	1	53	1	+	*м*м*
4	47	–1	0	0	4	1	b	*м*	30	12	34	2	1	54	2	=	*м*м*
5	47	–1	0	0	5	1	c	*м*	31	50	36	3	1	56	1	bp	б/роз.
6	47	–1	0	0	6	2	r	б/роз.	32	3	39	3	2	57	1	*	б/роз.
7	47	–1	0	0	8	1	k	*м*м*	33	12	42	2	2	58	2	=	б/роз.
8	47	–1	0	0	9	1	1	б/роз.	34	2	44	3	2	60	1	–	*м*м*
9	47	–1	0	0	10	2	m	*м*м*	35	12	47	2	2	61	2	=	*м*м*
10	47	–1	0	0	12	2	P	*м*м*	36	1	49	2	2	63	1	+	б/роз.
11	47	–1	0	0	14	1	s	*м*	37	12	51	2	2	64	2	=	б/роз.
12	47	–1	0	0	15	1	t	*м*м*	38	50	53	2	2	66	1	bp	б/роз.
13	12	0	2	0	16	4	=	*м*	39	54	55	2	3	67	1	l.o	б/роз.
14	12	2	2	0	20	2	=	*м*	40	53	57	2	3	68	1	a.o	*м*м*
15	12	4	2	0	22	1	=	*м*	41	53	59	2	3	69	1	a.o	б/роз.
16	3	6	2	0	23	1	*	*м*м*	42	53	61	2	3	70	1	a.o	*м*м*
17	12	8	2	0	24	4	=	*м*м*	43	2	63	3	3	71	1	–	*м*м*
18	5	10	2	0	28	1	%	б/роз.	44	12	66	2	3	72	2	=	*м*м*
19	12	12	2	0	29	5	=	б/роз.	45	3	68	2	3	74	1	*	*м*м*
20	2	14	2	0	34	1	–	*м*	46	4	70	2	3	75	1	/	*м*
21	25	16	2	0	35	1	<	б/роз.	47	12	72	2	3	76	2	=	*м*
22	51	18	1	0	36	5	upl	б/роз.	48	50	74	2	3	78	1	bp	б/роз.
23	57	–1	0	1	41	5	C2_	б/роз.	49	49	76	1	4	–1	0	stop	б/роз.
24	5	19	3	1	46	1	%	*м*м*	50	48	77	1	4	–1	0	s_out	*м*м*
25	3	22	2	1	47	1	*	*м*м*	51	48	78	1	4	–1	0	t_out	*м*

Висновки.

Нині у багатьох галузях науки і техніки знаходять застосування часопараметризовані мультипаралельні програми. У зв'язку з цим на перше місце виходять питання верифікації і тестування програм такого класу.

Розроблений метод компіляційно-семантичної верифікації часопараметризованих мультипаралельних програм забезпечує облік наступних груп чинників, що роблять істотний вплив на ефективність програмних засобів паралельних обчислювальних систем:

– використання реального часу як один з основних параметрів формального синтезу паралельних програм і часових паралельних процесів, що їм відповідають;

– явне відображення в конструкціях паралельних програм складу фактично використовуваних методів паралельної обробки даних;

– явне відображення в конструкціях паралельних програм одиниць виміру (семантики) даних, що обробляються;

– підтримка в явному виді структурами часових паралельних програмних і апаратних продуктів вимог архітектурної і/або проблемної орієнтації;

– підтримка в явному виді структурами паралельних програмних і апаратних продуктів вимог і обмежень користувачів (наприклад, забезпечення необхідного часу виконання програми, заданої тактової частоти обробки даних цифровим пристроєм та ін.).

СПИСОК ЛІТЕРАТУРИ

1. Поляков Г. А. Синтез и анализ параллельных процессов в адаптивных времяпараметризованных вычислительных системах / Г. А. Поляков, С. И. Шматков, Е. Г. Толстолужская, Д. А. Толстолужский: монография. – Х.: ХНУ имени В. Н. Каразина, 2012. – 670с.
2. Дорогий Я. Ю., Цуркан В. В. Огляд методів верифікації параметризованих моделей. Збірник наукових праць Національного університету кораблебудування імені адмірала Макарова. Миколаїв : НУК, 2020. № 1 (479). С. 82–90. URI http://eir.nuos.edu.ua/handle/123456789/3802.
3. Коцовський В. М. Теорія паралельних обчислень: навчальний посібник. Ужгород: ПП «АУТДОР-Шарк», 2021. 188 с.
4. Moroz, O. Y., Tolstoluzka, O. G., & Savchenko, R. V. Analysis of existing verification technologies for parallel programs. Bulletin of V.N. Karazin Kharkiv National University series «Mathematical modeling. Information technology. Automated control systems» issue 46, 2020. P. 76–81. [in Ukrainian] https://doi.org/10.26565/2304-6201-2020-46-07

REFERENCES

1. Polyakov G. A. Sintez i analiz parallel'nykh protsessov v adaptivnykh vremyaparametrizovannykh vychislitel'nykh sistemakh: monografiya / G. A. Polyakov, S. I. Shmatkov, E. G. Tolstoluzhskaya, D. A. Tolstoluzhskii. Khar'kov: KhNU im. V. N. Karazina, 2012. 670 s [in Ukrainian].
2. Dorogy Y.Yu., Tsurkan V.V. Review of methods of verification of parameterized models. Collection of scientific works of the Admiral Makarov National Shipbuilding University. Mykolaiv: NUK, 2020. No. 1 (479). P. 82–90. [in Ukrainian] URL: http://eir.nuos.edu.ua/handle/123456789/3802. (Last accessed: 28.11.2022).
3. Kotsovsky V. M. The theory of parallel computing: a textbook. Uzhhorod: PE "AUTDOR-Shark", 2021. 188 p. [in Ukrainian].
4. Moroz, O. Y., Tolstoluzka, O. G., & Savchenko, R. V. (2020). Analysis of existing parallel programs verification technologies. Bulletin of V.N. Karazin Kharkiv National University, Series «Mathematical Modeling. Information Technology. Automated Control Systems», 46, P. 76-81. https://doi.org/10.26565/2304-6201-2020-46-07

Moroz Olha *Senior lecturer of the Department of Theoretical and Applied Systems Engineering, Faculty of Computer Science; VN Karazin Kharkiv National University, 4 Svobody Square, Kharkiv, Ukraine, 61022*

Compilation-semantic verification of time-parameterized multi-parallel programs for information management systems

Abstract: The article provides a definition of time-parameterized multi-parallel programs, which (in contrast to the generally accepted interpretation of parallel programs) contain specifications for the start of operations/functions, as well as the subsets of such operations/functions. The need to develop new methods for verifying time-parameterized parallel programs is substantiated. The stages of performing the task of compilation-semantic verification of time-parameterized multi-parallel programs in the interests of creating systems of automatic synthesis of highly efficient parallel programs for computer systems of various classes are presented. **Topicality.** The need to solve the scientific problem of developing new methods for verifying time-parameterized multi-parallel programs, focused on the application of the format of semantic-numerical specification structures, is necessary. The **goal** is to describe the method of compilation-semantic verification of time-parameterized multi-parallel programs in the interests of creating systems of automatic synthesis of highly efficient parallel programs for computer systems of various classes. **Research method.** Compilation-semantic verification of time-parameterized multiparallel programs. **Results.** The real time is used as one of the main parameters of the formal synthesis of parallel programs and time-parallel processes corresponding to them. The actually used methods of parallel data processing are clearly presented in the constructions of parallel programs. The units of measurement (semantics) of the processed data are clearly presented in the constructions of parallel programs. An example illustrating the main stages of the method is given. **Conclusions.** The developed method of compilation-semantic verification of time-parameterized multi-parallel programs takes into account the groups of factors that have a significant impact on the effectiveness of software tools of parallel computing systems.

***Keywords**: time-parameterized multi-parallel programs, verification of parallel programs, compilation-semantic verification, semantic-numerical specifications.*

Надійшла у першій редакції 07.10.2022, в останній - 01.12.2022.
The first version has been received on 07.10.2022, the final version - on 01.12.2022.

DOI: https://doi.org/10.26565/2304-6201-2022-56-05

UDC 519.6

Pryimak Oleksii *Candidate of Engineering Sciences*
e-mail: pryimak@mail.com **https://orcid.org/0000-0003-2633- 7456**
Yanovsky Volodymyr *Doctor of Physical and Mathematical Sciences, Professor*
V. N. Karazin Kharkiv National University,
4 Svobody Sq., Kharkiv, 61022, Ukraine;
Institute for Single Crystals, NAS Ukraine,
60 Nauky Ave., Kharkiv, 61001, Ukraine
e-mail: yanovsky@isc.kharkov.ua **https://orcid.org/0000-0003-0461-749X**

Head-on collision of flocks

Relevance. The study of the collective behavior of flocks of intelligent agents by using the mathematical and numerical methods is related to the multi-agent systems and artificial intelligence, which are actively researched nowadays.
Goal. To reveal the patterns of flocks dispersion during their collision and to obtain the analytical ratios of flocks kinematics.
Research methods. The work is based on the methods of mathematical and numerical modeling of multi-agent systems.
The results. The main parameter that determines the flocks behavior during their interaction is the acceleration. When the impact parameter is increased, the changes in the characteristics of the flocks become less noticeable. The obtained dependence of the acceleration on the value of the aiming parameter resembles the dependence that is typical for phase transitions.
Conclusions. The main regularities of flocks dispersion are determined, as well as the analytical ratios of flocks kinematics, which are in good conformity with the simulation data.
Keywords: *collective behavior, multi-agent system, flock, intelligent agent, force vector, kinematics, acceleration, impact parameter.*

How to quote: Pryimak O.V., Yanovsky V.V., "Head-on collision of flocks", *Bulletin of V.N. Karazin Kharkiv National University, series Mathematical modelling. Information technology. Automated control systems*, vol. 56, pp. 51-65, 2022. https://doi.org/10.26565/2304-6201-2022-56-05

Як цитувати: Приймак О.В., Яновський В.В. Лобове зіткнення зграй. *Вісник Харківського національного університету імені В. Н. Каразіна, серія Математичне моделювання. Інформаційні технології. Автоматизовані системи управління*. 2022. вип. 56. С. 51-65. https://doi.org/10.26565/2304-6201-2022-56-05

1 Introduction

Currently the collective behavior of self-driven or motile elements is of great interest (see [1] for example). Such systems include flight of flocks of birds [2-4], movement of schools of fish [5-7], insect migrations [8, 9] and herds of animals [10]. The patterns of their collective motion and the nature of the appearance of coordinated motions are intensively studied [11]. However, that interest is not limited to natural objects. Similar problems arise with the emergence of artificial multi-agent systems capable of manifesting themselves in collective behavior [12-14]. Even the influence of artificial objects – robots on the behavior of natural systems is also considered [15, 16]. At the same time, on the one hand, such systems can be considered as simple models of natural objects, on the other hand, as the emergence of swarm intelligence in artificial intelligent systems. A new direction in physics has even appeared – active matter [17, 18].

In nature, the behavior of systems consisting of many interacting moving individuals is extremely diverse. Despite the widespread occurrence of such phenomena, there have been no systematic studies of self-propelled interacting objects till recent times. One of the first works [19] is devoted to modeling the movement of schools of fish using the rules: (a) approach movement to allow aggregation, (b) parallel orientation movement and (c) cohesion. The speed and direction of individuals were considered stochastic, and the direction of movement of individuals was determined by the position and direction of movement of their neighbors. It has been noted that a collective movement can arise even in the absence of a leader. Much more famous was the later work of Reynolds [20] in which he simulated the movement of bird-like objects – boyds. A more detailed discussion of the various patterns of movement of interacting individuals can be found in the review [1].

In this work, the behavior of flocks during their head-on collision is considered. Two flocks have been simulated by using the flocking algorithm and their behavior after the collision has been studied.

Actually, this type of collision in physics is the beginning of studying the scattering of bodies in a collision. The features of flocks collisions and the differences between them and the regularities of scattering of physical particles are discussed. The main patterns of collisions of such flocks have been determined.

2 Model

The collective behavior of flocks of agents has been modeled by using the flocking algorithm proposed by Reynolds [20]. In its basic form, flocking describes the collective movement of agents according to three simple rules: separation, alignment, cohesion. The process of moving is iterative. At each iteration, the change in the velocity of each agent is calculated as the sum of the changes in speed in accordance with the three rules of the flock. The change in the position of the i-th agent is determined by a simple iterative equation

$$\vec{x}_i(t+1) = \vec{x}_i(t) + \vec{v}_i(t+1)\cdot\Delta t. \tag{2.1}$$

The change in the velocity of the i-th agent depends on the neighboring agents marked with the index j, which falls into the sphere of radius R centered on the i-th particle in accordance with the equation

$$\vec{v}_i(t+1) = \vec{v}_i(t) + \Delta\vec{v}_i(t), \tag{2.2}$$

where $\vec{v}_i(t)$ is the velocity vector of the i-th agent at discrete time t. For flocking, the change in speed is determined by three factors, as noted above

$$\Delta\vec{v}(t)_i = 5\cdot\Delta\vec{v}_{separation,i}(t) + 3\cdot\Delta\vec{v}_{alignment,i}(t) + \Delta\vec{v}_{cohesion,i}(t).$$

Numeric multipliers determine the weights or significance of the respective contributions to the velocity change and may vary. To describe the model, we define these terms [21]. So let us start with the separation

$$\Delta\vec{v}_{sepi}(t) = \left(v_0 - v_i(t)\right)\frac{\left\langle x_i(t) - x\ (t)\right\rangle_R}{\left|\left\langle x_i(t) - x\ (t)\right\rangle_R\right|},$$

where v_0 is the magnitude of velocity vector of the agents and $v_i(t) = |\vec{v}_i(t)|$ is the magnitude of velocity vector of the i-th agent. The factor $\left(v_0 - v_i(t)\right)$ is present in all contributions and it is needed to return the velocity value to the value of v_0. We will also use the notation

$$\left\langle \vec{x}_i(t) - \vec{x}\ (t)\right\rangle_R = \frac{1}{n}\sum_j^n \frac{\vec{x}_i(t) - \vec{x}_j(t)}{\left|\vec{x}_i(t) - \vec{x}_j(t)\right| d_{ij}(t)}.$$

Here $\langle\ldots\rangle_R$ denotes averaging (or summation) of the velocities within a circle of radius R surrounding agent i. For each rule, the radii of the neighborhood can be chosen separately. Now we define the value of $\Delta\vec{v}_{separation,i}(t)$ as

$$\Delta\vec{v}_{separation,i}(t) = \frac{\Delta\vec{v}_{sep}(t)}{\left|\Delta\vec{v}_{sep}(t)\right|}\cdot\sigma \quad ; \quad \sigma = \begin{cases} 1 \ if\ \left|\Delta\vec{v}_{sep}(t)\right| \le 0.03 \\ 0.03 \ if\ \left|\Delta\vec{v}_{sep}(t)\right| > 0.03 \end{cases}.$$

The σ factor is called steering force. It is introduced to smooth non-physical sharp turns. The value $\sigma = 0.03$ is chosen for modeling and may change.

Let us move on to alignment and define

$$\Delta\vec{v}_{alig\,i}(t) = \left(v_0 - v_i(t)\right)\frac{\left\langle\vec{v}(t)\right\rangle_R}{\left|\left\langle\vec{v}(t)\right\rangle_R\right|}.$$

Here we again use the natural notation

$$\left\langle\vec{v}(t)\right\rangle_R = \frac{1}{n}\sum_j^n \vec{v}_j(t),$$

where $\langle\ldots\rangle_R$ - means averaging over the velocities of the agents inside the sphere of radius R surrounding the i-th agent. It is obvious that $\frac{\langle\vec{v}_j\rangle_R}{|\langle\vec{v}_j\rangle_R|}$ is a unit vector in the direction of the mean

motion of neighboring agents. This provides alignment. Let us define $\Delta v_{alignment}$ as

$$\Delta\vec{v}_{alignment,i}(t)=\frac{\Delta\vec{v}_{alig,i}(t)}{\left|\Delta\vec{v}_{alig,i}(t)\right|}\cdot\sigma \quad ; \quad \sigma=\begin{cases} 1 \ if \ \left|\Delta\vec{v}_{alig,i}(t)\right|\le 0.03 \\ 0.03 \ if \ \left|\Delta\vec{v}_{alig,i}(t)\right|>0.03 \end{cases}.$$

Let us proceed to the description of the last contribution of the person responsible for <<cohesion>> and define

$$\Delta\vec{v}_{coh\,i}\left(t\right)=\left(v_0-v_i\left(t\right)\right)\frac{\left\langle\Delta\vec{x}_i\left(t\right)\right\rangle}{\left|\left\langle\Delta\vec{x}_i\left(t\right)\right\rangle\right|},$$

where

$$\left\langle\Delta\vec{x}_i\right\rangle_R=\frac{1}{n}\sum_j^n\vec{x}_j\left(t\right)-\vec{x}_i\left(t\right)$$

deviation of the position of the i-th agent from the average position of the neighbors in the sphere of radius R. Finally

$$\Delta\vec{v}_{cohesion,i}(t)=\frac{\Delta\vec{v}_{coh,i}(t)}{\left|\Delta\vec{v}_{coh,i}(t)\right|}\cdot\sigma \quad ; \quad \sigma=\begin{cases} 1 \ if \ \left|\Delta\vec{v}_{coh,i}(t)\right|\le 0.03 \\ 0.03 \ if \ \left|\Delta\vec{v}_{coh,i}(t)\right|>0.03 \end{cases}.$$

When modeling, two flocks of agents are considered to move in a two-dimensional space without obstacles. When determining the change in the corresponding velocities of the agent, the different radii of the spheres, over which the averaging is performed, are chosen:

$$R_{separation}=500\ m,$$
$$R_{alignment}=1000\ m,$$
$$R_{cohesion}=2000\ m.$$

The velocity of the agent v in space per iteration is limited by the expression $v_{min}\le v\le v_{max}$, and the rotation angle is limited by the expression $\Delta A\le\Delta A_{max}$. The agent's velocity tends to v_0, which is taken into account in the three flocking rules. The magnitude of the velocity of each agent at the initial moment of time is equal to v_0. The listed characteristics are assigned the following values:

$$v_{min}=30\ m/1,$$
$$v_0=50\ m/1,$$
$$v_{max}=70\ m/1,$$
$$\Delta A_{max}=\frac{\pi}{30}.$$

At the initial moment of time, the agents of each flock are located in space in a "chessboard" order according to the following rules. In each column, the agents have the same position along the X axis, and the distance between the neighboring agents along the Y axis is 500 meters. The distance between adjacent columns along the X axis is 500 meters. There is one less agent in the even columns than in the odd ones, and the agents are located with a shift along the Y axis by 250 meters (Fig. 1). The cases with the following number of agents in a flock are considered: 3, 14, 33, 60, 77, 95.

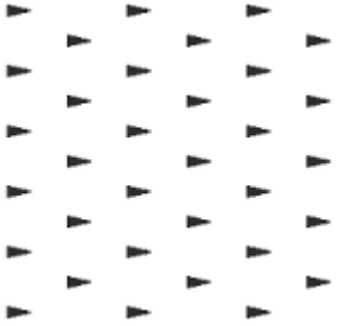

Fig.1 An example of the location of a flock of 33 agents at the initial time

In a numerical experiment, two flocks with the same number of agents collide. The centers of two colliding flocks at the initial moment of time are located at a distance of 10^5 meters from each other along the X axis. The center of a flock is determined as the arithmetic average of the positions of the agents of flocks separately for each dimension.

The direction of movement at the initial moment of time for the agents of the first flock is equal to 0 radians, and for the agents of the second flock to π radians.

The flocks move towards each other. The collection of statistics on the movement of flocks begins with an iteration when the distance between any two agents of two flocks does not exceed $R_{cohesion}$, i.e. agents of different flocks begin to interact with each other.

Flocks collide and fly past each other, after which the agents of different flocks stop interacting with each other. The interaction of agents of different flocks lasts for t_{int}, and the collection of flock movement statistics starts from the moment the interaction of agents of different flocks begins on the interval $4 \cdot t_{int}$ for flocks of sizes 3, 14, 33 agents and $8 \cdot t_{int}$ for flocks of 60, 77, 95 agents.

The average speed of the flock is equal to the arithmetic mean of the speed of the agents of the flock, and the average direction of movement of the flock is equal to the arithmetic mean of the direction of the agents of the flock.

The obtained simulation data are dimensionless. The characteristic scale for nondimensionalization is $S = R_1 + R_2 + R_{cohesion}$, where the flock radius R is equal to the maximum distance among flock agents from the center of the flock.

3 Collision of flocks

Let us consider a head-on collision between two flocks. The geometry of their scattering is shown in Fig. 2. This is the simplest and in some sense the canonical case of scattering. Initially, the agents of the respective flocks occupy certain areas. When modeling, they have been distributed over areas close to a circle. The initial distance between flocks across the direction of movement corresponds to the impact parameter ρ. During the simulation, the impact parameter changes from 0 to l_{int}. For large values of ρ, there is no interaction between flocks and, accordingly, their scattering.

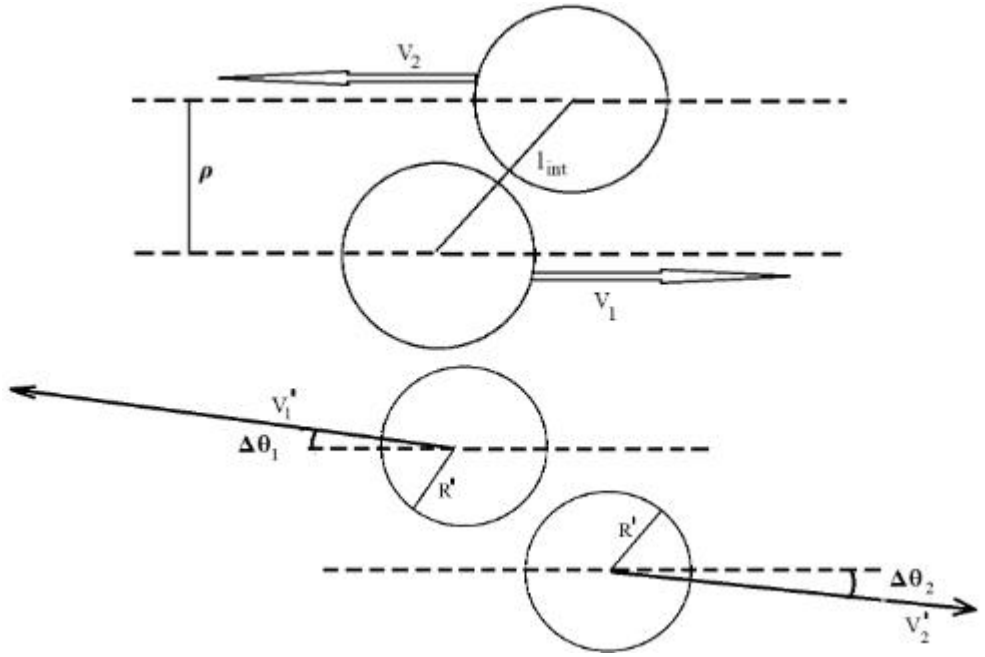

Fig.2 The top image shows the directions of movement of flocks, their velocity and sizes at the moment of the beginning of the interaction of agents of flocks. It is convenient to skip the free movement stage. Possible a priori changes in flock parameters and their movement after interaction are shown below. So, the directions of their movement can change, which are characterized by the scattering angles $\Delta\theta$, the indices indicate the flocks, the velocity of their movements and the characteristic sizes and even the shape of the flocks. The circles show the areas occupied by the agents of the respective flocks

There are specific features of the interaction of flocks. First, their interaction occurs at a finite distance not exceeding l_{int}, and, accordingly, takes a finite time interval from 0 to t_{int}. The flock characteristics may change during interaction, and even after interaction, some changes may persist. These features distinguish flock scattering from such a well-studied process as the scattering of interacting particles. In this sense, the stage of asymptotic return to free motion with new parameters may not occur. Therefore, it makes sense for flocks to determine scattering data starting from the end of scattering, and to track their change in the future at the moments of relaxation to some steady state, if it occurs.

Another a priori difference may lie in the dependence of the scattering pattern on the shape of the colliding flocks. For different forms with the same exposure parameters, different proportions of agents can participate in the interaction and, accordingly, affect their flocks in different ways.

The nature of the interaction between agents, based on the information they receive, complicates the analytical construction of the theory of flock dispersion. Therefore, in the future, we will use the simulation results to establish the main patterns of flock dispersion.

4 Flocks collision simulation results

Let us start with an analysis of the change in the distance between the centers of the flocks during interaction. Typical examples of distance changes obtained as a result of flock collision simulation are shown in Fig. 3. The behavior of distances is universal and most stable, in the sense of the absence of noticeable fluctuations.

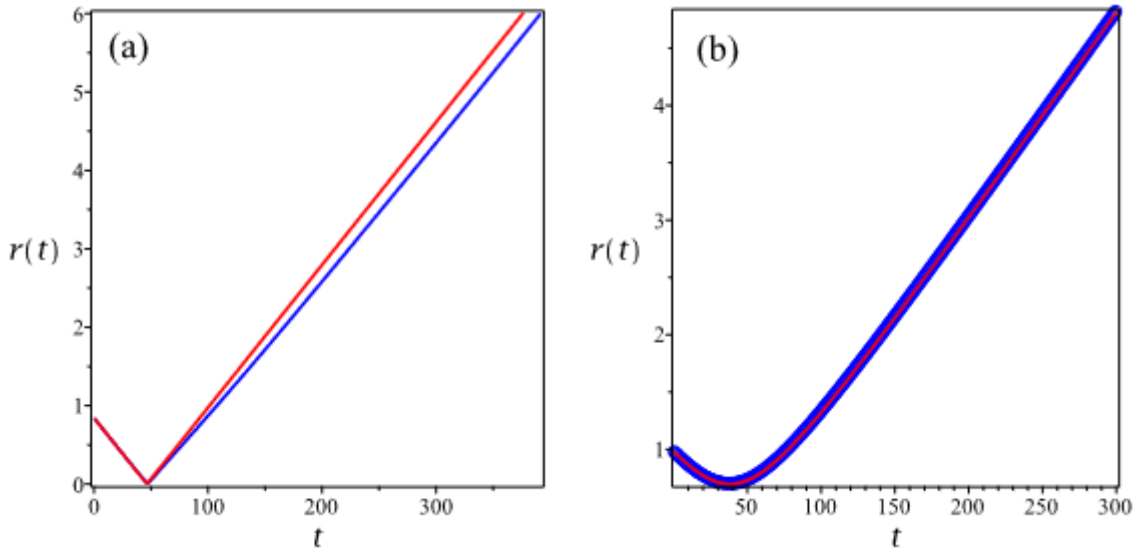

Fig.3 Typical changes in the distance between flocks over time, obtained as a result of numerical simulation. Red line is the distance between non-interacting (phantom) flocks, blue line is the distance between interacting flocks. (a) — impact parameter $\rho = 0.014$, *characteristic interaction scale* $l_{int} = 0.82608$, *and minimum position* $t_{min} = 47$. *(b) — impact parameter* $\rho = 0.0693$. *With the same number of agents in the flock* $N_1 = N_2 = 33$

We can note an important consequence of comparing the change in distances between interacting and non-interacting flocks. For all the initial parameters and the number of agents in the flocks, there is a close location of the minima and a good conformity between the minimum distance and the impact parameter. Noticeable differences can be observed in the asymptotic change of distances with time at times $t >> t_{int}$ or at distances $r >> l_{int}$ (see Fig. 3). The difference in the slope angles of the asymptotics means the difference in the velocities of these flocks. In other words, when flocks interact, it reduces their movement speed. In a certain sense, the differences between these dependences determine the degree of influence of the interaction of flocks on the impact parameter. So, for large values of the parameter, only a small part of the agents of both flocks interact, and this does not have a noticeable effect on the behavior of the flocks as a whole. Therefore, the interaction of agents does not always lead to the interaction of flocks.

Another important observation is related to the value of the minimum distance between flocks. For example, Fig. 4 shows the change in the minimum distance of approach of flocks from the impact parameter. The number of flocks is the same and equal to 95 individuals. In fact, it can be seen that the minimum distance of approach of interacting flocks coincides with the value of the impact parameter $r_m = \rho$. This dependence is retained for all considered numbers of flocks.

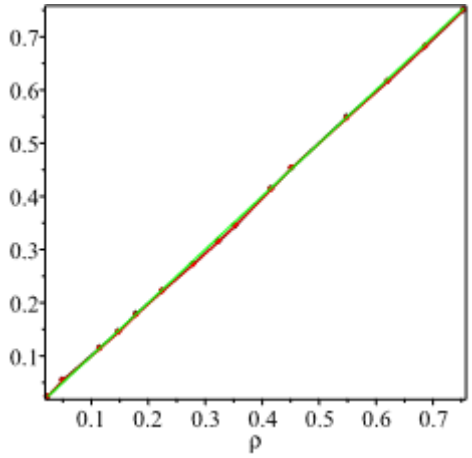

Fig.4 The dependence of the minimum distance of approach of flocks on the impact parameter is shown. Black line is for interacting flocks, red line is for phantom flocks, and green line is for $r_m = \rho$ *. One can see the complete coincidence of these dependencies for flocks* $N_1 = N_2 = 95$*. The same coincidence is observed for flocks of different numbers*

The coincidence of the minimum distance with the impact parameter means the absence of transverse displacements as a result of interaction. Therefore, a small scattering angle for any values of the impact parameter can be observed. Fig. 5 shows flock scattering angles $N_1 = N_2 = 60$ obtained by modeling flock collisions. Similar dependences are also observed for flocks with a different number of agents in flocks. It can be assumed that during a head-on collision, flocks retain their direction of movement after the collision due to symmetry considerations.

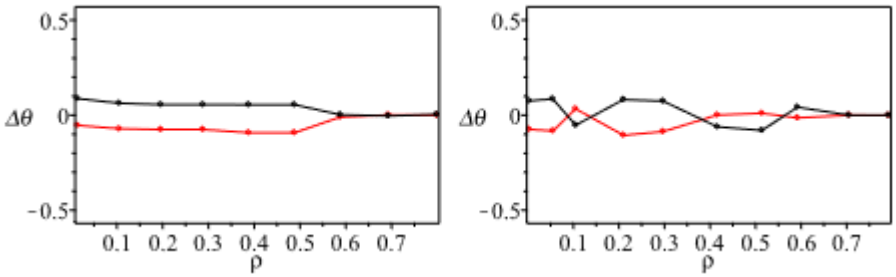

Fig.5 The dependence of the scattering angles of the first flock is shown in red, the second flock in black. Data about flocks with $N_1 = N_2 = 33$ *agents are presented on the left, and flocks with* $N_1 = N_2 = 60$ *on the right. In fact, the deviation of the directions of movement is small and does not have a systematic character*

It is important to remember that flocks interact at a finite distance l_{int} , after which the interaction stops and flocks continue to move freely with new parameters. In fact, if the direction of movement is preserved, then one of the important parameters is the speed of movement of flocks after interaction.

Let us now discuss in more detail how the speed of interacting flocks changes. The nature of the interaction depends on the impact parameter. Thus, at small values, the nature of flock speed changes is clearly expressed and has a typical form, shown in Fig. 6 with noticeable sharp decrease in the speed of the flock and a slower return to the initial speed of the flock. The characteristic velocity relaxation time for these parameters is $t_{rel} \approx 647$, and the interaction time is $t_{int} \approx 143$. Thus, the minimum is reached at the stage of interaction, and the increase in speed continues after the interaction of flocks. The ratio of times for this case is easy to establish. So for the first flock, the beginning of the decrease in speed is $t_{Sv1} \approx 10$, the time to reach the minimum is $t_{v1min} \approx 123$ and $t_{Fv1} \approx 657$ ($t_{rel} = t_{Fv} - t_{Sv}$), flock interaction

starts at $t = 0$ and lasts $t_{int} \approx 143$. For the second flock, similar values $t_{Sv2} \approx 10$, $t_{v2min} \approx 125$, and $t_{Fv2} \approx 641$ are realized. Thus, the relaxation times are much longer than the interaction time.

For large impact parameters, when a small part of agents from different flocks interact, the behavior of the velocities is significantly different (see Fig. 6). In fact, there are no noticeable changes in the speed of the flock. In such cases, the change in distances between interacting flocks and phantom flocks is indistinguishable.

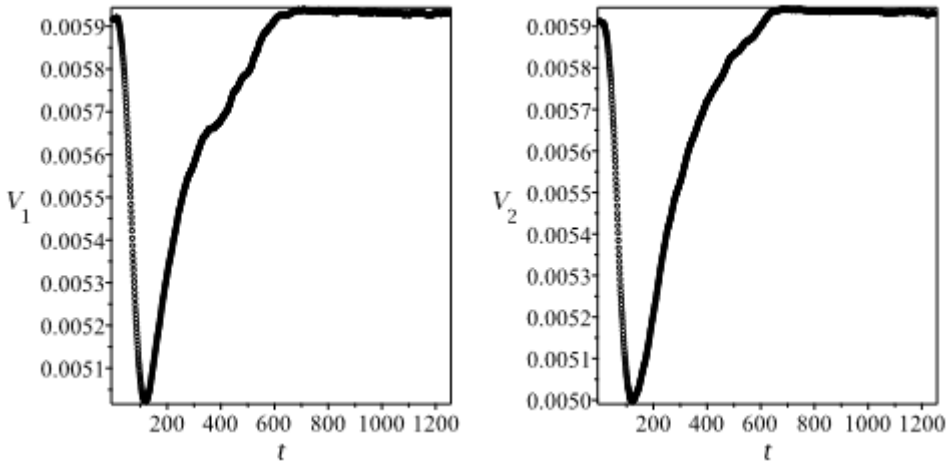

Fig.6 The change in the velocity of the first flock is shown on the left, the second on the right. The number of agents is $N_1 = N_2 = 95$, $\rho = 0.050$

This behavior is observed with a different number of agents in flocks. Fig. 7 shows the dependence of the jump in velocity and relaxation time on the impact parameter. One can see the disappearance of the jump in speed even at the stage of interaction of a certain proportion of the agents of the flocks. Similar dependences are observed for other numbers of flocks.

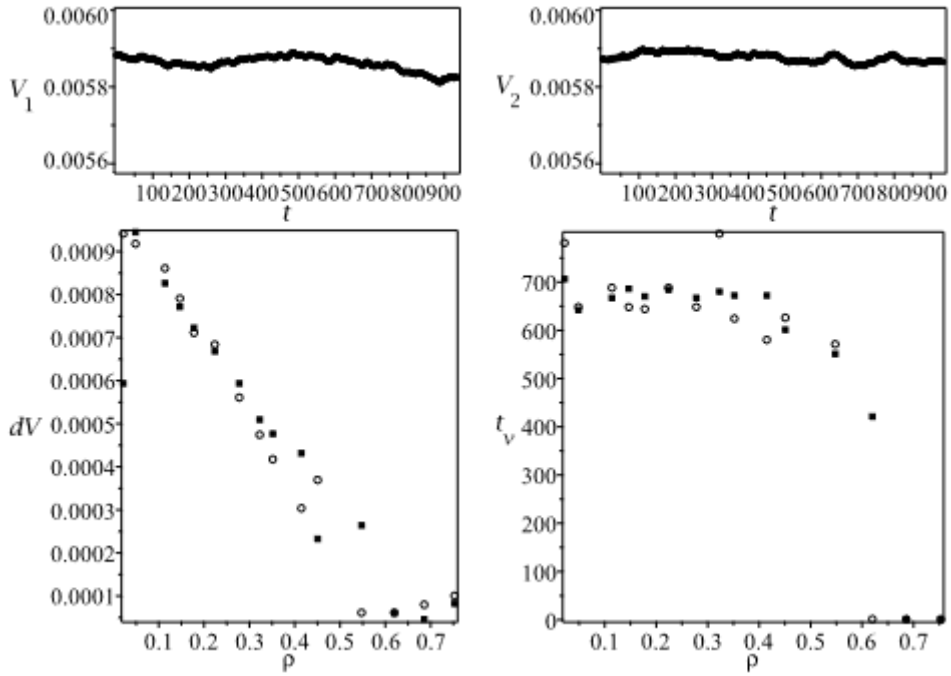

Fig.7 The change in the velocity of the first flock is on the left, the second is on the right. Number of agents is $N_1 = N_2 = 95$, $\rho = 0.687$ *.The magnitude of the jump in velocity is shown below on the left and the relaxation time on the right, depending on the impact parameter. The circles are for the first flock, the squares for the second one.*

Some important changes are also observed in the forms of flocks during interaction. The average radius of the flock has been chosen as a parameter characterizing the shape of the flock. The characteristic differences have been observed again depending on the values of the impact parameter.

Fig. 8 shows characteristic changes in the average radii of interacting flocks for different values of the impact parameter. A sharp change in the average radius is noticeable at small values of the impact parameter (see the bottom row of Fig. 8). The change starts at the stage of interaction and continues even in the absence of interaction. At times of the order of the velocity relaxation time, the stage of a slow decrease of the average radius begins. At large values of the impact parameter (see the top row of Fig. 8), a slow monotonous increase in the average radius is observed.

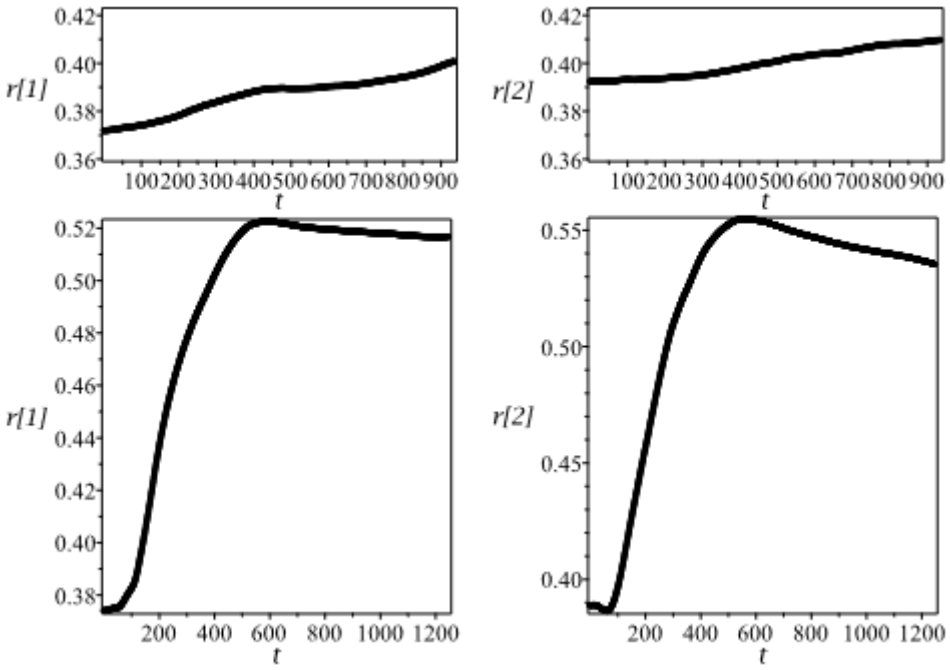

Fig.8 The changes in the average radius of the first flock is on the left, the second is on the right. The number of agents in flocks is $N_1 = N_2 = 95$. *For the top row* $\rho = 0.687$ *, for the bottom row* $\rho = 0.050$

It is interesting to consider the change in flock density over time for similar flocks and parameters. Fig. 9 shows the corresponding dependencies. It is easy to see the correlation with the behavior of the mean radius. In addition, an increase in the density of flocks during the interaction and a subsequent sharp decrease in density after the end of the interaction is noticeable.

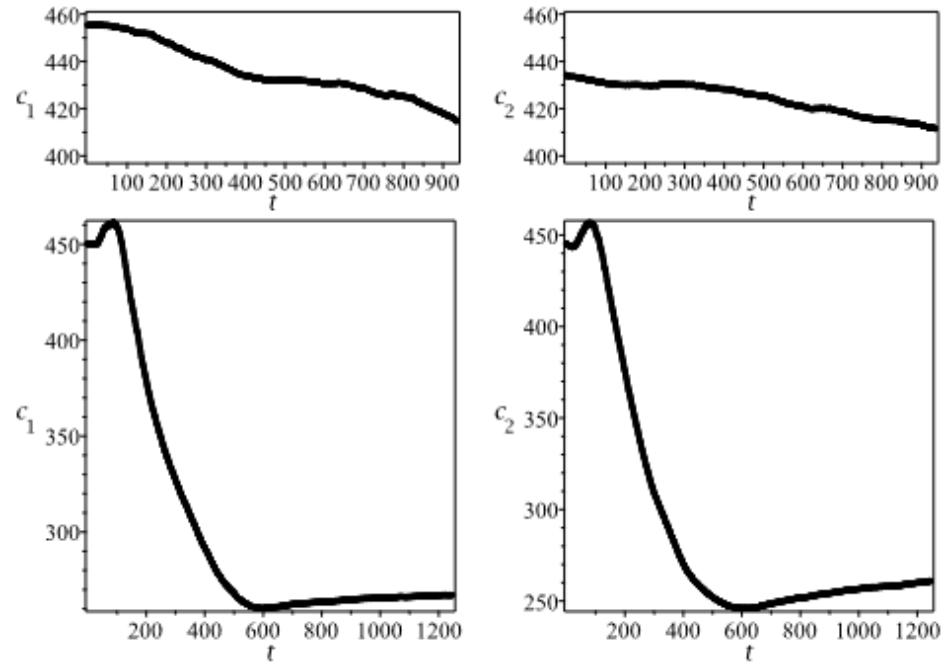

Fig.9 The change in the average density of the first flock is on the left, the second is on the right. The number of agents in flocks is $N_1 = N_2 = 95$. *For the top row* $\rho = 0.687$ *, for the bottom row* $\rho = 0.050$

We can say that there is a jump in the Δc density. After times of the order of velocity relaxation, a slow stage of density increase begins. The presence or absence of that jump, as well as the magnitude of the jump, determines the degree of influence of the interaction of flocks on their movement and behavior.

5 Flocks kinematics

Let us consider the kinematics of the flocks' movement. In this case, we consider two cases of flock movement with the same initial data. This is the movement of flocks without interaction and in the presence of interaction between flocks. Flocks without interaction are phantom flocks. Agents of this flock cannot see agents of another flock and pass through them unharmed. Let us start with this case. Let the centers of the flocks move without interaction, then the positions of the flocks change with time as

$$x_1 = x_{01} + v_1 t; \quad y_1 = y_{01};$$

$$x_2 = x_{02} - v_2 t; \quad y_2 = y_{02}.$$

Here, the number of the flock is marked by the index, and the speeds of the flock movement are oppositely directed along the X axis. Let us assume that the beginning of the flocks' movement starts with the distance between them coinciding with the characteristic scale of interaction l_{int}. In other words, $x_{02} = x_{01} + \sqrt{l_{int}^2 - \rho^2}$. Then the distance between the centers of the flocks changes according to

$$r_s(t) = \sqrt{(x_1 - x_2)^2 + (y_1 - y_2)^2} = \sqrt{\left((v_1 + v_2)t - \sqrt{l_{int}^2 - \rho^2}\right)^2 + \rho^2}, \tag{5.1}$$

where $r_s(t)$ is the distance between freely moving flocks without interaction. The minimum $r_s(t)$ is reached at time $t = t_m = \dfrac{\sqrt{l_{int}^2 - \rho^2}}{\Delta v}$ where the approach velocity is $\Delta v = v_1 + v_2$ and is equal in magnitude to $r_s(t_m) = \rho$. When comparing with experimental data, it is convenient to use an equivalent form, but depending on other parameters

$$r_s(t) = \sqrt{\left(\left(\frac{t}{t_m} - 1\right)\sqrt{l_{int}^2 - \rho^2}\right)^2 + \rho^2}. \tag{5.2}$$

In this relation, the time of the closest approach t_m appears as the main parameter. We also give the initial speed of approach

$$\frac{dr_s(t)}{dt}\Big|_{t=0} = -\frac{l_{int}^2 - \rho^2}{\sqrt{l_{int}^2}\, t_m}. \tag{5.3}$$

Comparing this expression with a similar form obtained from the relation (5.1), we recieve the initial approach velocity through the main parameters

$$v_1 + v_2 = \frac{\sqrt{l_{int}^2 - \rho^2}}{t_m}. \tag{5.4}$$

This relation can be used for an a priori estimate of t_m from the initial data.

Now let us calculate how the distance between the interacting flocks will change. Suppose that the interaction leads to the acceleration of the movement of the flock. We will assume that the acceleration at the moments of interaction is constant and oppositely directed for the first and second flocks. In fact, this assumption is related to the hypothesis of the fulfillment of Newton's third law (the force of action is equal to the force of reaction) and is based on simulation data. Then

$$x_1 = x_{01} + v_1 t - a_{x1}\frac{t^2}{2}; \quad y_1 = y_{01} + a_{y1}\frac{t^2}{2};$$

$$x_2 = x_{02} - v_2 t + a_{x2}\frac{t^2}{2}; \quad y_2 = y_{02} - a_{y2}\frac{t^2}{2}.$$

It remains to calculate the distance between the interacting flocks

$$r_{int}(t) = \sqrt{\left((v_1+v_2)t - \Delta a_x \frac{t^2}{2} - \sqrt{l_{int}^2 - \rho^2}\right)^2 + \rho^2}; \quad 0 \le t \le t_{int}, \tag{5.5}$$

where $\Delta a_x = a_{x1} + a_{x2}$ and for reasons of symmetry and simulation data, we neglect the lateral acceleration $a_y = 0$. This relation is satisfied when the flocks $t \le t_{int}$ interact, where $r_{int} \le l_{int}$. This dependence of the distance between flocks contains natural parameters. Minimum convergence is achieved at times that are easy to find

$$t_{1m} = \frac{v_1 + v_2 - \sqrt{(v_1+v_2)^2 - 2\Delta a_x \sqrt{l_{int}^2 - \rho^2}}}{\Delta a_x},$$

$$t_{2m} = \frac{v_1 + v_2 + \sqrt{(v_1+v_2)^2 - 2\Delta a_x \sqrt{l_{int}^2 - \rho^2}}}{\Delta a_x}.$$

It is easy to see that

$$t_{1m} \le t_{2m} \quad \text{if} \quad a_x > 0,$$

$$t_{1m} < 0, \quad t_{2m} > 0 \quad \text{if} \quad a_x < 0.$$

Therefore, t_{1m} is important for us if $\Delta a_x > 0$, and t_{2m} if $\Delta a_x < 0$. Further, we will be interested in the case $\Delta a_x > 0$. The choice of this case is justified by the data obtained in the simulation of collisions. The condition that these times are real gives an a priori constraint on the acceleration

$$0 \le \Delta a_x \le \frac{(v_1+v_2)^2}{2\sqrt{l_{int}^2 - \rho^2}}.$$

Assuming the acceleration being small, we can obtain a more convenient expression for the time to reach the minimum distance between flocks

$$t_{1m} \approx \frac{\sqrt{l_{int}^2 - \rho^2}}{v_1 + v_2} + \Delta a_x \frac{l_{int}^2 - \rho^2}{2(v_1+v_2)^3}. \tag{5.6}$$

Actually, this ratio explains the closeness of the minimum distances of approach for the phantom and interacting flocks (see the ratio (5.4)). Using the equation (5.6) it is easy to set the acceleration value from the simulation data. Similarly, we can estimate the interaction time $r_{int}(t_{int}) = l_{int}$

$$t_{int} = \frac{(v_1+v_2) - \sqrt{(v_1+v_2)^2 - 4\Delta a_x \sqrt{l_{int}^2 - \rho^2}}}{\Delta a_x}. \tag{5.7}$$

Assuming the acceleration being small, we also obtain an approximate value

$$t_{int} \approx 2\frac{\sqrt{l_{int}^2 - \rho^2}}{v_1 + v_2} + 2\Delta a_x \frac{l_{int}^2 - \rho^2}{(v_1+v_2)^3}. \tag{5.8}$$

The minimum approach distance is still $r_{int}(t_{1m}) = \rho$, as well as the initial approach velocity

$$\frac{dr_{int}(t)}{dt}\Big|_{t=0} = -\frac{2v_1\sqrt{l_{int}^2 - \rho^2}}{\sqrt{l_{int}^2}}.$$

Thus, the dependence (5.5) agrees well with the experimental data. It includes a single unknown parameter Δa_x.

Actually, in a certain sense, it is the parameter which determines the <<force>> of the interaction of flocks. Naturally, we use simulation data to determine it. So, for example, the acceleration of flocks approach Δa_x can be determined by comparing the t_m time to reach the minimum distance with the value t_e obtained in the simulation

$$\Delta a_x = \frac{2((v_1+v_2)t_e - \sqrt{l_{int}^2 - \rho^2})}{t_e^2}. \tag{5.9}$$

Using this ratio, it is easy to set the acceleration values from the simulation data.

Finally, after the interaction, the distance changes, as in non-interacting flocks, but with different velocities. These new speeds are the same as $v_1' + v_2' = v_1 + v_2 - \frac{\Delta a_x}{2} t_{int}$. Thus, the change in distance with time $t_{int} \le t$ occurs as

$$r(t) = \sqrt{((v_1'+v_2')t - (l_{int}^2 - \rho^2))^2 + \rho^2} + \sqrt{((v_1+v_2)t_{int} - \frac{\Delta a_x}{2} t_{int}^2 - (l_{int}^2 - \rho^2))^2 + \rho^2} + l_{int}. \tag{5.10}$$

This equation is used below for comparison with the simulation data.

6 Results and conclusions

Let us start by comparing the simulation data on the change in the distance between flocks with the obtained dependencies. Fig. 10 shows the simulation data and the corresponding dependencies for the set value of approach acceleration Δa_x. For the chosen initial conditions $\Delta a_x = 0.134 \cdot 10^{-4}$ according to the relation (5.9). There is a noticeable good conformity between the dependence (5.5) and the simulation data during the interaction. The conformity of the minimum distance with the impact parameter and the achievement of l_{int} at time $t = t_{int}$ has been shown as well. At times $t \ge t_{int}$, the dependency (5.10) is shown in green against the simulation data (Fig. 10). The differences between these dependencies are hard to notice. Thus, the hypothesis of uniformly accelerated deceleration of the flocks at the moments of interaction conforms with the simulation data. Such a good match is observed for a different number of agents in flocks and impact parameters. In this sense, acceleration is actually the only parameter that determines the interaction of flocks in a head-on collision. It is natural to assume that it is the acceleration that determines the <<force>> of the interaction of flocks. Therefore, it is of interest to establish its dependence on the impact parameter and on the number of agents.

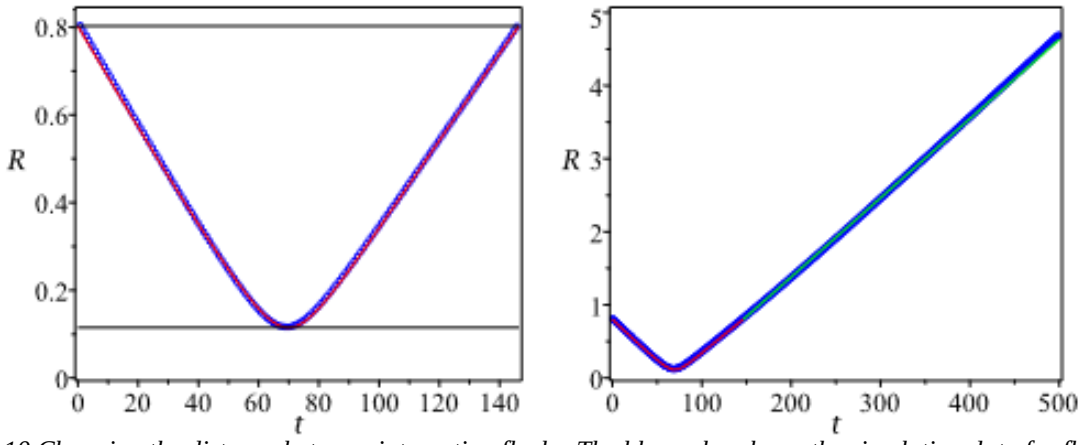

Fig.10 Changing the distance between interacting flocks. The blue color shows the simulation data for flocks $N_1 = N_2 = 95$ *and* $\rho = 0.115$. *The red line corresponds to the dependency (5.5). On the left, at times of flock interaction* $0 \le t \le t_{int}$, *on the right, at times* $t \ge t_{int}$. *The two horizontal lines on the left side correspond to* l_{int} *and* ρ. *On the right, the dependence (5.10) of the distance change after the end of the interaction of flocks is shown in green*

The characteristic change in the approach acceleration Δa_x as a function of the impact parameter is shown in Fig. 11.

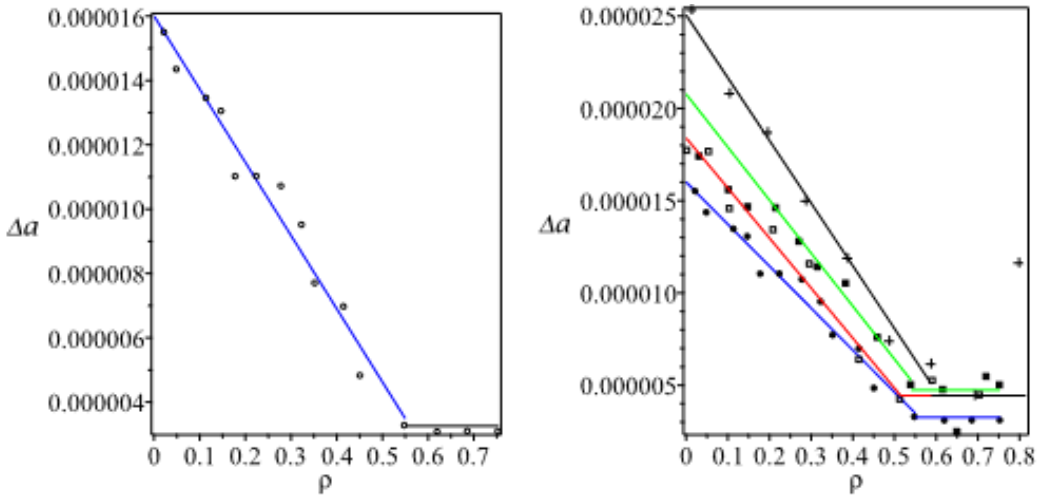

Fig.11 On the left the dependence of acceleration on impact parameter ρ *for* $N_1 = N_2 = 95$ *is shown. Circles are simulation data, blue line is root-mean-square approximation in the region of decline, black line is a constant value corresponding to the absence of acceleration. On the right the dependence of acceleration on the impact parameter for different numbers of flocks is shown. Blue line –* $N_1 = N_2 = 95$, *black line –* $N_1 = N_2 = 33$, *green line –* $N_1 = N_2 = 77$ *, and red line –* $N_1 = N_2 = 60$

This behavior is typical of the order parameter in phase transitions. This means the disappearance of the interaction of flocks at a certain value of the impact parameter, despite the presence of a certain proportion of interacting agents in the flocks. If we use a linear approximation of the given data in Fig. 11, then the value of the impact parameter at which $\Delta a_x = 0$ for all numbers of flocks is $\rho_c \approx 0.7$. This value is less than l_{int} and, accordingly, part of the agents continues to interact with this value of the impact parameter. In other words, the interaction of agents does not mean the interaction of flocks.

Thus, in a head-on collision at the stage flock interactions, the main parameter acceleration Δa_x is determined by the relation (5.9) and determines the main characteristics of their behavior.

СПИСОК ЛІТЕРАТУРИ

1. T. Vicsek, A. Zafeiris. Collective motion. *Physics reports*. 2012. Vol. 517, issues 3-4. P. 71-140. URL: https://arxiv.org/pdf/1010.5017 (Last accessed: 01.02.2022).
2. C. Keys, L. Dugatkin. Flock size and position effects on vigilance, aggression, and prey capture in the European starling. *The Condor*. 1990. Vol. 92. P. 151-159. https://sora.unm.edu/sites/default/files/journals/condor/v092n01/p0151-p0159.pdf
3. K. Bhattacharya, T. Vicsek. Collective decision making in cohesive flocks. *New Journal of Physics*. 2010. Vol. 12. 13 p. https://iopscience.iop.org/article/10.1088/1367-2630/12/9/093019/pdf
4. J. Parrish, W. Hamner. Animal Groups in Three Dimensions. *Cambridge, England: Cambridge University Phys. Rev. Ess*. 1997. 378 p. https://www.cambridge.org/core/books/animal-groups-in-three-dimensions/910F9DF579FCC43241F3560A2964E4F8
5. Y. Katz, K. Tunstrom, C. Ioannou, C. Huepe, I. Couzin. Inferring the structure and dynamics of interactions in schooling fish. *Proceedings of the National Academy of Sciences*. 2011. Vol. 108, no. 46. P. 18720-18725. https://www.pnas.org/doi/full/10.1073/pnas.1107583108
6. A. Ward, D. Sumpter, I. Couzin, P. Hart, J. Krause. Quorum decisionmaking facilitates information transfer in fish shoals. *Proceedings of the National Academy of Sciences*. 2008. Vol. 105, no. 19. P. 6948-6953. https://www.pnas.org/doi/pdf/10.1073/pnas.0710344105

7. Y. Hayakawa. Spatiotemporal dynamics of skeins of wild geese. *Europhysics Letters*. 2010. Vol. 89, no. 4. 48004 (6 p.). https://iopscience.iop.org/article/10.1209/0295-5075/89/48004/meta
8. S. Bazazi, J. Buhl, J. Hale, M. Anstey, G. Sword, S. Simpson, I. Couzin. Collective motion and cannibalism in locust migratory bands. *Current biology*. 2008. Vol. 18, issue 10. P. 735-739. https://www.sciencedirect.com/science/article/pii/S0960982208005216
9. S. Bazazi, C. Ioannou, S. Simpson, G. Sword, C. Torney, P. Lorch, I. Couzin. The social context of cannibalism in migratory bands of the mormon cricket. *PloS One*. 2010. Vol. 5, issue 12. 7 p. https://journals.plos.org/plosone/article/file?id=10.1371/journal.pone.0015118&type=printable
10. N. Bode, J. Faria, D. Franks, J. Krause, A. Wood. How perceived threat increases synchronization in collectively moving animal groups. *Proceedings of the Royal Society B: Biological Sciences*. 2010. Vol. 277. P. 3065-3070. https://www.ncbi.nlm.nih.gov/pmc/articles/PMC2982070/pdf/rspb20100855.pdf
11. U. Erdmann, B. Blasius, L. Schimansky-Geier. Active Motion and Swarming. *The European physical journal. Special topics*. 2008. P. 157. https://pascal-francis.inist.fr/vibad/index.php?action=getRecordDetail&idt=20331961
12. C. Frederick, M. Egerstedt, H. Zhou. Collective Motion Planning for a Group of Robots Using Intermittent Diffusion. 2022. 18 p. URL: https://arxiv.org/pdf/1904.02804.pdf (Last accessed: 01.02.2022).
13. M. Raoufi, A. Turgut, F. Arvin. Self-organized Collective Motion with a Simulated Real Robot Swarm. 2019. 12 p. URL: https://arxiv.org/pdf/1904.03230.pdf (Last accessed: 01.02.2022).
14. K. Sugawara, R. Arai, M. Sano. Collective motion of interacting simple robots. *IECON'01, 27th Annual Conference of the IEEE Industrial Electronics Society (Cat. No.37243)*, Denver, CO, USA. 2001. Vol.1. P. 428-432. https://ieeexplore.ieee.org/abstract/document/976520
15. G. Caprari, A. Colot, R. Siegwart, J. Halloy, J. Deneubourg. Animal and Robot Mixed Societies - Building Cooperation Between Microrobots and Cockroaches. *IEEE Robotics and Automation Magazine*. 2005. Vol. 12. P. 58-65. https://www.researchgate.net/publication/3344719
16. J. Halloy, G. Sempo, G. Caprari, C. Rivault, M. Asadpour, F. Tache, I. Said, V. Durier, S. Canonge, J. Ame, C. Detrain, N. Correll, A. Martinoli, F. Mondada, R. Siegwart, J. Deneubourg. Social integration of robots into groups of cockroaches to control self-organized choices. *Science*. 2007. Vol. 318. P. 1155-1158. https://www.cns.nyu.edu/events/spf/SPF_papers/HalloyDeneubourgS07.pdf
17. S. Ramaswamy. The Mechanics and Statistics of Active Matter. *Annual Review of Condensed Matter Physics*. 2010. Vol. 1. P. 323–345. URL: https://arxiv.org/pdf/1004.1933.pdf (Last accessed: 01.02.2022).
18. M. Marchetti, J. Joanny, S. Ramaswamy, T. Liverpool, J. Prost, M. Rao, R. Aditi Simha. Hydrodynamics of soft active matter. *Reviews of Modern Physics*. 2013. Vol. 85, no. 3. P. 1143–1189. http://dspace.rri.res.in/jspui/bitstream/2289/5838/1/2013_RevModPhys_85_1143.pdf
19. I. Aoki. A simulation study on the schooling mechanism in fish. *Bulletin of the Japanese Society of Scientific Fisheries*. 1982. Vol. 48, issue 8. P. 1081-1088. https://www.jstage.jst.go.jp/article/suisan1932/48/8/48_8_1081/_pdf/-char/en
20. C. W. Reynolds. Flocks, herds, and schools: A distributed behavioral model. *Computer graphics*. 1987. Vol. 21, no. 4. P. 25-34. https://dl.acm.org/doi/pdf/10.1145/37401.37406
21. D. Shiffman. *The nature of code*. New York: Magic Book Project. 2012. 520 p. https://natureofcode.com/book

REFERENCES

1. T. Vicsek and A. Zafeiris. "Collective motion," *Physics reports*, vol. 517, issues 3-4, 2012, pp. 71-140. URL: https://arxiv.org/pdf/1010.5017 (Last accessed: 01.02.2022).
2. C. Keys and L. Dugatkin. "Flock size and position effects on vigilance, aggression, and prey capture in the European starling", *The Condor*, vol. 92, 1990, pp. 151-159. https://sora.unm.edu/sites/default/files/journals/condor/v092n01/p0151-p0159.pdf

3. K. Bhattacharya and T. Vicsek. “Collective decision making in cohesive flocks,” *New Journal of Physics*, vol. 12, 2010, 13 p. https://iopscience.iop.org/article/10.1088/1367-2630/12/9/093019/pdf
4. J. Parrish and W. Hamner. “Animal Groups in Three Dimensions,” *Cambridge, England: Cambridge University Phys. Rev. Ess*, 1997, 378 p. https://www.cambridge.org/core/books/animal-groups-in-three-dimensions/910F9DF579FCC43241F3560A2964E4F8
5. Y. Katz, K. Tunstrom, C. Ioannou, C. Huepe and I. Couzin. “Inferring the structure and dynamics of interactions in schooling fish,” *Proceedings of the National Academy of Sciences*, vol. 108, no. 46, 2011, pp. 18720-18725. https://www.pnas.org/doi/full/10.1073/pnas.1107583108
6. A. Ward, D. Sumpter, I. Couzin, P. Hart and J. Krause. “Quorum decisionmaking facilitates information transfer in fish shoals,” *Proceedings of the National Academy of Sciences*, vol. 105, no. 19, 2008, pp. 6948-6953. https://www.pnas.org/doi/pdf/10.1073/pnas.0710344105
7. Y. Hayakawa. “Spatiotemporal dynamics of skeins of wild geese,” *Europhysics Letters*, vol. 89, no. 4, 2010, 48004 (6 p). https://iopscience.iop.org/article/10.1209/0295-5075/89/48004/meta
8. S. Bazazi, J. Buhl, J. Hale, M. Anstey, G. Sword, S. Simpson and I. Couzin. “Collective motion and cannibalism in locust migratory bands,” *Current biology*, vol. 18, issue 10, 2008, pp. 735-739. https://www.sciencedirect.com/science/article/pii/S0960982208005216
9. S. Bazazi, C. Ioannou, S. Simpson, G. Sword, C. Torney, P. Lorch and I. Couzin. “The social context of cannibalism in migratory bands of the mormon cricket,” *PloS One*, vol. 5, issue 12, 2010, 7 p. https://journals.plos.org/plosone/article/file?id=10.1371/journal.pone.0015118&type=printable
10. N. Bode, J. Faria, D. Franks, J. Krause and A. Wood. “How perceived threat increases synchronization in collectively moving animal groups,” *Proceedings of the Royal Society B: Biological Sciences*, vol. 277, 2010, pp. 3065-3070. https://www.ncbi.nlm.nih.gov/pmc/articles/PMC2982070/pdf/rspb20100855.pdf
11. U. Erdmann, B. Blasius and L. Schimansky-Geier. “Active Motion and Swarming,” *The European physical journal. Special topics*, 2008, p. 157. https://pascal-francis.inist.fr/vibad/index.php?action=getRecordDetail&idt=20331961
12. C. Frederick, M. Egerstedt and H. Zhou. “Collective Motion Planning for a Group of Robots Using Intermittent Diffusion,” 2020, 18 p. URL: https://arxiv.org/pdf/1904.02804.pdf (Last accessed: 01.02.2022).
13. M. Raoufi, A. Turgut and F. Arvin. “Self-organized Collective Motion with a Simulated Real Robot Swarm,” 2019, 12 p. URL: https://arxiv.org/pdf/1904.03230.pdf (Last accessed: 01.02.2022).
14. K. Sugawara, R. Arai and M. Sano. “Collective motion of interacting simple robots,” *IECON’01, 27th Annual Conference of the IEEE Industrial Electronics Society (Cat. No.37243)*, Denver, CO, USA, vol.1, 2001, pp. 428-432. https://ieeexplore.ieee.org/abstract/document/976520
15. G. Caprari, A. Colot, R. Siegwart, J. Halloy and J. Deneubourg. “Animal and Robot Mixed Societies - Building Cooperation Between Microrobots and Cockroaches,” *IEEE Robotics and Automation Magazine*, vol. 12, 2005, pp. 58-65. https://www.researchgate.net/publication/3344719
16. J. Halloy, G. Sempo, G. Caprari, C. Rivault, M. Asadpour, F. Tache, I. Said, V. Durier, S. Canonge, J. Ame, C. Detrain, N. Correll, A. Martinoli, F. Mondada, R. Siegwart and J. Deneubourg. “Social integration of robots into groups of cockroaches to control self-organized choices,” *Science*. vol. 318, 2007, pp. 1155-1158. https://www.cns.nyu.edu/events/spf/SPF_papers/HalloyDeneubourgS07.pdf
17. S. Ramaswamy. “The Mechanics and Statistics of Active Matter,” *Annual Review of Condensed Matter Physics*, vol. 1, 2010, pp. 323–345. URL: https://arxiv.org/pdf/1004.1933.pdf (Last accessed: 01.02.2022).
18. M. Marchetti, J. Joanny, S. Ramaswamy, T. Liverpool, J. Prost, M. Rao and R. Aditi Simha. “Hydrodynamics of soft active matter,” *Reviews of Modern Physics*, vol. 85, no. 3, 2013, pp. 1143–1189. http://dspace.rri.res.in/jspui/bitstream/2289/5838/1/2013_RevModPhys_85_1143.pdf

19. I. Aoki. “A simulation study on the schooling mechanism in fish,” *Bulletin of the Japanese Society of Scientific Fisheries*, vol. 48, issue 8, 1982, pp. 1081-1088. https://www.jstage.jst.go.jp/article/suisan1932/48/8/48_8_1081/_pdf/-char/en
20. C. W. Reynolds. “Flocks, herds, and schools: A distributed behavioral model,” *Computer graphics*, vol. 21, no. 4, 1987, pp. 25-34. https://dl.acm.org/doi/pdf/10.1145/37401.37406
21. D. Shiffman. *The nature of code*. New York: Magic Book Project, 2012, 520 p. https://natureofcode.com/book

Приймак О.В. *Кандидат технічних наук*
Яновський В.В. *Доктор фізико-математичних наук, професор*
Харківський національний університет ім. В.Н. Каразіна,
майдан Свободи 4, м. Харків, 61022;
Інститут монокристалів НАН України,
проспект Науки 60, м. Харків, 61001

Лобове зіткнення зграй

Актуальність. Дослідження колективної поведінки зграй інтелектуальних агентів з використанням методів математичного та чисельного моделювання пов’язане з вирішенням задач у активно досліджуваних у наш час сферах багатоагентних систем та штучного інтелекту.

Мета. Виявити закономірності розсіяння зграй інтелектуальних агентів при їхньому зіткненні та отримати аналітичні співвідношення кінематики зграй.

Методи дослідження. В основі роботи лежать принципи та методи математичного та чисельного моделювання багатоагентних систем. Колективна поведінка агентів змодельована з використанням алгоритму флокування, що належить до методів моделювання руху, заснованих на векторах сил. Використано аналітичні методи опису кінематики поведінки стай, які добре узгоджуються з результатами моделювання.

Результати. Отримано дані, які визначають головні зміни, що відбуваються зі зграями в наслідок їх зіткнення. Визначено особливості, які відбуваються при взаємодії зграй при зміні кількості агентів у зграях. Визначено, що при збільшенні прицільного параметру зміни в характеристиках зграй стають менш помітними, незважаючи на існуючу взаємодію агентів двох зграй. Визначено, що головний параметр, який визначає поведінку зграй, є величина прискорення на стадії їх взаємодії. Отримана залежність прискорення від значення прицільного параметру нагадує залежність, яка є типовою для фазових переходів.

Висновки. В роботі отримано нові наукові результати, що полягають у виявленні головних закономірностей розсіяння зграй інтелектуальних агентів при їхньому зіткненні та отриманні аналітичних співвідношень кінематики зграй, які добре узгоджуються з даними моделювання.

Ключові слова: *колективна поведінка, багатоагентна система, зграя, інтелектуальний агент, флокування, вектор сили, кінематика, прискорення, прицільний параметр.*

Надійшла у першій редакції 12.10.2022, в останній - 16.11.2022.
The first version has been received on 12.10.2022, the final version - on 16.11.2022.

Наукове видання

Вісник Харківського національного університету імені В. Н. Каразіна

Серія «Математичне моделювання. Інформаційні технології. Автоматизовані системи управління»

Випуск 56

Збірник наукових праць

Українською та англійською мовами

Комп'ютерне верстання О.О. Афанасьєва

Підписано до друку 26.12.2022 р.
Формат 60x84/8. Папір офсетний. Друк цифровий.
Ум. друк. арк. – 5,5.
Обл.– вид. арк. – 6,8.
Наклад 50 пр. Зам. № 36/2022
Безкоштовно

Видавець і виготовлювач
Харківський національний університет імені В. Н. Каразіна
61022, м. Харків, майдан Свободи, 4
Свідоцтво суб'єкта видавничої справи ДК №3367 від 13.01.09

Видавництво Харківський національний університет імені В. Н. Каразіна
тел.: 705-24-32